Applications of Cone Beam Computed Tomography in Orthodontics and Endodontics

By: Bassam Hassan

The printing of this thesis was financially supported by the
ACTA Research Institute and the VU University of Amsterdam

Printed by: Drukkers GVO vormgevers http://www.p-l.nl/

VRIJE UNIVERSITEIT

Applications of Cone Beam Computed Tomography in Orthodontics and Endodontics

ACADEMISCH PROEFSCHRIFT

ter verkrijging van de graad Doctor aan
de Vrije Universiteit Amsterdam,
op gezag van de rector magnificus
prof.dr. L.M. Bouter,
in het openbaar te verdedigen
ten overstaan van de promotiecommissie
van de faculteit der Tandheelkunde
op donderdag 17 juni 2010 om 13.45 uur
in het auditorium van de universiteit,
De Boelelaan 1105

door

Bassam Abdulsstar Hassan
geboren te Baghdad, Irak

promotor: prof.dr. P.F. van der Stelt

copromotor: dr. G.C.H. Sanderink

Dedication:

This thesis is dedicated to Ginan and Amer for their continuous and unbounded love and support for me over the years.

Contents:

Chapter I Introduction and aims

Part of this chapter is published as:

Bassam Hassan and Reinhilde Jacobs. Cone Beam Computed Tomography 3D imaging in Oral and Maxillofacial Surgery. Euro Medical Imaging Review 2008 1(1): 38-40.

Three-dimensional imaging technologies in dentistry

Imaging plays an important role in diagnosis and treatment planning in dentistry. A thorough history and clinical examination are vital in establishing diagnosis; yet, the value of radiographic imaging cannot be overstated. Two-dimensional (2D) projection radiography has been in use for more than half a century for diagnosing congenital and developmental deformities in the maxillofacial region. Still, in the last decades, the introduction of three-dimensional imaging characterized by Computed Tomography (CT) and Magnetic Resonance Imaging (MRI) technologies had a tremendous impact on the practice and teaching of dentistry. The tomographic nature of CT and MRI provides thin slices at much higher inherent detail than what is achievable with 2D projection radiography, which in turn allows for a better delineation of the bone and soft-tissue boundaries and a deeper appreciation of the intricate interrelations of the complex anatomy in the maxillofacial region.

Conventional Computed Tomography (CT) vs. Cone Beam CT (CBCT)

Conventional helical or spiral CT is used in maxillofacial imaging for diagnosing osseous lesions and deformities, pre-operative planning of surgical interventions, intra-operative surgical navigation and fabrication of surgical stents and implants. [1-4] Those systems are largely accessible to clinicians residing in public and private hospitals in medical radiology departments. For small dental hospitals and private clinics, though, the installation, operating and maintenance costs and labour of a conventional CT could prove prohibitive in most cases. [5,6] In the last decade, a CT system specifically dedicated for the maxillofacial region has been developed and became increasingly popular. These so called Cone Beam Computed Tomography (CBCT) scanners capture the entire maxillofacial region by a single rotation of the x-ray tube and detector around the patient's head while providing sub-millimeter resolution. [7-10]

There are several characteristic differences between CBCT and conventional spiral CT with respect to data acquisition and

reconstruction method, image spatial resolution, contrast, artifacts and patient radiation dose. [11, 12] CBCT is advantageous over MDCT in terms of radiation dose reduction, lesser cost and increased availability. However, CBCT images suffer from several artifacts due to inferior detector efficiency and beam inhomogeneity. [13, 14] The influence those artifacts have on image quality and diagnostic accuracy is variable among the different manufacturers and the different scanning and reconstruction settings.

Cone Beam Computed Tomography (CBCT) technology

CBCT scanning technology has its roots in medicine in angiography, radiation therapy and intra-operative imaging procedures. [15-17] The technology was initially developed as an alternative to the fan-based conventional CT scanners due to an increasing demand for rapid imaging coupled with the ability to cover large scan area in a single arm rotation. The principle of CBCT is based on a fixed x-ray source and detector with a rotating gantry. The x-ray source emits a cone-shaped beam of ionizing radiation that passes through the centre of the scan region of interest (ROI) in the patient's head to the x-ray detector on the other side. The gantry bearing the x-ray source and detector rotates around the patient's head in full 360^{o}, or sometimes, partial 180^{o}-270^{o}arcs. While rotating, the x-ray source emits radiation in a continuous or pulsed mode allowing the detector to acquire multiple 'basis' projection radiographs (figure1.1a). Those two-dimensional projections are then reconstructed with the help of a special reconstruction algorithm into a 3D volume (figure1.1b).

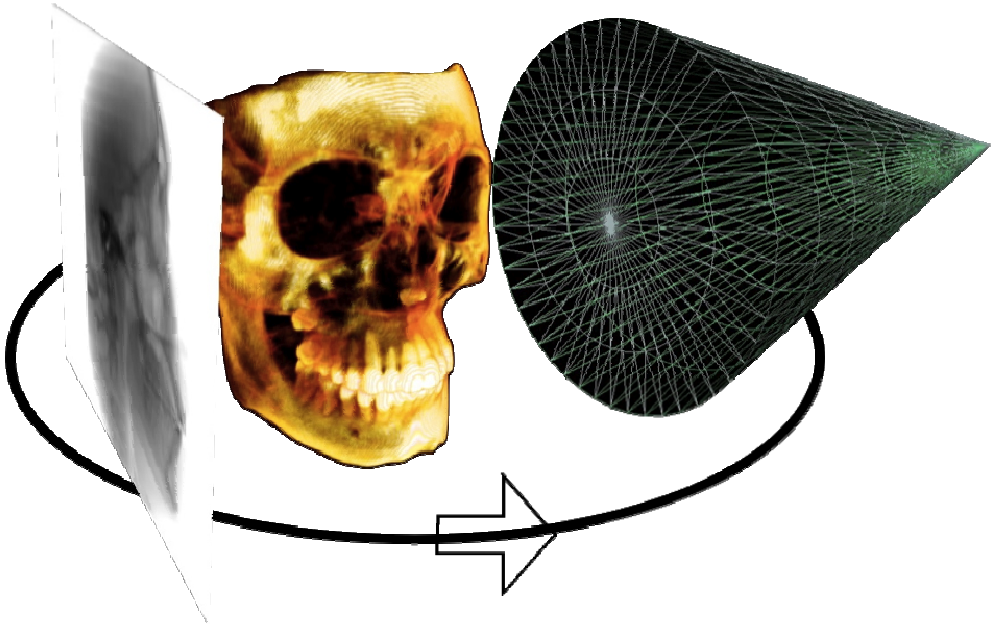

Figure 1.1a Principle of action of Cone Beam Computed Tomography technology step1:Acquisition of the basis projections.

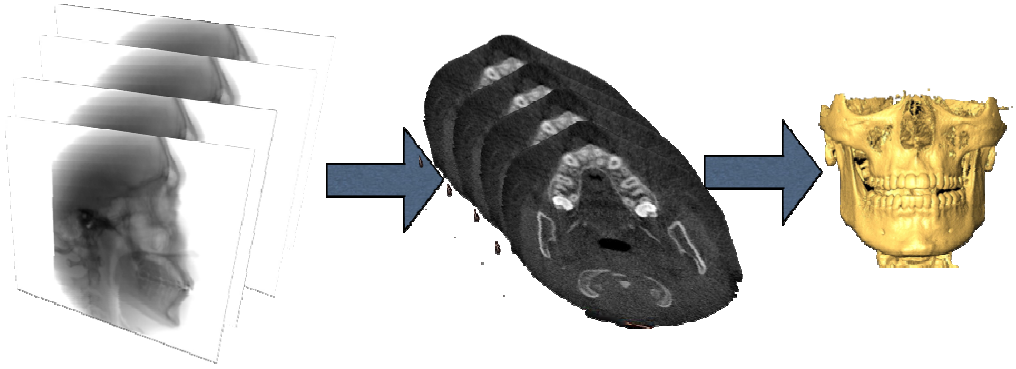

Figure 1.1b Principle of action of Cone Beam Computed Tomography technology step 2: Reconstruction of the basis projections to a 3D volume.

The detectors that capture x-rays in CBCT are divided into two groups based on their design technology. The older technology dubbed Image Intensifier Tube/ Charged Coupled Device or (IIT/CCD) utilizes a phosphor screen to convert x-rays into visible light. The light is then projected onto a photo cathode that converts the light into electrons. The electrons are then accelerated in a vacuum tube and directed a second time to a small phosphor screen; at that stage, the electrons are converted again into light photons, which are detected by the CCD chip. This arrangement allows coupling of a large detector area with a small camera lens and allows for efficient detection of light. However, several elements in the IIT/CCD arrangement introduce artifacts and increased noise levels in the resulting clinical images. [18] Therefore, a second technology called Flat Panel Detector or (FPD) was proposed and became widely adopted in the more recent generations of commercial CBCT systems. In FPD technology detection of x-rays occurs in sensor elements, which are produced in a thin film of hydrogenated amorphous silicon. The sensor elements in the scintillator layer are composed of terbium-activated gadolinium oxysulphide or thallium-doped cesium iodide. Those sensor elements detect x-rays and convert them into light photons. The photons are detected by an arranged array of photodiodes and then are converted into an electrical signal, which is in turn is read out by switching devices. This arrangement is less complicated than IIT/CCD and offers greater dynamic range. The detector also has less distortion and smaller detector pitch in comparison with IIT/CCD. [19]

In addition to the detector design, each CBCT acquisition is governed by a host of scanning and reconstruction parameters, which are equally important. Those parameters directly influence image quality and radiation dose delivered to the patient. CBCT patient scanning parameters include x-ray beam energy as defined by tube voltage in kilo Volt peak (kVp) and tube current in milli-Ampere (mA), scan field of views (FoV) selection, patient positioning in the machine, patient movement during the scan and mouth opening. Data reconstruction parameters include reconstruction algorithm, number of basis projections used for reconstruction and voxel size. Variability of those scanning and reconstruction parameters in isolation and in combination with each

other largely influences image quality in CBCT and in turn its efficacy for certain clinical applications in dentistry.

Image artifacts including scatter, beam hardening, metal streaks, low contrast to noise ratio (increased image noise level), increased inhomogeneity, image density variability and poor soft-tissue visibility are all well-known and largely well-understood artifacts associated with CBCT scanning technology. Those artifacts are mainly caused by limitations in CBCT hardware and software and the variability of the scanning and reconstruction parameters mentioned above. Moreover, commercial CBCT systems come with different technical specifications from different manufacturers. This large variation among the different CBCT systems did not improve with the introduction of the next generation CBCT scanners. Standardized comparisons among the different scanners are difficult and results of scientific studies are usually confines to the type of CBCT system employed and the specific model used.

Applications of CBCT in dentistry

A phenomenal and unprecedented interest in CBCT from all fields of dentistry is currently underway. CBCT has revolutionized maxillofacial imaging, facilitating the transition of dental diagnosis from 2D to 3D images and expanding the role of imaging from diagnosis to image guidance of operative and surgical procedures. Not only that we are able now to provide more accurate diagnosis with this imaging modality, but also we are able based on the new radiographic data to guide and assess various surgical and clinical interventions. What follows is a brief review of the most frequent applications of CBCT as cited in the literature.

Tooth impaction:

Surgical removal of impacted teeth demands precise knowledge of the tooth location in the jaw and its relation to other teeth and surrounding anatomical structures. For instance, in the mandible the relationship of the roots of impacted third molars to the mandibular dental canal must be accurately assessed since the canal is frequently very closely associated with an impacted molar and post-operative complications due to nerve impingement are reported. [20, 21] It is necessary to assess whether a physical contact between the root and the border of the canal is present or not. In the maxilla, localization of impacted canines relative to the lateral and central incisors is central to their management. Information regarding the palatal orientation of an impacted canine and its proximity to the root of the lateral incisor is vital to allow for an effective and timely surgical intervention[22, 23]

Conventional panoramic radiographs are routinely obtained to evaluate tooth impaction preoperatively. However, when compared with CT, the 2D nature of the image and the superimposition of adjacent anatomical structures impede precise assessment of the tooth relative to adjacent anatomical structures. [24-26]CBCT orthographic tomographic slices and panoramic reconstructions are superior to conventional panoramic radiographs in determining the location, orientation of an impacted tooth and its relationship to adjacent vital structures in the maxilla and the mandible(Figure2).[27-34]

Figure2: Visualization of the intimate relation of the mandibular canal and an impacted wisdom tooth, imaged with the Scanora 3D (Soredex, Tuusula, Finland)

Pathological conditions:

CBCT diagnostic applications in the maxillofacial region include evaluating the presence of osseous defects in the jaws, cysts, lesions, calcifications, teeth and bone traumas and fractures. CBCT is also playing an increasingly important role in the detection of 'incidental' pathology in patients referred to dental treatment. Since most CBCT systems currently available acquire volumes that extend beyond the dentition and the surrounding alveolus, unsuspected lesions in the para-nasal sinuses, parotic region, masticatory space, floor of the mouth and the hyoid region are frequently detected and reported. [35-41] Evidently the three-dimensional nature of CBCT allows determination of the exact extension of the lesion in the affected region (figure3).

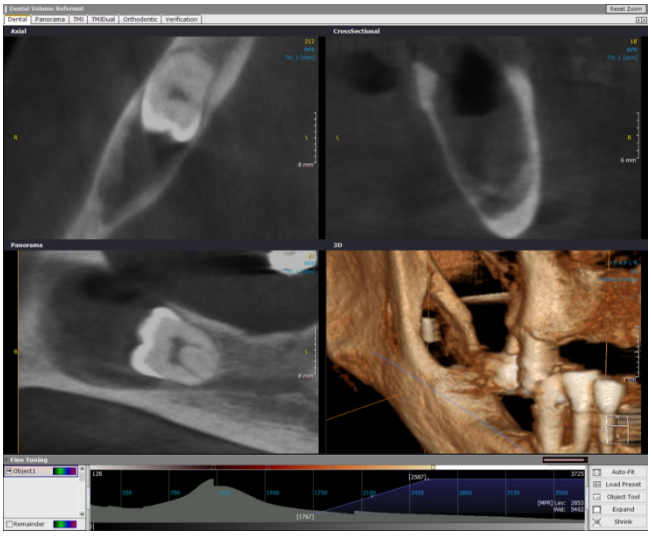

Figure3: Folicular dentigerous cyst in the right mandible associated with an impacted tooth, imaged with the Scanora 3D (Soredex, Tuusula, Finland) and presented in the On-Demand 3D software (CyberMed, Seoul, South Korea).Courtesy R. Jacobs and P. Couto, Oral Imaging Centre, KU Leuven, Leuven, Belgium.

Orthognathic surgery:

Several applications of CBCT in orthognathic surgery treatment simulation, guidance and outcome assessment have been developed. CBCT 3D surface reconstructions of the jawbones are used for pre-operative surgical planning and simulation in patients with traumas and skeletal malformations (Figure4). [42-44] Coupled with dedicated software tools, simulations of virtual re-positioning of the jaws, osteotomies, distraction osteogenesis and other interventions can now be successfully implemented. Pre and post-operative 3D CBCT skull models can also be registered (i.e. superimposed on each other) to assess the amount and position of alterations in the mandibular rami and condylar head following orthognathic surgery of the maxilla and the mandible. [45, 46]

3D reconstructions of the jawbones from CBCT are of sufficient quality for clinical work. However, 3D models of the dentition still suffer from deformations due to streak artifacts caused by metal fillings, crowns and bridges, orthodontic brackets and other metallic dental appliances. [47] Therefore, virtual 3D models of the dentition are obtained by scanning the dental cast using a high-resolution surface laser scanner. Custom made inter-occlusal wafers can also be scanned separately and then combined with CBCT 3D reconstructions of the jaws to create composite skull models.[48-51]These so-called 'double scanning' techniques have been successfully applied to patients with jaw asymmetry and severe malocclusion cases. [52-54]

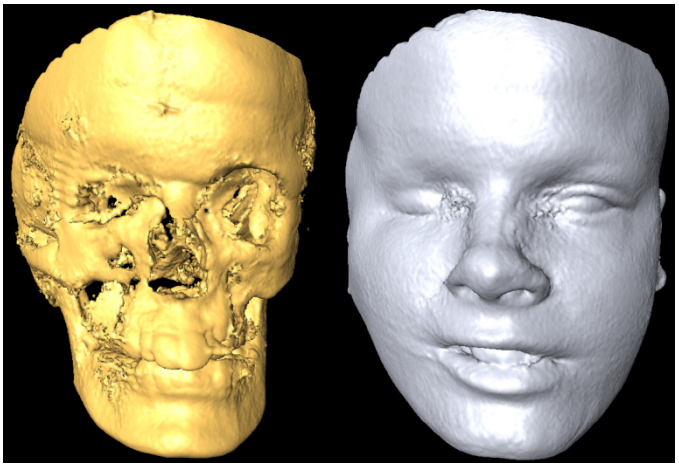

Figure4: A patient with deviation in the face in the right side, imaged with the NewTom 3G (QR SLR, Verona, Italy) presented with Amira software (Visage Imaging, Carlsbad, California).

TMJ imaging:

The temporomandibular joint (TMJ) is a complex entity with hard and soft tissue components. TMJ disorders (TMDs) are common but widely variable. MRI has sustained its position as the gold standard imaging modality for diagnosing TMDs since it provides excellent visibility of the disk and the associated joint muscles. Nonetheless, most TMJ examinations start with a panoramic radiograph to visualize any gross changes in the condylar head and temporal components. Panoramic radiography, however, has a low diagnostic accuracy in detecting TMDs that a negative indicator on a panoramic radiograph does not exclude the presence of osseous defect. [55-57] CBCT para-sagittal and coronal slices show clear images of the condylar head and the glenoid fossa. Additionally, provides images from different orientations and different reconstruction views thus providing axial, coronal and para-sagittal imaging of the condylar head. CBCT is more accurate than panoramic radiography and conventional tomography for detecting TMDs (Figure5). [58-62]CBCT exam was also recommended before image-guided puncture operation of the superior compartment of the joint space. [63]

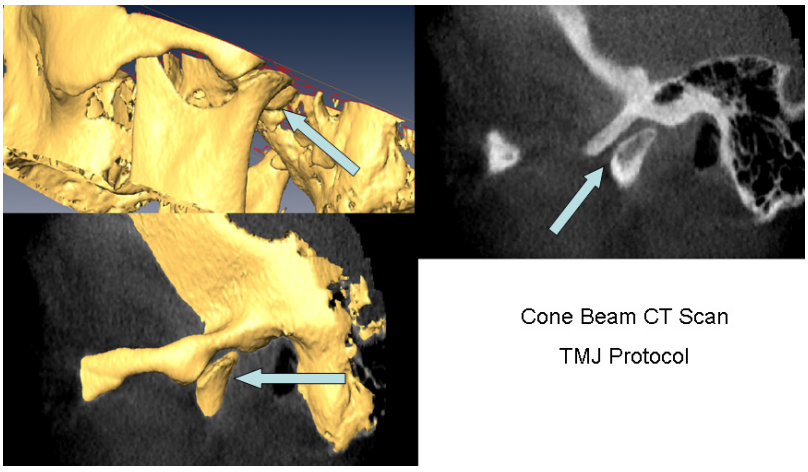

Figure5: Patient with flattening in the temporomandibular joint, imaged with the NewTom 3G (QR SLR, Verona, Italy) presented with Amira software (Visage Imaging, Carlsbad, California)

Cleft lip and palate:

In cleft lip and palate patients, information regarding the number and orientation of teeth, dental and skeletal age, the amount and quality of available bone and bone graft in the cleft region are considered vital for the clinical management of such cases. Panoramic radiographs are often used to investigate the incidence and number of missing teeth and to determine dental and skeletal age in cleft lip and palate patients. [64,65] However, the amount and quality of available bone cannot be accurately assessed on panoramic radiograph. Therefore, medical CT is typically used to quantify the amount of bone present. Yet, the young age of cleft patients makes the routine use of medical CT problematic due to the relatively high radiation dose involved.

CBCT is rapidly replacing medical CT for this task since it provides excellent 3D visualization of the palate at the pre-maxilla region at a lower patient dose (Figure6). [66]CBCT is used to determine dental age and when a large scan field of view FoV selection is available, 3D reconstructions of the cervical vertebra can be made and employed to determine skeletal age. [67] Additionally, CBCT has been used to show any deformities in the piriform margin in the nasal platform and the antero-posterior depression of the nasal alar base. [68] Three-dimensional CBCT reconstructions of the skin surface of the face and nose for cleft lip assessment are also possible.

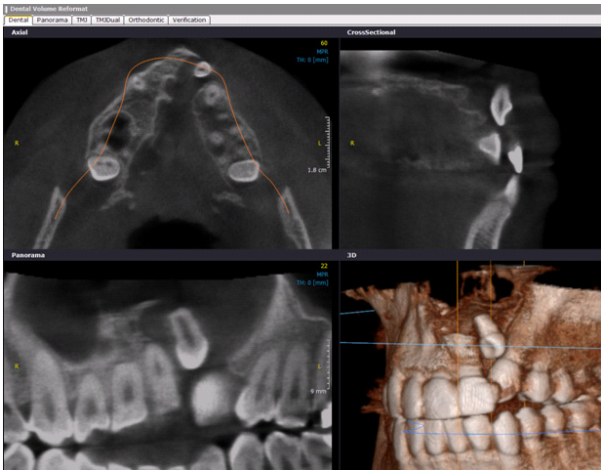

Figure6: Patient with unilateral cleft palate with tooth impaction, imaged with the Scanora 3D (Soredex, Tuusula, Finland) and presented in the On-Demand 3D software

Dental implants and bone grafts:

Imaging plays a crucial role in the preoperative assessment of oral implant placement. After a thorough clinical examination, imaging should be used to evaluate bone quality and quantity, its morphology and relation to vital anatomic structures such as the mandibular canal. Panoramic and intra-oral radiographs are widely used in implant evaluation; yet the inherent 2D nature of those techniques hamper a detailed pre-operative planning that would allow to integrate all necessary parameters with respect to the anatomical restrictions, the required implant position and axis in relation to anatomy, neurovascularisation, biomechanics and esthetics. [69,70] Moreover, the inherent distortion of panoramic images makes those images less suited for reliable implant planning. The introduction of CBCT, offering imaging in 3 dimensions at relatively low dose and costs, has increased the applicability and strengthened the justification of cross-sectional preoperative imaging. In addition, the convenience and easy access to CBCT has drastically expanded its use. [71] The benefits for 3D imaging in a virtual planning environment are an improved integration of all information on esthetics, biomechanics and anatomy (Figure7). [69,70] In fact, the rapid increase in the number of CBCT units installation is deemed to go hand in hand with the steep increase in implant therapy. The latter holds especially true for computer aided surgery applications where implant placement is first simulated then transferred to the operation site, using either navigation or surgical templates or so-called drill-guides. [72,73] This technique surely has advantages for more complicated surgery, such as planning grafting procedure. [74,75] Indeed, the graft can then be virtually modelled that the receptor bed may be well prepared to precisely fit to the *a priori* optimally shaped graft (Figure8). From the statements above, it is obvious that CBCT is striving to become

the method of choice for presurgical planning procedures.

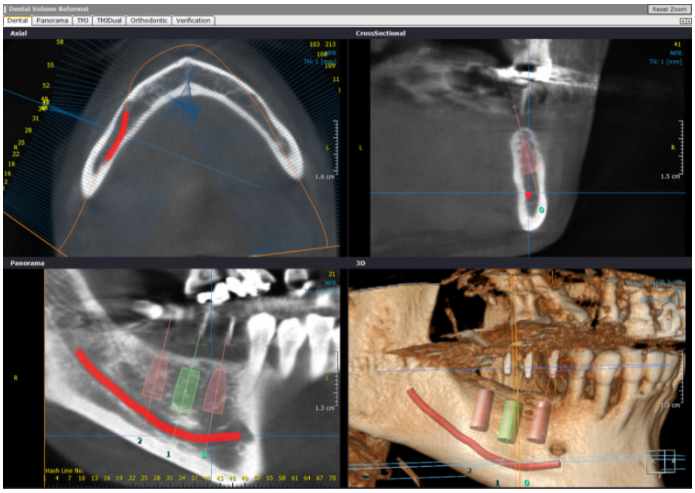

Figure7: Example of preparing a radiographic template with gutta percha cylinders to integrate the information on preferred implant axis and implant position, biomechanics and esthetics with consideration to anatomic restrictions. The mandibular nerve has been visualised (Ondemand 3D screenshot of Scanora 3D dataset) to allow interactive planning of implant placement without hitting this canal. Courtesy of Filip Van de Velde, periodontologist, Antwerp Belgium

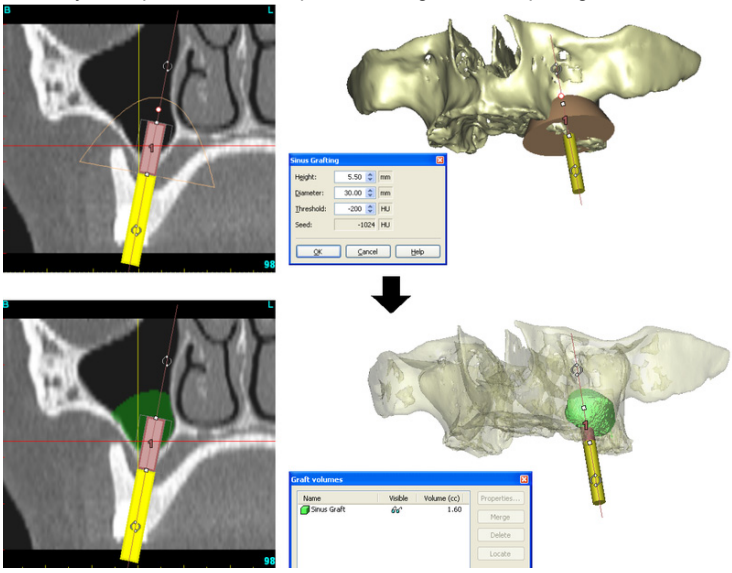

Figure8: Bone graft simulation in the right maxillary sinus prior to implant placement. Courtesy of Materialise, Haasrode, Belgium

Endodontics:

CBCT role in endodontics is increasingly expanding. Mounting scientific evidence reveals superior accuracy of CBCT to conventional periapical and panoramic radiographs in detection of apical periodontitis. Indeed, the efficacy of CBCT in detecting periapical lesions has been verified both in ex-vivo as well as in-vivo samples (Figure9). [76-78] CBCT imaging was also recommended before endodontic surgery since the three-dimensional nature of the images reveals the relationship of the root apex to important anatomical structures such as the inferior dental canal or the maxillary sinus. [79-81] However, the applicability of CBCT in detecting horizontal and vertical root fractures is yet not very much evidenced. Vertical root fractures are difficult to visualize on conventional periapical radiographs due to the super-imposition artiracts inherent in 2D imaging. Thin fractures are masked by the thick cortical bone and other structures in the projection plane. On the other hand, scarce evidence exists on the value of CBCT in detecting horizontal and vertical root fractures in endodontically treated teeth and more research is needed in this area (Figure10). Also, another potentially important role for CBCT in endodontics is to follow-up patients to assess treatment outcomes. It has been suggested that CBCT can provide a more objective and accurate measure of treatment outcomes than 2D periapical and panoramic radiographs. [81] However, little evidence exists on the value of CBCT in assessing endodontic treatment outcome.

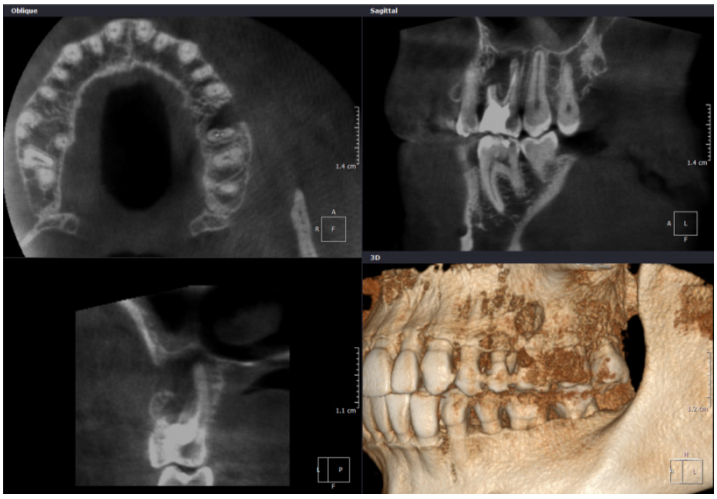

Figure9: Large periapical lesion associated with the root of the 26 endodontically treated tooth. Imaged with the Scanora 3D (Soredex, Tuusula, Finland) and presented in the On-Demand 3D software (CyberMed, Seoul, South Korea).

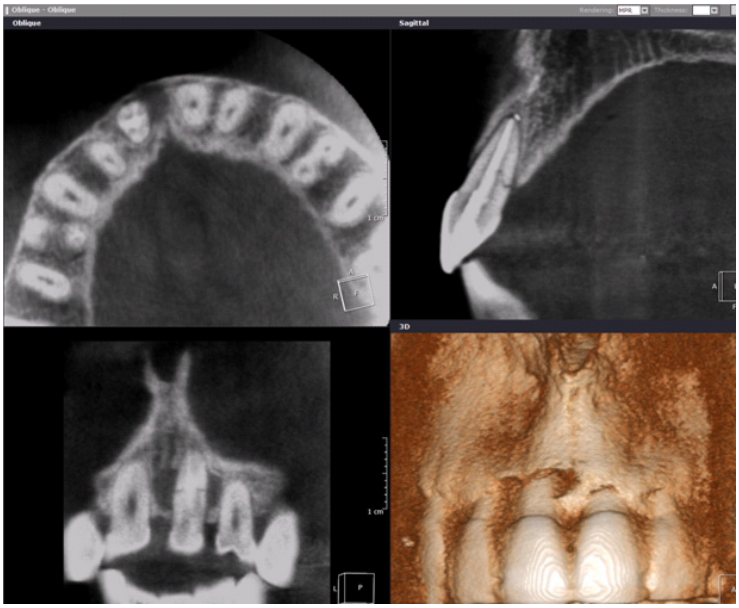

Figure10: Horizontal root fracture on the 21 endodontically treated tooth. Imaged with the Scanora 3D (Soredex, Tuusula, Finland) and presented in the On-Demand 3D software (CyberMed, Seoul, South Korea).Courtesy R. Jacobs and P. Couto, Oral Imaging Centre, KU Leuven, Leuven, Belgium.

Orthodontics:

It is difficult to categorize the scope of applications of CBCT in orthodontics since it is difficult to narrow down the scope of orthodontic practice to specific clinical interventions. However, all the applications previously discussed in characterization of tooth impaction, assessment of cleft lip and palate and TMJ imaging could equally fall under the category of orthodontic applications. What is more important and more relevant, however, is the potential application of CBCT in mainstream orthodontic practice in routine diagnosis and treatment planning. The orthodontic record is comprised of panoramic radiograph and lateral cephalogram plus light photographs of the patient in profile and frontal positions and the upper and lower dental casts mounted on an articulator in occlusion. With several practical limits related to time, cost and labour involved in producing, utilizing and maintaining this

‘analogue’ record, a conscious and steady effort was put forward to find a digital alternative. CBCT provides three-dimensional reconstructions of hard tissue including bone and teeth and soft-tissue reconstructions of air-bound surfaces including the skin and airway spaces. Also, two-dimensional reconstructions of panoramic and cephalometric radiographs are possible plus it can be combined with 2D or 3D light photographs of the patient face and scalp to create an accurate depiction of the patient’s head. All this has nourished the speculation that CBCT can and in fact will *replace* all conventional orthodontics records as the modality of choice to create a digital orthodontic record. However, before those 3D models can be used in the clinic, their accuracy needs to be assessed.

Aims of this thesis

The aims of this thesis are to assess the value and accuracy of CBCT for selected applications in the fields of orthodontics and endodontics. Research in those two fields was selected to illustrate the versatility and the wide scope of CBCT applications in dentistry. In orthodontics, the aim is to assess the accuracy and adequacy of 3D surface models of the dental arches created from CBCT systems for orthodontic diagnosis and treatment planning. In endodontics, the aims are to assess the accuracy of CBCT in detecting vertical root fractures in endodontically treated teeth and to assess the applicability of CBCT in assessing treatment outcomes of endodontic therapy.

The specific research questions dealt with in this work are:

Orthodontics:

1. What is the accuracy of linear measurements made on 3D CBCT models with respect to varying patient scanning position?

2. What is the influence of field size selection and data reconstruction parameters on the quality of 3D CBCT models of the dental arches for orthodontic treatment planning and simulation?

3. What is the accuracy of the 3D CBCT models of the occlusal surfaces of teeth?

Endodontics:

1. What is the value of CBCT in enhancing the diagnosis of vertical root fractures (VRF) in endodontically treated teeth?

2. What are the differences among the different CBCT scanners in their efficiency for detecting VRF and what is the influence of the reconstruction orientation on fracture line visibility?

3. What is the value of CBCT in detecting periapical lesions and assessing treatment outcomes of one visit and two visits endodontic therapy?

References:

1) Chen Y, Duan P, Meng Y, Chen Y. Three-dimensional spiral computed tomographic imaging: a new approach to the diagnosis and treatment planning of impacted teeth. Am J OrthodDentofacialOrthop. 2006 Jul ;130(1):112-6.

2) Terajima M, Yanagita N, Ozeki K, Hoshino Y, Mori N, Goto TK, et al. Three-dimensional analysis system for orthognathic surgery patients with jaw deformities. Am J OrthodDentofacialOrthop. 2008 Jul ;134(1):100-11.

3) Kwon T, Park H, Ryoo H, Lee S. A comparison of craniofacial morphology in patients with and without facial asymmetry--a three-dimensional analysis with computed tomography. Int J Oral Maxillofac Surg. 2006 Jan ;35(1):43-8.

4) Maeda M, Katsumata A, Ariji Y, Muramatsu A, Yoshida K, Goto S, et al. 3D-CT evaluation of facial asymmetry in patients with maxillofacial deformities. Oral Surg Oral Med Oral Pathol Oral RadiolEndod. 2006 Sep ;102(3):382-90.

5) Quereshy FA, Savell TA, Palomo JM. Applications of cone beam computed tomography in the practice of oral and maxillofacial surgery. J Oral Maxillofac Surg. 2008 Apr ;66(4):791-6.

6) Kawamata A, Ariji Y, Langlais RP. Three-dimensional computed tomography imaging in dentistry. Dent Clin North Am. 2000 Apr ;44(2):395-410.

7) Danforth RA, Dus I, Mah J. 3-D volume imaging for dentistry: a new dimension. J Calif Dent Assoc. 2003 Nov ;31(11):817-23.

8) Yamamoto K, Ueno K, Seo K, Shinohara D. Development of dento-maxillofacial cone beam X-ray computed tomography system. OrthodCraniofac Res. 2003 ;6Suppl 1160-2.

9) Danforth RA. Cone beam volume tomography: a new digital imaging option for dentistry. J Calif Dent Assoc. 2003 Nov ;31(11):814-5.

10) Ganz SD. Conventional CT and cone beam CT for improved dental diagnostics and implant planning. Dent Implantol Update. 2005 Dec ;16(12):89-95.

11) Loubele M, Guerrero ME, Jacobs R, Suetens P, van Steenberghe D. A comparison of jaw dimensional and quality assessments of bone characteristics with cone-beam CT, spiral tomography, and multi-slice spiral CT. Int J Oral Maxillofac Implants. 22(3):446-54.

12) Loubele M, Maes F, Jacobs R, van Steenberghe D, White SC, Suetens P. Comparative study of image quality for MSCT and CBCT scanners for dentomaxillofacial radiology applications. Radiat Prot Dosimetry. 2008 ;129(1-3):222-6.

13) Loubele M, Jacobs R, Maes F, Denis K, White S, Coudyzer W, et al. Image quality vs radiation dose of four cone beam computed tomography scanners. DentomaxillofacRadiol. 2008 Sep ;37(6):309-19.

14) Katsumata A, Hirukawa A, Okumura S, Naitoh M, Fujishita M, Ariji E, et al. Relationship between density variability and imaging volume size in cone-beam computerized tomographic scanning of the maxillofacial region: an in vitro study [Internet]. Oral Surg Oral Med Oral Pathol Oral RadiolEndod. 2008 Aug 18.

15) Robb RA. Dynamic spatial reconstruction: an x-ray video fluoroscopic CT scanner for dynamic volume imaging of moving organs. IEEE Trans Med Imag 1982;M1:22–3.

16) Cho PS, Johnson RH, Griffin TW. Cone-beam CT for radiotherapy applications. Phys Med Biol 1995;40:1863–83.

17) Ning R, Chen B. Cone beam volume CT mammographic imaging: feasibility study. In: Antonuk LE, Yaffe MJ, editors. Medical imaging

2001: physics of medical imaging proceedings of SPIE. vol. 4320. San Diego (CA): CA SPIE; 2001. p. 655–64.

18) Katsumata A, Hirukawa A, Okumura S, Naitoh M, Fujishita M, Ariji E, Langlais RP (2007) Effects of image artifacts on gray value density in limited-volume cone-beam computerized tomography. Oral Surg Oral Med Oral Pathol Oral RadiolEndod 104 (6):829–836

19) Suetens P 2002 Fundamentals of Medical Imaging Cambridge: Cambridge University Press (2002), ISBN 0-521-80362-4

20) Bouloux GF, Steed MB, Perciaccante VJ. Complications of third molar surgery. Oral MaxillofacSurgClin North Am. 2007 Feb ;19(1):117-28, vii.

21) Rood JP. Permanent damage to inferior alveolar and lingual nerves during the removal of impacted mandibular third molars. Comparison of two methods of bone removal. Br Dent J. 1992 Feb 8;172(3):108-10.

22) Ericson S, Kurol PJ. Resorption of incisors after ectopic eruption of maxillary canines: a CT study. Angle Orthod. 2000 Dec ;70(6):415-23.

23) Kojima R, Taguchi Y, Kobayashi H, Noda T. External root resorption of the maxillary permanent incisors caused by ectopically erupting canines. J ClinPediatr Dent. 2002 ;26(2):193-7.

24) de Melo Albert DG, Gomes ACA, do Egito Vasconcelos BC, de Oliveira e Silva ED, Holanda GZ. Comparison of orthopantomographs and conventional tomography images for assessing the relationship between impacted lower third molars and the mandibular canal. J Oral Maxillofac Surg. 2006 Jul ;64(7):1030-7.

25) Nakagawa Y, Ishii H, Nomura Y, Watanabe NY, Hoshiba D, Kobayashi K, et al. Third molar position: reliability of panoramic radiography. J Oral Maxillofac Surg. 2007 Jul ;65(7):1303-8.

26) Chen Y, Duan P, Meng Y, Chen Y. Three-dimensional spiral computed tomographic imaging: a new approach to the diagnosis and treatment planning of impacted teeth. Am J OrthodDentofacialOrthop. 2006 Jul ;130(1):112-6.

27) Tantanapornkul W, Okouchi K, Fujiwara Y, Yamashiro M, Maruoka Y, Ohbayashi N, et al. A comparative study of cone-beam computed tomography and conventional panoramic radiography in assessing the topographic relationship between the mandibular canal and impacted third molars. Oral Surg Oral Med Oral Pathol Oral RadiolEndod. 2007 Feb ;103(2):253-9.

28) Angelopoulos C, Thomas S, Hechler S, Parissis N, Hlavacek M. Comparison between digital panoramic radiography and cone-beam computed tomography for the identification of the mandibular canal as

part of presurgical dental implant assessment. J Oral Maxillofac Surg. 2008 Oct ;66(10):2130-5.

29) Neugebauer J, Shirani R, Mischkowski RA, Ritter L, Scheer M, Keeve E, et al. Comparison of cone-beam volumetric imaging and combined plain radiographs for localization of the mandibular canal before removal of impacted lower third molars. Oral Surg Oral Med Oral Pathol Oral RadiolEndod. 2008 May ;105(5):633-42; discussion 643.

30) Sawamura T, Minowa K, Nakamura M. Impacted teeth in the maxilla: usefulness of 3D Dental-CT for preoperative evaluation. Eur J Radiol. 2003 Sep ;47(3):221-6.

31) Liu D, Zhang W, Zhang Z, Wu Y, Ma X. Localization of impacted maxillary canines and observation of adjacent incisor resorption with cone-beam computed tomography. Oral Surg Oral Med Oral Pathol Oral RadiolEndod. 2008 Jan ;105(1):91-8.

32) Walker L, Enciso R, Mah J. Three-dimensional localization of maxillary canines with cone-beam computed tomography. Am J OrthodDentofacialOrthop. 2005 Oct ;128(4):418-23.

33) Ohman A, Kivijärvi K, Blombäck U, Flygare L. Pre-operative radiographic evaluation of lower third molars with computed tomography. DentomaxillofacRadiol. 2006 Jan ;35(1):30-5.

34) Flygare L, Ohman A. Preoperative imaging procedures for lower wisdom teeth removal. Clin Oral Investig. 2008 Dec ;12(4):291-302.

35) Ogura I, Kurabayashi T, Amagasa T, Okada N, Sasaki T. Mandibular bone invasion by gingival carcinoma on dental CT images as an indicator of cervical lymph node metastasis. DentomaxillofacRadiol. 2002 Nov ;31(6):339-43.

36) Closmann JJ, Schmidt BL. The use of cone beam computed tomography as an aid in evaluating and treatment planning for mandibular cancer. J Oral Maxillofac Surg. 2007 Apr ;65(4):766-71.

37) Siraci E, Cem Gungor H, Taner B, Cehreli ZC. Buccal and palatal talon cusps with pulp extensions on a supernumerary primary tooth. DentomaxillofacRadiol. 2006 Nov ;35(6):469-72.

38) Araki M, Kameoka S, Mastumoto N, Komiyama K. Usefulness of cone beam computed tomography for odontogenicmyxoma. DentomaxillofacRadiol. 2007 Oct ;36(7):423-7.

39) Nair MK, Pettigrew JC, Mancuso AA. Intracranial aneurysm as an incidental finding. DentomaxillofacRadiol. 2007 Feb ;36(2):107-12.

40) Ogura I, Kurabayashi T, Amagasa T, Okada N, Sasaki T. Mandibular bone invasion by gingival carcinoma on dental CT images as an

indicator of cervical lymph node metastasis. DentomaxillofacRadiol. 2002 Nov ;31(6):339-43.

41) Closmann JJ, Schmidt BL. The use of cone beam computed tomography as an aid in evaluating and treatment planning for mandibular cancer. J Oral Maxillofac Surg. 2007 Apr ;65(4):766-71.

42) Cevidanes LH, Styner MA, Proffit WR. Image analysis and superimposition of 3-dimensional cone-beam computed tomography models. American Journal of Orthodontics and DentofacialOrthopedics. 2006 May ;129(5):611-618.

43) Swennen GRJ, Schutyser F. Three-dimensional cephalometry: spiral multi-slice vs cone-beam computed tomography. Am J OrthodDentofacialOrthop. 2006 Sep ;130(3):410-6.

44) Chan HJ, Woods M, Stella D. Three-dimensional computed craniofacial tomography (3D-CT): potential uses and limitations. AustOrthod J. 2007 May ;23(1):55-64.

45) Cevidanes LHS, Bailey LJ, Tucker GR, Styner MA, Mol A, Phillips CL, et al. Superimposition of 3D cone-beam CT models of orthognathic surgery patients. DentomaxillofacRadiol. 2005 Nov ;34(6):369-75.

46) Cevidanes LHS, Bailey LJ, Tucker SF, Styner MA, Mol A, Phillips CL, et al. Three-dimensional cone-beam computed tomography for assessment of mandibular changes after orthognathic surgery. Am J OrthodDentofacialOrthop. 2007 Jan ;131(1):44-50.

47) Macchi A, Carrafiello G, Cacciafesta V, Norcini A. Three-dimensional digital modeling and setup. Am J OrthodDentofacialOrthop. 2006 May ;129(5):605-10.

48) Metzger MC, Hohlweg-Majert B, Schwarz U, Teschner M, Hammer B, Schmelzeisen R. Manufacturing splints for orthognathic surgery using a three-dimensional printer. Oral Surg Oral Med Oral Pathol Oral RadiolEndod. 2008 Feb ;105(2):e1-7.

49) Nkenke E, Zachow S, Benz M, Maier T, Veit K, Kramer M, et al. Fusion of computed tomography data and optical 3D images of the dentition for streak artefact correction in the simulation of orthognathic surgery. DentomaxillofacRadiol. 2004 Jul ;33(4):226-32.

50) Nkenke E, Vairaktaris E, Neukam FW, Schlegel A, Stamminger M. State of the art of fusion of computed tomography data and optical 3D images. Int J Comput Dent. 2007 Jan ;10(1):11-24.

51) Gateno J, Xia J, Teichgraeber JF, Rosen A. A new technique for the creation of a computerized composite skull model. J Oral Maxillofac Surg. 2003 Feb ;61(2):222-7.

52) Uechi J, Okayama M, Shibata T, Muguruma T, Hayashi K, Endo K, et al. A novel method for the 3-dimensional simulation of orthognathic surgery by using a multimodal image-fusion technique. Am J OrthodDentofacialOrthop. 2006 Dec ;130(6):786-98.

53) Swennen GRJ, Barth E, Eulzer C, Schutyser F. The use of a new 3D splint and double CT scan procedure to obtain an accurate anatomic virtual augmented model of the skull. Int J Oral Maxillofac Surg. 2007 Feb ;36(2):146-52.

54) Swennen GRJ, Mommaerts MY, Abeloos J, De Clercq C, Lamoral P, Neyt N, et al. The use of a wax bite wafer and a double computed tomography scan procedure to obtain a three-dimensional augmented virtual skull model. J Craniofac Surg. 2007 May ;18(3):533-9.

55) Dahlström L, Lindvall AM. Assessment of temporomandibular joint disease by panoramic radiography: reliability and validity in relation to tomography. DentomaxillofacRadiol. 1996 Sep ;25(4):197-201.

56) Schmitter M, Gabbert O, Ohlmann B, Hassel A, Wolff D, Rammelsberg P, et al. Assessment of the reliability and validity of panoramic imaging for assessment of mandibular condyle morphology using both MRI and clinical examination as the gold standard. Oral Surg Oral Med Oral Pathol Oral RadiolEndod. 2006 Aug ;102(2):220-4.

57) Crow HC, Parks E, Campbell JH, Stucki DS, Daggy J. The utility of panoramic radiography in temporomandibular joint assessment. DentomaxillofacRadiol. 2005 Mar ;34(2):91-5.

58) Tsiklakis K, Syriopoulos K, Stamatakis HC. Radiographic examination of the temporomandibular joint using cone beam computed tomography. DentomaxillofacRadiol. 2004 May ;33(3):196-201.

59) Honda K, Arai Y, Kashima M, Takano Y, Sawada K, Ejima K, et al. Evaluation of the usefulness of the limited cone-beam CT (3DX) in the assessment of the thickness of the roof of the glenoidfossa of the temporomandibular joint. DentomaxillofacRadiol. 2004 Nov ;33(6):391-5.

60) Hintze H, Wiese M, Wenzel A. Cone beam CT and conventional tomography for the detection of morphological temporomandibular joint changes. DentomaxillofacRadiol. 2007 May ;36(4):192-7.

61) Schlueter B, Kim KB, Oliver D, Sortiropoulos G. Cone beam computed tomography 3D reconstruction of the mandibular condyle. Angle Orthod. 2008 Sep ;78(5):880-8.

62) Honey OB, Scarfe WC, Hilgers MJ, Klueber K, Silveira AM, Haskell BS, et al. Accuracy of cone-beam computed tomography imaging of the temporomandibular joint: comparisons with panoramic radiology and

linear tomography. Am J OrthodDentofacialOrthop. 2007 Oct ;132(4):429-38.

63) Honda K, Bjørnland T. Image-guided puncture technique for the superior temporomandibular joint space: value of cone beam computed tomography (CBCT). Oral Surg Oral Med Oral Pathol Oral RadiolEndod. 2006 Sep ;102(3):281-6.

64) Shapira Y, Lubit E, Kuftinec MM. Congenitally missing second premolars in cleft lip and cleft palate children. Am J OrthodDentofacialOrthop. 1999 Apr ;115(4):396-400.

65) Baek S, Kim N. Congenital missing permanent teeth in Korean unilateral cleft lip and alveolus and unilateral cleft lip and palate patients. Angle Orthod. 2007 Jan ;77(1):88-93.

66) Wörtche R, Hassfeld S, Lux CJ, Müssig E, Hensley FW, Krempien R, et al. Clinical application of cone beam digital volume tomography in children with cleft lip and palate. DentomaxillofacRadiol. 2006 Mar ;35(2):88-94.

67) Shi H, Scarfe WC, Farman AG. Three-dimensional reconstruction of individual cervical vertebrae from cone-beam computed-tomography images. Am J OrthodDentofacialOrthop. 2007 Mar ;131(3):426-32.

68) Miyamoto J, Nagasao T, Nakajima T, Ogata H. Evaluation of cleft lip bony depression of piriform margin and nasal deformity with cone beam computed tomography: "retruded-like" appearance and anteroposterior position of the alar base. PlastReconstr Surg. 2007 Nov ;120(6):1612-20.

69) Jacobs R, Adriansens A, Verstreken K, Suetens P, van Steenberghe D. Predictability of a three-dimensional planning system for oral implant surgery. Dentomaxillofac Radiol. 1999 Mar ;28(2):105-11.

70) Jacobs R, Adriansens A, Naert I, Quirynen M, Hermans R, Van Steenberghe D. Predictability of reformatted computed tomography for pre-operative planning of endosseous implants. Dentomaxillofac Radiol. 1999 Jan ;28(1):37-41.

71) Guerrero ME, Jacobs R, Loubele M, Schutyser F, Suetens P, van Steenberghe D. State-of-the-art on cone beam CT imaging for preoperative planning of implant placement. Clin Oral Investig. 2006 Mar ;10(1):1-7.

72) van Steenberghe D, Malevez C, Van Cleynenbreugel J, Bou Serhal C, Dhoore E, Schutyser F, et al. Accuracy of drilling guides for transfer from three-dimensional CT-based planning to placement of zygoma implants in human cadavers. Clin Oral Implants Res. 2003 Feb ;14(1):131-6.

73) Van Assche N, van Steenberghe D, Guerrero ME, Hirsch E, Schutyser F, Quirynen M, et al. Accuracy of implant placement based on pre-surgical planning of three-dimensional cone-beam images: a pilot study. J Clin Periodontol. 2007 Sep ;34(9):816-21.

74) Hamada Y, Kondoh T, Noguchi K, Iino M, Isono H, Ishii H, et al. Application of limited cone beam computed tomography to clinical assessment of alveolar bone grafting: a preliminary report. Cleft Palate Craniofac J. 2005 Mar ;42(2):128-37.

75) Draenert FG, Gebhart F, Neugebauer C, Coppenrath E, Mueller-Lisse U. Imaging of bone transplants in the maxillofacial area by NewTom 9000 cone-beam computed tomography: a quality assessment. Oral Surg Oral Med Oral Pathol Oral Radiol Endod. 2008 Jul ;106(1):e31-5.

76) Lofthag-Hansen S, Huumonen S, Gro¨ndahl K, Gro¨ndahl H-G (2007) Limited cone-beam CT and intraoral radiography for the diagnosis of periapical pathology. Oral Surgery, Oral Medicine, Oral Pathology, Oral radiology and Endodontology 103, 114–9.

77) Estrela C, Bueno MR, Leles CR, Azevedo B, Azevedo JR (2008) Accuracy of cone beam computed tomography and panoramic radiography for the detection of apical periodontitis. Journal of Endodontics 34, 273–9

78) Stavropoulos A, Wenzel A (2007) Accuracy of cone beam dental CT, intraoral digital and conventional film radiography for the detection of periapical lesions: an ex vivo study in pig jaws. Clinical Oral Investigations 11, 101–6.

79) Rigolone M, Pasqualini D, Bianchi L, Berutti E, Bianchi SD (2003) Vestibular surgical access to the palatine root of the superior first molar: ‘‘low-does cone-beam’’ CT analysis of the pathway and its anatomic variations. Journal of Endodontics 29, 773–5.

80) Tsurumachi T, Honda K (2007) A new cone beam computertized tomography system for use in endodontic surgery. International Endodontic Journal 40, 224–32.

81) Patel S. New dimensions in endodontic imaging: Part 2. Cone beam computed tomography. IntEndod J. 2009 Jun ;42(6):463-475.

Chapter II Applications of CBCT in orthodontics

Part 2.1: Accuracy of CBCT measurements on 3D surface models for cephalometric analysis

Hassan B, van der Stelt P, Sanderink G. Accuracy of three-dimensional measurements obtained from cone beam computed tomography surface-rendered images for cephalometric analysis: influence of patient scanning position. Eur J Orthod. 2009 Apr ;31(2):129-134.

Part 2.2: Influence of scanning and reconstruction parameters on quality of CBCT 3D models of the dental arches

Hassan B, Couto Souza P, Jacobs R, de Azambuja Berti S, van der Stelt P. Influence of scanning and reconstruction parameters on quality of three-dimensional surface models of the dental arches from cone beam computed tomography [Internet]. Clinical Oral Investigations 2009 Aug [e-pub]

Part 2.3: Accuracy assessment of three-dimensional surface reconstructions of teeth from Cone Beam Computed Tomography scans

B. Al-Rawi, **B. Hassan**, Bart Vandenberge, Reinhilde Jacobs

Journal or Oral Rehabilitation February (2010). [Epub ahead of print]

Part 2.1: Accuracy of three-dimensional measurements obtained from cone beam computed tomography surface-rendered images for cephalometric analysis: influence of patient scanning position

Bassam Hassan, Paul van der Stelt and Gerard Sanderink

European Journal of Orthodontics 31 (2009) 129–134

SUMMARY

The aims of this study were to assess the accuracy of linear measurements on three-dimensional (3D) surface-rendered images generated from cone beam computed tomography (CBCT) in comparison with two-dimensional (2D) slices and 2D lateral and postero-anterior (PA) cephalometric projections, and to investigate the influence of patient head position in the scanner on measurement accuracy. Eight dry human skulls were scanned twice using NewTom 3G CBCT in an ideal and a rotated position and the resulting datasets were used to create 3D surface-rendered images, 2D tomographic slices, and 2D lateral and PA projections. Ten linear distances were defi ned for cephalometric measurements. The physical and radiographic measurements were repeated twice by three independent observers and were compared using repeated measures analysis of variance ($P = 0.05$). The radiographic measurements were also compared between the ideal and the rotated scan positions. The radiographic measurements of the 3D images were closer to the physical measurements than the 2D slices and 2D projection images. No statistically significant difference was found between the ideal and the rotated scan measurements for the 3D images and the 2D tomographic slices. A statistically significant difference ($P < 0.001$) was observed between the ideal and rotated scan positions for the 2D projection images. The findings indicate that measurements based on 3D CBCT surface images are accurate and that small variations in the patient's head position do not infl uence measurement accuracy.

Introduction

Two-dimensional (2D) projection radiographs have been traditionally considered the modality of choice for the assessment of craniofacial structures for orthodontic cephalometric analysis. However, the superimposition of structures of the left and right side of the skull, the unequal enlargement ratios of the left and right side, and the possible distortion of the mid-facial structures are well-recognized shortcomings of this imaging technique (Chen *et al.* , 2004 ; Bruntz *et al.* , 2006). This led to the development of alternative cephalometric analysis approaches. The most recent method is three-dimensional (3D) cephalometry in which the linear and angular measurements are made directly on 3D surface and volume-rendered images obtained from computed tomography (CT) scans (Halazonetis, 2005 ; Park *et al.* , 2006). The accuracy of these 3D-rendered images has been previously evaluated and the findings showed that direct 3D measurements are highly accurate with no significant discrepancies from physical measurements (Cavalcanti and Vannier, 1998 ; Cavalcanti *et al.* , 2004). However, the relatively high radiation dose, costs, and limited availability associated with CT scans impede its adoption to routine clinical orthodontic diagnosis and treatment planning (Kau *et al.* , 2005). Cone beam computed tomography (CBCT) has emerged as a promising technology with the potential to replace CT as the method of choice for 3D cephalometric analysis as it provides tomographic views and volumetric reconstructions at substantially reduced radiation doses and expense (Swennen and Schutyser, 2006). CBCT has become a frequently utilized imaging modality in clinical orthodontics, implant planning, temporomandibular joint imaging, and maxillofacial surgery (Walker *et al.*, 2005; Sakabe *et al*., 2006).

There are several types of radiographic images which can be generated from CBCT data including 2D tomographic multi-planar reformatted (MPR) slices, 2D virtual lateral and postero-anterior (PA) cephalometric projections, 3D surface and volume-rendered images, and panoramic reconstruction. Several reports have established the accuracy of linear measurements of different CBCT systems based on 2D tomographic slices and 2D virtual lateral cephalographic images (Lascala *et al.* , 2004; Hilgers *et al.* , 2005; Kumar *et al.* , 2007; Ludlow *et al.* , 2007). However, the accuracy of linear measurements based on 3D surface and volume rendered CBCT images is

still to be assessed. Due to the dissimilarity in the image acquisition methodology, reconstruction algorithms, and detector characteristics, CBCT reconstructed 3D surface-rendered images of the maxillofacial region are inferior in quality in comparison with CT (Loubele *et al.* , 2006). This raises questions regarding the accuracy of CBCT 3D-rendered models for direct 3D cephalometry.

In practice, the position of the patient's head during the scanning procedure could deviate from a true vertical and horizontal orientation. It is therefore important not only to assess the accuracy of craniofacial measurements on 3D surface bone models generated from CBCT scans in ideal scanning settings, but also to examine the influence of head positioning during the scanning procedure on the accuracy of the measurements. It is also necessary to investigate whether a retrospective correction of the patient scanning position using software tools as previously suggested (Swennen and Schutyser, 2006) is required. The influence of head position in the scanner on the accuracy of measurements of the mandibular anatomy based on CBCT 2D axial slices and panoramic reconstructions has been reported. The results showed that head position did not have a significant influence on measurement accuracy (Moshiri *et al.*, 2007). The aims of this study were to assess the accuracy of linear measurements on 3D surface-rendered images generated from CBCT datasets and to compare them with those made on 2D tomographic slices and on 2D lateral and PA cephalometric projections. The influence of head position of the patient in the scanner on measurement accuracy for the three image types was also evaluated to establish recommendations for CBCT in orthodontic practice.

Materials and methods

Physical measurements

Eight dry human skulls, which were not identified by gender, age, or ethnicity, were used in the study. To undertake the measurements 10 linear distances were selected in the maxilla and mandible. The selected lines were orientated horizontally, vertically, and obliquely to account for linear measurements made in all three dimensions. The gold standard was obtained for each of the 10 lines by physical measurements using a digital calliper with an accuracy of 0.01 mm (Gamma, Amsterdam, The

Netherlands). The physical measurements were repeated twice by three independent observers. (Table 1)

Radiographic scan

The radiographic scans were obtained using the NewTom 3G CBCT system (Quantitative Radiology, Verona, Italy). Each skull was placed in a plastic box with the mid-sagittal plane coinciding with that of the box. The skull was then fixed in the box using dental wax and wrapped in plastic sheets. The box was filled with water. The skulls were kept dry during the scan to avoid possible expansion due to absorption of water which can influence measurement accuracy. The skulls were positioned according to the recommendations of the CBCT manufacturer with the Frankfort plane perpendicular to the floor. Each skull was scanned twice: first in an 'ideal' position and second in a 'rotated' position. The rotated scan was obtained by placing a wooden wedge under the right edge of the box and rotating the plastic box around the *Z* scanning axis by approximately 15 – 18 degrees. The scans were later checked using the software tools to ensure consistency in skull rotation angle and orientation. (Figure 1) The imaging parameters were 3.24 mAs, 110 kVp, and a 20 second scan time using the 9 inch detector field. The raw data were reconstructed using the high-resolution reconstruction algorithm setting provided by the CBCT software (QR NNT v2.0.4, Quantitative Radiology). The resulting volume had an isotropic voxel size of 0.25 mm and the datasets were exported as 512 × 512 matrices in DICOM 3 file format and saved on an external hard disk.

Radiographic measurements

The DICOM datasets were imported into commercial software (Amira v.4.2, Mercury Computer Systems, Chelmsford, Massachusetts, USA) for analysis. Each skull dataset was processed to create three types of images; 3D surface-rendered images of the maxilla and mandible (Figure 2), 2D tomographic MPR slices with a thickness of
0.5 mm (Figure 3), and 2D lateral and PA projections (Figure 4). The original scan position was left unchanged with no corrections. The 3D surface models were created automatically in the software by specifying a single threshold grey level value of an average of 650 ± 50 for the mandible and 450 ± 30 for the maxilla. Different values for the maxilla and mandible were used because of the difference in bone thickness and density between the maxilla and mandible which influence the bone surface rendering quality

and the visibility of the anatomical landmarks. The condylar head showed some artefacts which had to be corrected manually using segmentation tools available in the software.

The 2D lateral and PA projections were created using orthographic 1:1 true scale and a reference system was established in the *X*, *Y*, and *Z* directions. The 2D and 3D measurement tools in Amira are calibrated by the software manufacturer to produce length measurements expressed as millimeters with an accuracy of 0.01 mm. Three observers were trained to use the software for this study. Each observer repeated the radiographic measurements twice for each image type for both scan positions (ideal and rotated) independently which resulted
in a total of 12 radiographic measurements per line, per skull per observer (3 × 2 ideal + 3 × 2 rotated). The total number of radiographic measurements for the three observers for the eight skulls was 2880.

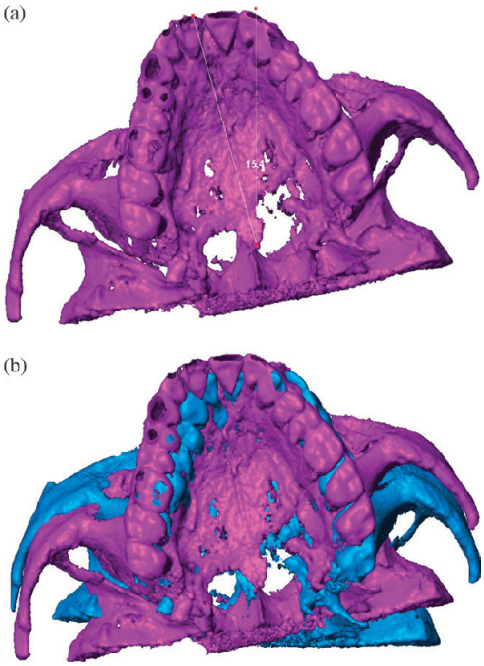

Figure 1 Three-dimensional surface-rendered model of the maxilla shown with a rotation angle of 15.4 degrees (a) (the left line represents the true mid-sagittal plane when the skull is in an ideal scanning position and the right line the deviation from true mid-sagittal when the skull is rotated) and in an ideal (blue) and rotated (purple) position superimposed on each other (b).

Table 1 Physical measurements of the gold standard (all measurements are given in mm; standard deviation in brackets).

Anatomical landmarks										
Skull number	Maxillary landmarks				Mandibular landmarks					
	Orbital(L)-orbital(R)	Orbital(L)-anterior nasal spine	Orbital(R)-anterior nasal spine	Anterior nasal spine-posterior nasal spine	Condyle(L)-condyle(R)	Coronoid(L)-coronoid(R)	Condyle(L)-coronoid(L)	Condyle(R)-coronoid(R)	Condyle(L)-coronoid(R)	Condyle(R)-coronoid(L)
1	73.69 (0.16)	43.73 (0.16)	45.71 (0.11)	50.40 (0.22)	81.54 (0.26)	85.94 (0.27)	30.02 (0.09)	27.22 (0.09)	90.26 (0.11)	86.51 (0.12)
2	71.62 (0.15)	46.81 (0.08)	43.83 (0.11)	54.21 (0.11)	99.77 (0.48)	95.48 (0.09)	26.92 (0.22)	27.61 (0.12)	99.69 (0.14)	102.75 (0.07)
3	80.29 (0.10)	47.30 (0.13)	53.12 (0.10)	55.35 (0.14)	90.14 (0.29)	81.93 (0.19)	34.58 (0.12)	33.21 (0.13)	91.90 (0.04)	93.59 (0.12)
4	74.31 (0.12)	43.48 (0.19)	47.12 (0.25)	51.55 (0.17)	87.82 (0.13)	85.65 (0.11)	27.74 (0.14)	26.97 (0.05)	91.09 (0.14)	90.71 (0.25)
5	64.12 (0.13)	39.61 (0.27)	41.04 (0.15)	46.39 (0.34)	88.78 (0.16)	81.62 (0.12)	34.08 (0.19)	34.57 (0.19)	91.46 (0.06)	91.46 (0.11)
6	66.05 (0.45)	41.59 (0.13)	39.75 (0.37)	48.73 (0.26)	85.94 (0.13)	79.83 (0.05)	30.33 (0.16)	30.00 (0.20)	87.45 (0.21)	88.86 (0.19)
7	59.27 (0.13)	38.75 (0.13)	40.20 (0.14)	43.47 (0.19)	108.81 (0.13)	90.71 (0.09)	38.01 (0.13)	40.26 (0.07)	105.89 (0.15)	107.37 (0.09)
8	61.27 (0.33)	38.75 (0.12)	36.41 (0.08)	45.55 (0.22)	97.14 (0.19)	94.23 (0.09)	34.04 (0.06)	31.69 (0.09)	101.90 (0.23)	100.34 (0.27)

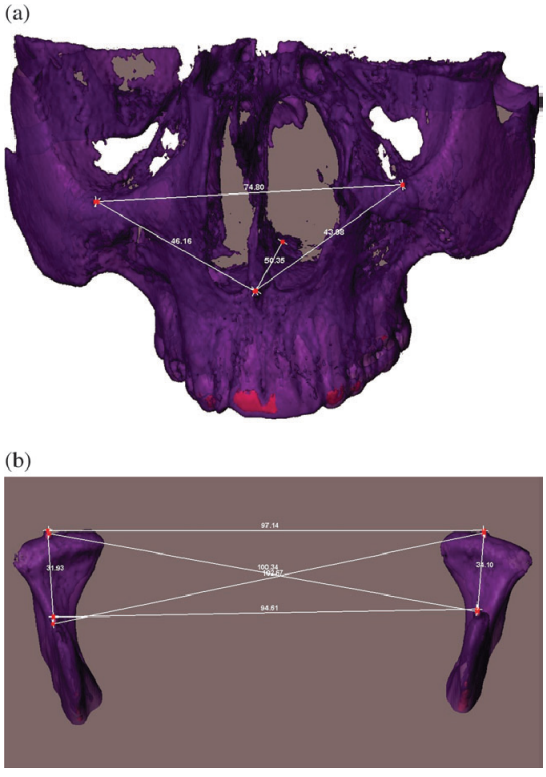

Figure 2 Linear measurements on the three-dimensional surface rendered model of (a) maxilla: between OI(R)-OI(L), ANS-PNS, OI(R)-
ANS, and OI(L)-ANS and (b) mandible: between Con(R)-Con(L), Cor(R)- Cor(L), Con(R)-Cor(R), Con(L)-Cor(L), Con(R)-Cor(L), and Con(L)-Cor(R).

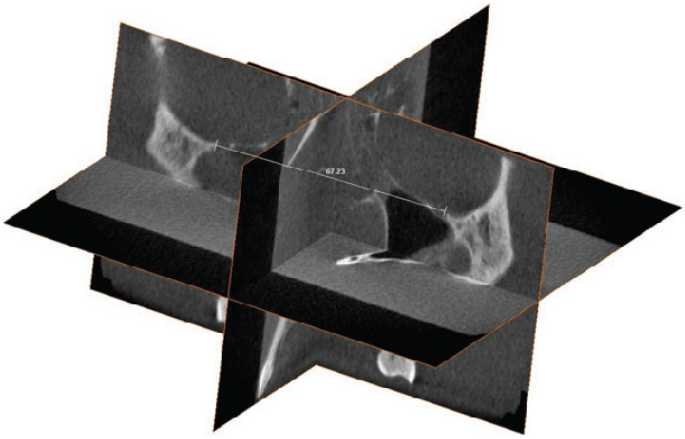

Figure 3 Two-dimensional multi-planar reformatted slices with a thickness of 0.5 mm (axial, coronal 'frontal' and sagittal). Linear measurement between OI(R) and OI(L).

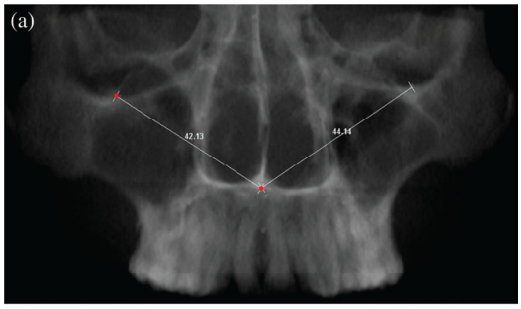

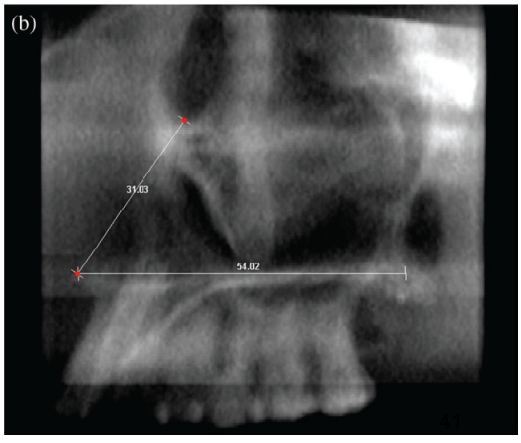

Figure 4 Linear measurements on two-dimensional radiographs. (a) Postereo-anterior projection: between OI(R)-ANS and OI(L)-ANS. (b) Lateral cephalogram: between ANS-PNS OI-ANS.

Table 2 Mean absolute differences (and standard deviations) of radiographic measurements and the gold standard for the selected distances.

Anatomical landmarks	Scan position					
	Optimal scan position			Rotated scan position		
	3D models	2D tomographic slices	2D cephalometric (lateral and PA) projections	3D models	2D tomographic slices	2D cephalometric (lateral and PA) projections
Orbital(L)-orbital(R)	0.39 (0.29)	0.34 (0.24)	0.37 (0.22)	0.43 (0.30)	0.66 (0.61)	**2.25 (2.59)**
Orbital(L)-anterior nasal spine	0.18 (0.18)	0.37 (0.84)	**3.53 (1.95)**	0.22 (0.11)	0.44 (0.44)	**3.97 (1.01)**
Orbital(R)-anterior nasal spine	0.22 (0.20)	0.33 (0.62)	**4.1 (2.23)**	0.27 (0.22)	0.31 (0.24)	**9.27 (4.36)**
Anterior nasal spine-posterior nasal spine	0.26 (0.25)	0.27 (0.26)	0.29 (0.32)	0.33 (0.46)	0.30 (0.51)	**1.78 (1.28)**
Condyle(L)-condyle(R)	0.22 (0.15)	0.15 (0.12)	0.17 (0.12)	0.18 (0.12)	0.15 (0.10)	**12.73 (2.55)**
Coronoid(L)-coronoid(R)	0.16 (0.11)	0.11 (0.09)	0.10 (0.08)	0.15 (0.10)	0.12 (0.07)	**12.42 (1.83)**
Condyle(L)-coronoid(L)	0.12 (0.10)	0.11 (0.08)	0.25 (0.36)	0.10 (0.77)	0.10 (0.07)	**5.71 (2.22)**
Condyle(R)-coronoid(R)	0.10 (0.08)	0.16 (0.10)	0.34 (0.28)	0.10 (0.14)	0.13 (0.09)	**2.93 (1.26)**
Condyle(L)-coronoid(R)	0.11 (0.06)	0.13 (0.32)	**3.21 (1.33)**	0.11 (0.17)	0.13 (0.41)	**6.06 (4.11)**
Condyle(R)-coronoid(L)	0.14 (0.08)	0.19 (0.22)	**4.08 (2.21)**	0.14 (0.16)	0.21 (0.11)	**6.97 (4.68)**

Differences of >1 mm between the radiographic measurements and the gold standard are shown in **bold.**
Differences of >1 mm for the 2D cephalometric measurements between the ideal and rotated scan position are underlined.

Statistical analysis

The accuracy of the gold standard for the selected distances was established by averaging the physical measurements of the three observers. The mean of each radiographic measurement for each image type was compared with the mean of the gold standard using analysis of variance of repeated measurements with the Statistical Package for Social Sciences version 14, (SPSS Inc., Chicago, Illinois, USA). The significance level was set to $P \leq 0.05$. Corresponding image types were assessed for both scan positions to minimize the influence of the interaction effect on the statistical results.

Results

The gold standard measurements are summarized in Table 1. The accuracy of the gold standard measurements was within 0.5 mm as the largest standard deviation (SD) was 0.48 mm. All radiographic measurements in both scan positions (ideal and rotated) were statistically different from the gold standard measurements at $P = 0.05$. However, as not all the differences were equal and some were relatively small, it can be argued that their relevance in clinical practice is limited. In the ideal position, the largest observed difference between the mean 3D models and gold standard

measurements was less than 0.5 mm [mean deviation (MD) = 0.39 mm, SD = 0.29], for 2D tomographic slices, the largest observed difference with the gold standard measurements was less than 1.0 mm (MD = 0.37 mm, SD = 0.84), and for 2D cephalometric (lateral and PA) projection images, less than 5 mm (MD = 4.1 mm, SD = 2.23). The measurements in the rotated position were compared with the optimal position measurements for each image type. For 3D surface images and 2D tomographic slices, no statistically significant differences were found between the optimal and rotated scan data ($P = 0.73$ and $P = 0.93$, respectively). For 2D cephalometric lateral and PA projections, a statistically significant difference ($P < 0.001$) was observed between both scan positions (e.g. IO(R)-ANS line) (Table 2).

Discussion

This study was performed to investigate the effect of image type and patient head positioning on the accuracy of CBCT measurements for cephalometric analysis. For scanning positions (ideal and rotated), the difference between the 3D surface image measurements and the gold standard was relatively small (within 0.5 mm). This may be due to the fact that hard tissue transformations are rigid in nature, so scan position does not influence the location of the anatomical landmarks relative to each other. It is noteworthy though that soft tissue transformation is not necessarily rigid when the patient is positioned incorrectly in the scanner which may influence the outcome of the measurements. However, this could not be assessed as dry skulls were used in this research. The difference between 2D tomographic slice measurements and the gold standard was also small (within 1.0 mm) in both scan positions and the findings are consistent with previous studies (Lascala *et al.* , 2004 ; Hilgers *et al.*, 2005 ; Kumar *et al.*, 2007; Ludlow *et al.*, 2007). However, the problems with 2D tomographic slices remain that typically the two anatomical landmarks between which a line is drawn are not identifiable on the same slice when thin slices are utilized (0.5 – 1.0 mm). This is due to variations in the location of anatomical landmarks and also because of
patient positioning errors. As such, it necessitates scrolling through the slices back and forth or right and left to identify the anatomical landmarks on both sides bilaterally or anteroposteriorly. This complicates the measurement process and typically requires more time and effort and can be considered inappropriate for cephalometric analysis.

Virtual lateral cephalograms and PA projections reconstructed from CBCT scan data have gained increasing popularity in recent years and are routine in the diagnostic report for each CBCT orthodontic patient. However, the results presented show that the measurements based on virtual lateral and PA cephalograms for some measurements (obliquely defined lines) deviated from the gold standard by more than 1 mm even when the scan was in an optimal
position (Table 2). When the skulls were rotated, a larger difference of more than 10 mm was found, which means that virtual cephalometric projection images created from CBCT data are sensitive to small variations in patient scanning position. Virtual 2D projection images measurements were the least accurate among the three image types.
The accuracy of the radiographic measurements was limited by the voxel size employed (0.25 mm) and by the ability of the observer in determining the exact position of the anatomical landmarks. It is also possible that the rotation angle used in this study did not reflect the 'real' average patient positioning error in the CBCT apparatus, but no information could be found in the literature with regard to the incidence and extent of patient positioning errors in a scanner. Patient positioning discrepancies occur in all three dimensions (x , y , z). However, in this study only the influence of angular rotation around the z -axis on measurement accuracy was assessed.

Conclusions

Small variations in patient head position when a CBCT examination is performed do not affect the accuracy of linear measurements based on 3D surface-rendered models. The measurements based on 2D tomographic slices are also accurate but there is an increase in observer time and more effort is required to identify the anatomical landmarks using 2D slices; thus, from the point of view of an orthodontist, it might be considered impractical for cephalometric analysis. Linear measurements based on 2D virtual lateral and PA projections were sensitive to small variations in head position which means that retrospective correction for patient position using software tools is required as was previously suggested if 2D virtual cephalograms are to be used for tracing (Swennen and Schutyser, 2006). This raises issues regarding how accurate an orthodontist can compensate for an incorrectly positioned patient in the absence of automatic software tools to perform this task. When introducing protocols for 3D analysis with CBCT images in orthodontics, it is important to emphasize the advantages and limitations of the different visualization techniques available with this imaging modality.

The results of this study suggest that performing cephalometric analysis on 3D-rendered models seems to be the most appropriate approach with regard to accuracy and convenience.

Acknowledgement
We would like to thank Dr Hans Verheij for carrying out the statistical analysis and for his scientific support.

References

1. Bruntz L Q, Palomo J M, Baden S, Hans M G 2006 A comparison of scanned lateral cephalograms with corresponding original radiographs. American Journal of Orthodontics and Dentofacial Orthopedics 130: 340 – 348
2. Cavalcanti M G, Vannier M W 1998 Quantitative analysis of spiral computed tomography for craniofacial clinical applications. Dentomaxillofacial Radiology 27: 344 – 350
3. Cavalcanti M G, Rocha S S, Vannier M W 2004 Craniofacial measurements based on 3D-CT volume rendering: implications for clinical applications. Dentomaxillofacial Radiology 33: 170 – 176
4. Chen Y J, Chen S K , Yao J C , Chang H F 2004 The effects of differences in landmark identifi cation on the cephalometric measurements in traditional versus digitized cephalometry . Angle Orthodontist 74: 155 – 161
5. Halazonetis D J 2005 From 2-dimensional cephalograms to 3-dimensional computed tomography scans. American Journal of Orthodontics and Dentofacial Orthopedics 127: 627 – 637
6. Hilgers M L, Scarfe W C, Scheetz J P, Farman A G 2005 Accuracy of linear temporomandibular joint measurements with cone beam computed tomography and digital cephalometric radiography. American Journal of Orthodontics and Dentofacial Orthopedics 128: 803 – 811
7. Kau C H, Richmond S, Palomo J M , Hans M G 2005 Three-dimensional cone beam computerized tomography in orthodontics. Journal of Orthodontics 32: 282 – 293
8. Kumar V, Ludlow J B, Mol A, Cevidanes L 2007 Comparison of conventional and cone beam CT synthesized cephalograms. Dentomaxillofacial Radiology 36: 263 – 269
9. Lascala C A, Panella J, Marques M M 2004 Analysis of the accuracy of linear measurements obtained by cone beam computed tomography (CBCT-NewTom). Dentomaxillofacial Radiology 33: 291 – 294
10. Loubele M , Maes F , Schutyser F , Marchal G , Jacobs R , Suetens P 2006 Assessment of bone segmentation quality of cone-beam CT versus multislice spiral CT: a pilot study . Oral Surgery, Oral Medicine, Oral Pathology, Oral Radiology, and Endodontology 102: 225 – 234
11. Ludlow J B, Laster W S, See M, Bailey L J, Hershey H G 2007 Accuracy of measurements of mandibular anatomy in cone beam computed tomography images. Oral Surgery, Oral Medicine, Oral Pathology, Oral Radiology, and Endodontology 103: 534 – 542
12. Moshiri M, Scarfe W C , Hilgers M L , Scheetz J P , Silveira A M , Farman A G 2007 Accuracy of linear measurements from imaging plate and lateral cephalometric

images derived from cone-beam computed tomography. American Journal of Orthodontics and Dentofacial Orthopedics 132: 550 – 560
13. Park S H, Yu H S, Kim K D, Lee K J, Baik H S 2006 A proposal for a new analysis of craniofacial morphology by 3-dimensional computed tomography. American Journal of Orthodontics and Dentofacial Orthopedics 129: 623 – 634
14. Sakabe R, Sakabe J, Kuroki Y, Nakajima I, Kijima N, Honda K 2006 Evaluation of temporomandibular disorders in children using limited cone-beam computed tomography: a case report. Journal of Clinical Pediatric Dentistry 31: 14 – 16
15. Swennen G R J, Schutyser F 2006 Three-dimensional cephalometry: spiral multi-slice vs cone-beam computed tomography. American Journal of Orthodontics and Dentofacial Orthopedics 130: 410 – 416
16. Walker L , Enciso R , Mah J 2005 Three-dimensional localization of maxillary canines with cone-beam computed tomography . American Journal of Orthodontics and Dentofacial Orthopedics 128: 418 – 423

Part 2.2: Influence of scanning and reconstruction parameters on quality of three-dimensional surface models of the dental arches from cone beam computed tomography

Bassam Hassan, Paulo Couto Souza, Reinhilde Jacobs, Soraya de Azambuja Berti, Paul van der Stelt

Abstract

The study aim is to investigate the influence of scan field, mouth opening, voxel size, and segmentation threshold selections on the quality of the three-dimensional
(3D) surface models of the dental arches from cone beam computed tomography (CBCT). 3D models of 25 patients scanned with one image intensifier CBCT system (NewTom 3G, QR SLR, Verona, Italy) using three field sizes in open and closed-mouth positions were created at different voxel size resolutions. Two observers assessed the quality of the models independently on a five-point scale using specified criteria. The results indicate that large-field selection reduced the visibility of the teeth and the interproximal space. Also, large voxel size reduced the visibility of the occlusal surfaces and bone in the anterior region in both maxilla and mandible. Segmentation threshold was more variable in the maxilla than in the mandible. Closed-mouth scan complicated separating the jaws and reduced teeth surfaces visibility. The preliminary results from this imageintensifier system indicate that the use of medium or small scan fields in an open-mouth position with a small voxel is recommended to optimize quality of the 3D surface model reconstructions of the dental arches from CBCT. More research is needed to validate the results with other flat panel detector-based CBCT systems.

Keywords: Cone beam computed tomography. Three-dimension models. Image quality. Dentistry. Surface rendering.

Introduction

Computerized three-dimensional (3D) models of the craniofacial region are a recent trend in dentistry. 3D models of the hard-tissue dental arches including the teeth and the jawbones have been used for various clinical applications including pre-operative treatment planning of dental implants and craniofacial surgical procedures, fabrication of dental and craniofacial prosthesis, analysis of arch dimensions, virtual treatment simulation in orthodontics, and postoperative treatment outcome assessment [1–6]. 3D models of the dental arches are typically obtained by digitizing the dental cast with high-resolution surface laser scanning [7–10]. Those models can be used to evaluate the dentition and inter-occlusal space; however, they do not provide information regarding the amount of alveolar bone available and the relation of the tooth root to its socket. In addition, the accuracy of the digitized model is limited by the accuracy of the dental impression and cast, which could be variable and inconsistent overtime depending on several factors [11–13]. 3D models of the dental arches can also be obtained from computed tomography (CT) scans. Conventional CT technology provides accurate reconstructions of the alveolar bone but not the teeth due to limited spatial resolution and strong streak artifacts caused by metallic dental restorations and orthodontic brackets when present. Therefore, “composite models” were developed where the high quality 3D reconstructions of the alveolar bone and the roots of the teeth obtained from CT were combined with the high-quality 3D reconstructions of the teeth crowns obtained from laser surface scanning of the dental cast. And, while this technique produced satisfactory results, it was deemed unsuitable for the clinical practice due to time and cost constraints associated with complicated setup and the extensive user experience required for correct implementation [2, 14–20].

Cone beam CT (CBCT) specifically developed for the maxillofacial region provides comparable images to conventional CT at reduced radiation dose and cost [21–26]. CBCT reconstructions at present have smaller voxels in comparison with conventional CT [27], which could be advantageous in obtaining more accurate 3D surface models of the teeth crowns. However, CBCT subjective image quality is still inferior in comparison with conventional CT. Several artifacts including beam hardening and inhomogeneity and truncation influence image contrast and bone border definition in CBCT [28–31]. The Feldkamp filtered back-projection reconstruction algorithm employed by most CBCT manufacturers is exactly identical to the Radon inverse-transform algorithm used in conventional CT

in the mid-plane [32]. As such, it does not inherently reduce the effect of streak artifacts caused by metallic dental filling and orthodontic brackets. Moreover, since CBCT is inferior to CT in terms of contrast resolution, the effect of metal streak artifacts may be even more pronounced [33]. Several reconstruction algorithms and techniques were proposed to reduce those artifacts in CBCT images, but they remain to date computationally expensive and not yet widely adopted by CBCT manufacturers [34]. There are currently many CBCT systems which are commercially available. Those systems are categorized according to detector design technology into: (1) image intensifier tube/charged coupled devices (IIT/CCD) combination or (2) flat panel detector (FPD) [34]. It has been reported that IIT/CCD suffers from more artifacts and increased noise levels compared to FPD systems [35]. Also, in practice several patient scanning and data reconstruction parameters have influence on CBCT subjective image quality [35, 36]. All those factors combined could thus directly influence the quality of the 3D surface models reconstructions of the dental arches from CBCT. It is necessary to assess the quality of those models and the influence those parameters might have in order to optimize patient scanning, data reconstruction, and 3D surface model creation protocols. This is important in order to assess whether it is possible to obtain accurate 3D surface models of the dental arches from CBCT or not. Few studies based on dry skull samples assessed the accuracy of 3D models reconstructions from CBCT [37, 38]. However, 3D surface models created from phantoms, dry skulls, or even formalin-fixed cadavers are not realistic and do not represent actual patient. The quality of the segmented model could deviate largely from what is observed clinically. The objective of this study is to assess the quality of 3D surface models of the dental arches with respect to the influence of different scanning and reconstruction parameters in one IIT-based CBCT system (NewTom 3G) in an in vivo sample of patients.

Materials and methods

Sample selection

Twenty-five datasets scanned with the IIT/CCD system Newtom 3G CBCT (QR SLR, Verona, Italy) were selected from a larger database of CBCT patients. The datasets were divided into three groups: Group (A) consisted of ten patients scanned with the 12-in. (large) detector scan field of view (FoV). Group (B) consisted of ten patients scanned with the 9-in. (medium)

scan FoV. Group (C) consisted of five patients scanned with the 6-in. (small) scan FoV. Groups (A) and (B) were scanned in a closed-mouth position with the teeth in maximum intercuspid relation, while group (C) was scanned in an open-mouth position. Additional selection criteria were that (1) the upper and the lower jaws are both visible in the scan, (2) no more than four teeth are missing for both jaws excluding the third molars, and that (3) there are no orthodontic brackets or large metal restorations. Informed consent was obtained from the patients to use their data for research purposes.
Datasets were exported according to the manufacturer's default settings for each scan field in DICOM 3 file format at the isotropic voxel size of (0.3, 0.25, and 0.2 mm_3) for the 12-, 9-, and 6-in. scan FoVs, respectively. The datasets were 12 bits in depth, and the gray values (2_{12}=4,096) range was (−1,000 to 3,095). The datasets were imported into 3D analysis software (Amira v4.2, Visage Imaging, Carlsbad, CA, USA) for making the 3D models. Creating the 3D models

Segmentation threshold

The histogram of a CBCT dataset is composed of a wide range of gray-scale values that represent the X-ray attenuation profiles of the different soft and hard tissues. It is generally more difficult to specify the correct threshold value to separate the bone from soft tissue and background in CBCT than in conventional CT due to inherent inconsistencies in the histogram. A single threshold value was specified to segment the bone and teeth from the background and soft tissue for each 3D model. The surface models were created using the marching cube algorithm [39]. To determine an optimal threshold value, the histogram of each model was approximated as a mixture of Gaussians by using the stochastic expectation maximization (SEM) algorithm. The threshold value was then specified in the region of the intersection of the two Gaussians representing soft tissue and bone. To eliminate the stochastic part of the SEM, the average of three threshold values was taken [29, 40]. Threshold values were determined using this method separately for the maxilla and for the mandible when the jaws were separated (Fig. 1).

Scan field selection

For groups (A), (B), and (C), a smaller region of interest (ROI) limited only to the dental arches was selected, and the rest was digitally removed (Fig. 2). In each group, the upper arch was separated from the lower arch by using a

cubic ROI selection. For this experiment, the isotropic voxel size of 0.3 mm^3 was chosen for each model. Fifty 3D surface models were created in total (25 upper and 25 lower arches) for the three groups (A, B, C).

Voxel size selection

Group (C) was selected to assess the influence of the voxel size on 3D model quality. This was done in order to assess the influence of voxel size selection on the definition of the occlusal surfaces since groups (A) and (B) were scanned in closed-mouth position that the occlusal surfaces were difficult to visualize. To assess the influence of each level of the “voxel size” factor independently, voxels were
categorized into two components: (a) pixel resolution in the (x,y) scan plane (PRxy) and (b) axial slice thickness (AST) in the (z) plane. First, PRxy was fixed at 0.3 mm, and AST was increased from 0.3 to 1.2 mm using 0.3 mm steps. Then, AST was fixed at 0.3 mm and PRxy was increased from 0.3 to 1.2 mm using 0.3 mm steps. A 3D bicubic resampling filter was used to manipulate the voxel size to change the pixel resolution and the axial slice thickness. The bi-cubic resampling filter uses information from 16 adjacent points to each voxel for resampling the data. This has the added advantage of smoother resampling and less interpolation artifact compared to bilinear or the nearest neighbor filtering. In total, eight voxel combinations were obtained per model (AST 0.3, 0.6, 0.9, 1.2 and PRxy 0.3, 0.6, 0.9, 1.2). A total of 80 models were created (40 upper and 40 lower) dental arches.

Observations:

A single investigator who did not participate in the observations created the models. All 3D models were coded, and two observers (one maxillofacial radiologist and one maxillofacial surgeon) assessed the quality of all the models independently. The observers were blind to the scan field and voxel size selections. The models were presented to the observers in a random order. All models were viewed on a 19-in. flat panel screen (1,280×1,024, Philips Brilliance 200WP, Brussels, Belgium). The observers were allowed to rotate, scale (zoom), and translate (move) the models to improve visibility of certain structures, but adjusting the threshold value was not permitted. The observers were asked to assess the subjective visibility of the following structures for each model in the maxilla and the mandible on a five-point scale (1 = very poor, 2 = poor, 3 = satisfactory, 4 = good, 5 = very good):

1. External surfaces of the teeth and the occlusal surfaces in group (C)
2. Alveolar bone anteriorly and posteriorly
3. Palate region
4. Interproximal space between the teeth anteriorly and posteriorly separately
5. Overall image noise which represented the “soft tissue” and background noise that routinely appears in most CBCT surface reconstructions due to the difficulty in specifying a single threshold value to segment bone.

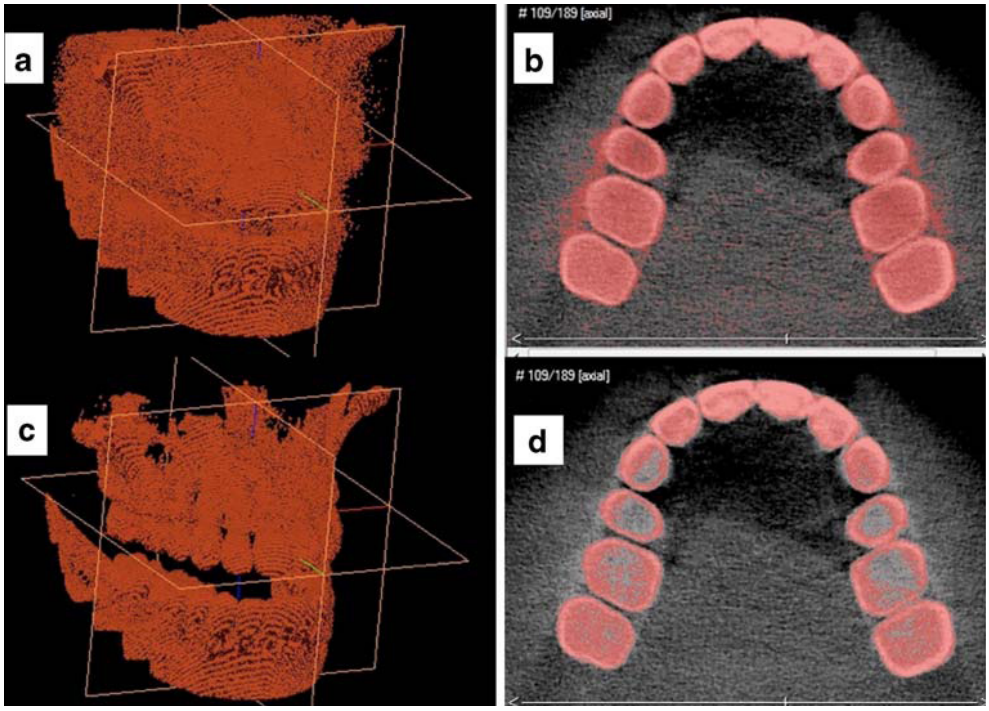

Fig. 1 An example of the segmentation procedure and threshold value determination for a 3D model from group (C) in 3D (a, c) and on 2D axial slices (b, d). The model can have an increased noise level due to threshold underestimation (a and b) or several holes in the bone and teeth due to threshold overestimation (c and d)

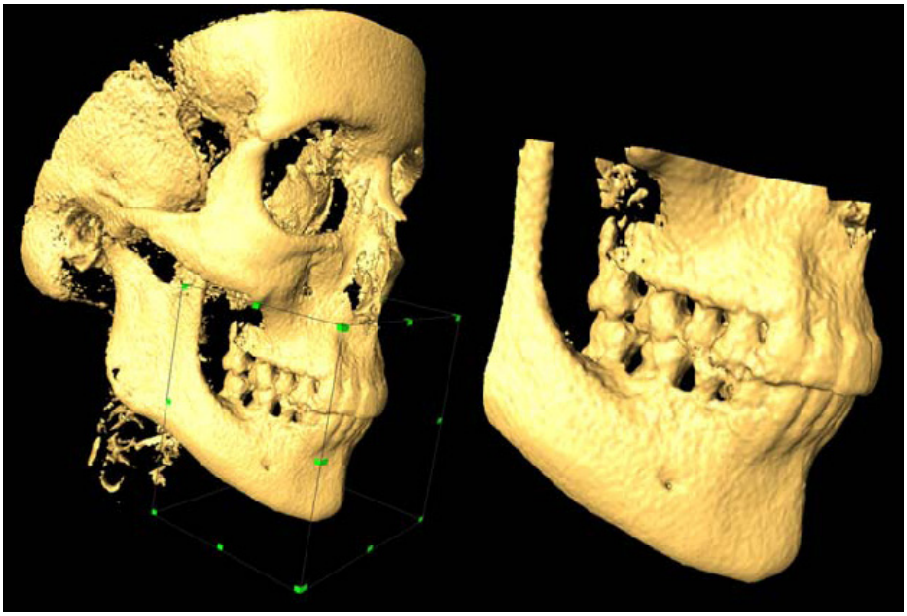

Fig. 2 A dataset from group (A) large scan field. Example of limiting the selection to the dental arches by using a cubic region of interest. The original dataset (left) and the cropped model (right)

Statistical analysis

The observation data were entered and analyzed using SPSS software (SPSS v.15, SPSS, Chicago, IL, USA). The observers' ratings were entered into a multivariate analysis of variance (MANOVA) with the Wilk's lambda test to assess the influence of scan field, voxel size, and segmentation threshold on visibility of the different structures of the 3D models. The three scan field groups and the different voxel combinations were compared to each other using Helmert planned contrasts. Inter-observer agreement was determined using Cohen kappa, and observers' interaction with scan FoV selection was calculated in the MANOVA analysis. Alpha level was set to 0.05.

Results

Segmentation threshold

Mean threshold values were (660±44.72, 850±51.63, and 784±60.82) for groups (A), (B), and (C), respectively. There was a statistically significant

difference in the threshold value among the three groups (p=0.001). Mean threshold and standard deviation value were (847± 33.21) and (662±121.2)\ for the mandible and maxilla, respectively.

Field size selection

There was an overall statistically significant difference among the three groups (A, B, and C) in 3D surface model quality (p=0.0001). Inter-observer agreement was moderate (kappa=0.53). There was no statistically significant interaction between the observers and the scan field groups (p=0.12). Specifically, the visibility of the external surfaces of the teeth in the maxilla and the interproximal space between the teeth in the anterior region in the maxilla and the mandible was better in group (C) than in group (A) (p=0.0001) with no significant differences from group (B) (p=0.48; Fig. 3). Image noise was significantly less in group (A) than in groups (B) and (C) (p=0.0001, 0.001), respectively.

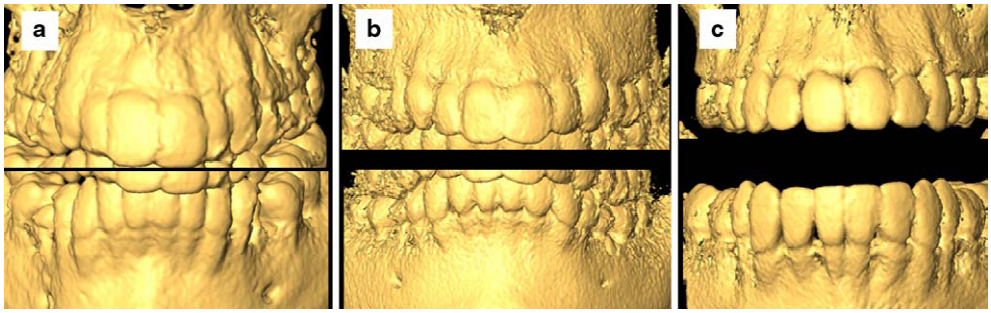

Fig. 3 Influence of scan field selection on the quality of the 3D model reconstruction. The difference in the visibility of the teeth and interproximal space between a large, b medium, and c small fields

Voxel size selection

There was an overall statistically significant difference in 3D model quality in group (C) due to manipulating pixel resolution in the scan plane (PRxy; p=0.0001) but not due to axial slice thickness manipulation (p=0.87). There was no significant interaction between the observers and PRxy (p=0.08). Specifically, the visibility of the external and occlusal surfaces of the teeth, anterior alveolar bone, and interproximal space anteriorly in the maxilla and the mandible was significantly improved by the small pixel resolution PRxy=0.3 mm in comparison with other selections (p=0.001; Fig. 4). There were no significant differences in subjective image quality between (PRxy=

0.6 mm) and (PRxy=0.9 mm) selections (p=0.17) but a significant difference between (PRxy=0.6 mm) and (PRxy= 1.2 mm) selections (p=0.03).

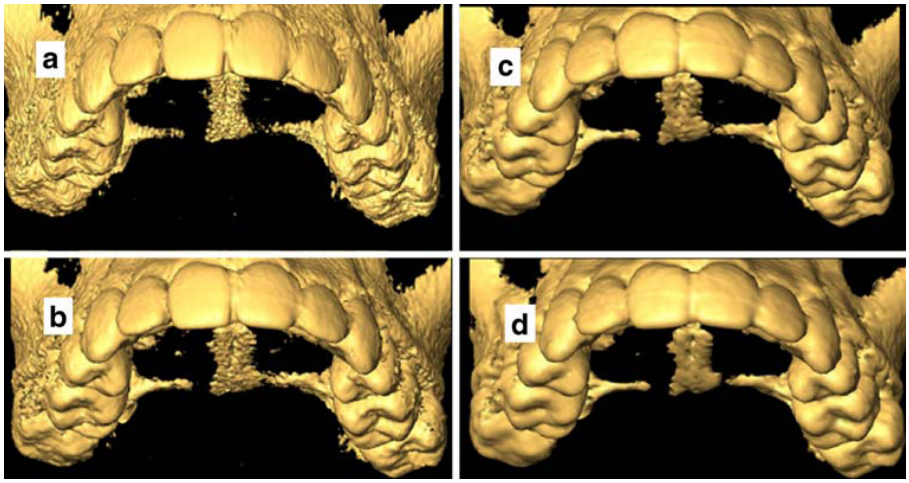

Fig. 4 Influence of voxel size manipulation on the quality of the 3D model reconstruction. Changing the pixel resolution in the scan plane PRxy influences the visibility of the occlusal surfaces of the teeth between **a** 0.3 mm, **b** 0.6 mm, **c** 0.9 mm, and **d** 1.2 mm. Notice the decreased noise level associated with large voxel on d in comparison with **a**

Discussion

The results indicate that scan field selection has significant influence on the quality of the 3D models. The small scan field selection provided best visibility for the different structures of the 3D models. Interestingly, there was no significant difference between the small and the medium scan fields in the quality of the 3D models. This means that the medium field, which covers the temporomandibular
joints bilaterally and several other important anatomical regions including the maxillary sinus, can be used without loss in quality. The large field reduced the visibility of the teeth surfaces and the interproximal space between the teeth. This is significant because the standard scanning protocol of orthodontic patients with CBCT is with the large scan field. The results here show, however, that there is a significant loss in quality of the 3D models of the dental arches when the large field is used. Conversely, there were more image artifacts associated with the small scan field than with the large scan field. This could be due to cone truncation for small field selections.

An important factor when comparing different scan FoVs is the local tomography problem. When a small FoV is selected, the anatomical

structures outside the region of interest are imaged as well since the line integrals sampled by the detector pass through them. Due to the fact that those tissues are only sampled for a small angular range, the resulting image reconstruction is inconsistent [41–43]. Smaller CBCT scan FoVs suffer from greater variability in the density gray values as well (i.e., more inconsistencies) compared to larger scan FoVs [35, 44]. The different scan fields have different voxel sizes, and various CBCT scanners also differ from each other in voxel size selections for each scan field. The importance of voxel size stems from a practical observation that very small voxels (e.g., 0.2 or 0.3 mm_3 isotropic) result in an extremely large surface mesh model, which is difficult to process to create an accurate 3D surface model for preoperative treatment planning and simulation. The results here show that large pixel resolution of 0.6, 0.9, or 1.2 mm in the x,y plane significantly reduce the visibility of the occlusal surfaces of the teeth, interproximal space between the teeth, and alveolar bone. Interestingly, increasing the axial slice thickness in the z plane up to 0.9 mm did not significantly reduce the quality of the 3D models. That means that anisotropic voxels with small pixel area in the x,y plane and larger slice thickness can be used instead of the "standard" small isotropic voxels. This has the added advantage of significantly reducing the model size to facilitate processing while maintaining image quality and also to reduce image noise. The choice of larger voxels reduces image noise, which is caused by photon count statistics, by averaging the gray-level values across slices, which in turn, reduces the overall noise level in the image [45].

Segmentation threshold value was automatically determined and observer independent [29]. There was more variation in the threshold value due to scan field selection than due to the different samples within the same field. Variation in the threshold value was less in the mandible than in the maxilla. This can be explained that cortical bone in the mandible is thick enough to keep the attenuation profile uniform across the entire bone surface, while in the maxilla, the varied thin cortical bone especially in the palate and tuberosity regions creates significant "bone dehiscence and fenestration" artifacts effect in the 3D model. Due to limited contrast, the roots could not be separated from their sockets using binary thresholding alone without creating artifacts. No attempt was made to systematically evaluate the visibility of the roots since they were very difficult to visualize. A closed-mouth position made it extremely difficult to separate the jaws using a cubic ROI selection to visualize the occlusal surfaces of the teeth and to assess the interocclusal relationship. A closed-mouth position necessitates manual

segmentation to separate the teeth from each other, which was a tedious, time-consuming, and user-dependent procedure that resulted in unsatisfactory results. An open mouth position facilitates separating the teeth to visualize the interproximal space. The mandible can be then virtually rotated into maximum occlusion using software tools.

This study was conducted to evaluate the influence of several scanning and reconstruction parameters on the quality of 3D model reconstructions of the dental arches from one IIT/CCD CBCT scanner (NewTom 3G). The required surface description includes clear display of the teeth surfaces and the occlusal contacts, exact reconstruction of the alveolar bone, plus separation of the teeth from each other and each tooth root from its socket. The study results show that it is still difficult to meet all those demands since separating the root from its socket is still difficult to achieve. Also, to produce a “usable” 3D surface model with sufficient quality, several scanning and reconstruction parameters need to be optimized first, and an optimized segmentation approach must be adhered to. This study was limited in that no interaction between the scan field selection and the voxel size was assumed. For practical time and resources constraints, it was not possible to assess the influence of voxel size selection on all fields. Instead, the small field was selected a priori based on the hypothesis that it provides better subjective image quality. That hypothesis was supported by the study results. Also, the visibility of the occlusal surfaces with the large and medium fields were not assessed since it was not possible to obtain scan material with the 9- and the 12-in. scan fields with open-mouth position. The study is limited only to one IIT/CCD CBCT system (NewTom 3G). Other FPD based systems are different with respect to image quality and scan and reconstruction parameters. Therefore, caution should be exercised when extrapolating the results to other CBCT systems. Lastly, the influence of streak artifacts was not investigated to limit the number of assessed factors on subjective image quality. However, it is expected that streak artifacts will have a significant influence on the quality of the 3D models. In conclusion, within the limitations of the current study, several scanning and reconstruction parameters need to be optimized first before good-quality models can be created. The use of the small or medium field in an open-mouth scan position coupled with an anisotropic voxel of 0.3–0.4 mm pixel resolution in the scan plane and an axial slice thickness of 0.6–0.7 mm is recommended when creating 3D models of the dental arches from NewTom 3G CBCT (Fig. 5).

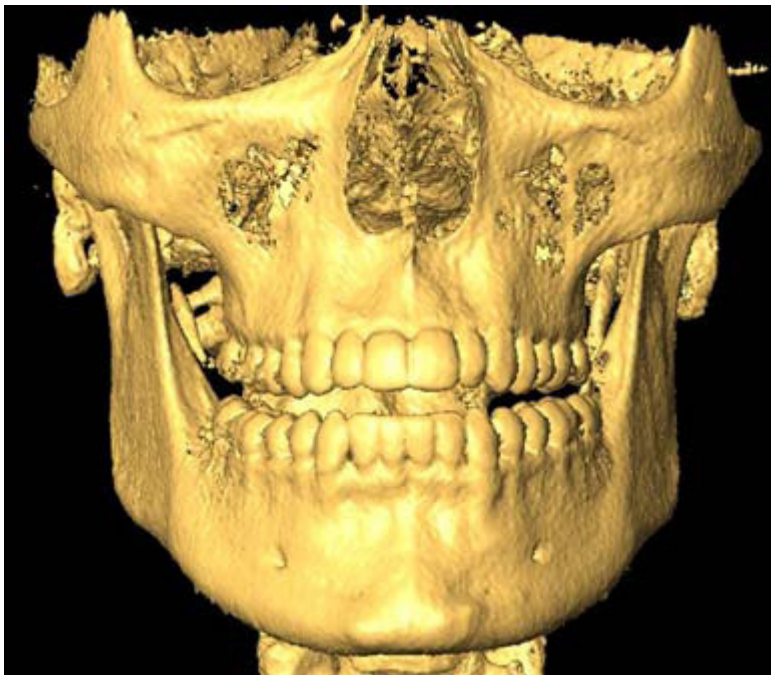

Fig. 5 Example of the recommended optimized scan protocol for making 3D reconstructions of the dental arches from CBCT. Medium field, open-mouth position with an anisotropic voxel of .4×0.6 mm

References

1. Cevidanes LH, Bailey LJ, Tucker SF et al (2007) Three dimensional cone-beam computed tomography for assessment of mandibular changes after orthognathic surgery. Am J Orthod Dentofacial Orthop 131:44–50
2. Caloss R, Atkins K, Stella JP (2007) Three-dimensional imaging for virtual assessment and treatment simulation in orthognathic surgery. Oral Maxillofac Surg Clin North Am 19:287–309
3. Van Steenberghe D, Malevez C, Van Cleynenbreugel J et al (2003) Accuracy of drilling guides for transfer from threedimensional CT-based planning to placement of zygoma implants in human cadavers. Clin Oral Implants Res 14:131–136
4. Van Assche N, van Steenberghe D, Guerrero ME et al (2007) Accuracy of implant placement based on pre-surgical planning of three-dimensional cone-beam images: a pilot study. J Clin Periodontol 34:816–821
5. Jacobs R, Adriansens A, Verstreken K (1999) Predictability of a three-dimensional planning system for oral implant surgery. Dento-maxillo-facial Radiol 28:105–111
6. Cevidanes LHS, Bailey LJ, Tucker GR et al (2005) Superimposition of 3D cone-beam CT models of orthognathic surgery patients. Dento-maxillo-facial Radiol 34:369–375
7. Wang Y, Zhao Y, Lv P et al (2006) A scanning method for the dental casts of intercuspal position. Beijing Da Xue Xue Bao 18 (38):298–300

8. Lu P, Li Z, Wang Y (1999) A study of dental cast by using 3D laser non-contact measurement and analysis. Zhonghua Kou Qiang Yi Xue Za Zhi 34:351–353
9. Da Silveira AC, Daw JL, Kusnoto B et al (2003) Craniofacial applications of three-dimensional laser surface scanning. J Craniofac Surg 14:449–456
10. Lu P, Li Z, Wang Y et al (2000) The research and development of noncontact 3-D laser dental model measuring and analyzing system. Chin J Dent Res 3:7–14
11. DeLong R, Heinzen M, Hodges JS et al (2003) Accuracy of a system for creating 3D computer models of dental arches. J Dent Res 82:438–442
12. Petrie CS, Walker MP, O'mahony AM et al (2003) Dimensional accuracy and surface detail reproduction of two hydrophilic vinyl polysiloxane impression materials tested under dry, moist, and wet conditions. J Prosthet Dent 90:365–372
13. DeLong R, Pintado MR, Ko CC et al (2001) Factors influencing optical 3D scanning of vinyl polysiloxane impression materials. J Prosthodont 10:78–85
14. Gateno J, Xia J, Teichgraeber JF et al (2003) A new technique for the creation of a computerized composite skull model. J Oral Maxillofac Surg 61:222–227
15. Uechi J, Okayama M, Shibata T et al (2006) A novel method for the 3-dimensional simulation of orthognathic surgery by using a multimodal image-fusion technique. Am J Orthod Dentofacial
Orthop 130:786–798
16. Swennen GRJ, Barth E, Eulzer C et al (2007) The use of a new 3D splint and double CT scan procedure to obtain an accurate anatomic virtual augmented model of the skull. Int J Oral Maxillofac Surg 36:146–152
17. Swennen GRJ, Mommaerts MY, Abeloos J et al (2007) The use of a wax bite wafer and a double computed tomography scan procedure to obtain a three-dimensional augmented virtual skull model. J Craniofac Surg 18:533–539
18. Nkenke E, Zachow S, Benz M et al (2004) Fusion of computed tomography data and optical 3D images of the dentition for streak artefact correction in the simulation of orthognathic surgery. Dento-maxillo-facial Radiol 33:226–232
19. Metzger MC, Hohlweg-Majert B, Schwarz U et al (2008) Manufacturing splints for orthognathic surgery using a threedimensional printer. Oral Surg Oral Med Oral Pathol Oral Radiol Endod 105:e1–e7
20. Nkenke E, Vairaktaris E, Neukam FW et al (2007) State of the art of fusion of computed tomography data and optical 3D images. Int J Comput Dent 10:11–24
21. Quereshy FA, Savell TA, Palomo JM (2008) Applications of cone beam computed tomography in the practice of oral and maxillofacial surgery. J Oral Maxillofac Surg 66:791–796
22. Loubele M, Bogaerts R, Van Dijck E, et al (2008) Comparison between effective radiation dose of CBCT and MSCT scanners for dentomaxillofacial applications. Eur J Radiol (July 2008; epub ahead of print)
23. Silva MAG, Wolf U, Heinicke F et al (2008) Cone-beam computed tomography for routine orthodontic treatment planning: a radiation dose evaluation. Am J Orthod Dentofacial Orthop 133
(640):e1–e5
24. Araki K, Maki K, Seki K et al (2004) Characteristics of a newly developed dentomaxillofacial X-ray cone beam CT scanner (CB MercuRay): system configuration and physical properties. Dentomaxillo- facial Radiol 33:51–59
25. Sukovic P (2003) Cone beam computed tomography in craniofacial imaging. Orthod Craniofac Res 6(Suppl):131–136 discussion 179–82
26. Yajima A, Otonari-Yamamoto M, Sano T et al (2006) Cone-beam CT (CB Throne) applied to dentomaxillofacial region. Bull Tokyo Dent Coll 47:133–141

27. Bartling SH, Majdani O, Gupta R et al (2007) Large scan field, high spatial resolution flat-panel detector based volumetric CT of the whole human skull base and for maxillofacial imaging. Dentomaxillo- facial Radiol 36:317–327
28. Loubele M, Guerrero ME, Jacobs R et al (2007) A comparison of jaw dimensional and quality assessments of bone characteristics with cone-beam CT, spiral tomography, and multi-slice spiral CT. Int J Oral Maxillofac Implants 22:446–454
29. Loubele M, Maes F, Schutyser F et al (2006) Assessment of bone segmentation quality of cone-beam CT versus multislice spiral CT: a pilot study. Oral Surg Oral Med Oral Pathol Oral Radiol Endod 102:225–234
30. Loubele M, Maes F, Jacobs R et al (2008) Comparative study of image quality for MSCT and CBCT scanners for dentomaxillofacial radiology applications. Radiat Prot Dosimetry 129:222–6
31. Loubele M, Jacobs R, Maes F et al (2008) Image quality vs radiation dose of four cone beam computed tomography scanners. Dento-maxillo-facial Radiol 37:309–319
32. Feldkamp LA, Davis LC, Kress JW (1984) Practical cone-beam algorithm. J Opt Soc Am A 1:612–619
33. Zhang Y, Zhang L, Zhu XR et al (2007) Reducing metal artifacts in cone-beam CT images by preprocessing projection data. Int J Radiat Oncol Biol Phys 1(67):924–932
34. Scarfe WC, Farman AG (2008) What is cone-beam CT and how does it work? Dent Clin North Am 52(4):707–730
35. Katsumata A, Hirukawa A, Okumura S, Naitoh M, Fujishita M, Ariji E, Langlais RP (2007) Effects of image artifacts on gray value density in limited-volume cone-beam computerized tomography. Oral Surg Oral Med Oral Pathol Oral Radiol Endod 104 (6):829–836
36. Kwong JC, Palomo JM, Landers MA et al (2008) Image quality produced by different cone-beam computed tomography settings. Am J Orthod Dentofacial Orthop 133:317–327
37. Periago DR, Scarfe WC, Moshiri M, Scheetz JP, Silveira AM, Farman AG (2008) Linear accuracy and reliability of cone beam CT derived 3-dimensional images constructed using an orthodontic volumetric rendering program. Angle Orthod 78(3):387– 395
38. Hassan B, van der Stelt P, Sanderink G (2009) Accuracy of threedimensional measurements obtained from cone beam computed tomography surface-rendered images for cephalometric analysis: influence of patient scanning position. Eur J Orthod 31(2):129–134
39. Lorensen WE, Cline HE (1987) Marching cubes: a high resolution 3D surface construction algorithm. SIGGRAPH Comput. Graph 21:163–169
40. Baillard C, Barillot C, Bouthemy P (2000) Robust adaptive segmentation of 3-D medical images with level sets. INRIA 4071:1–26
41. Siltanen S, Kolehmainen V, Järvenpää S, Kaipio JP, Koistinen P, Lassas M, Pirttilä J, Somersalo E (2003) Statistical inversion for medical x-ray tomography with few radiographs: I. General theory. Phys Med Biol 48(10):1437–1463
42. Kuchment P, Lancaster K, Mogilevskaya L (1995) On local tomography. Inverse Probl 11(3):571–589
43. Katsevich AI (1997) Local tomography for the limited-angle problem. J Math Anal Appl 213:160–182
44. Katsumata A, Hirukawa A, Okumura S, Naitoh M, Fujishita M, Ariji E, Langlais RP (2009) Relationship between density variability and imaging volume size in cone-beam computerized tomographic scanning of the maxillofacial region: an in vitro study. Oral Surg Oral Med Oral Pathol Oral Radiol Endod 107 (3):420–425
45. Salvado O, Hillenbrand CM, Wilson DL (2006) Partial volume reduction by interpolation with reverse diffusion. Int J Biomed Imaging Volume 2006:920–922

Part 2.3: Accuracy assessment of three-dimensional surface reconstructions of teeth from Cone Beam Computed Tomography scans

Bassam Al-Rawi, Bassam Hassan, Bart Vandenberge, Reinhilde Jacobs

Journal or Oral Rehabilitation February (2010). [Epub ahead of print]

ABSTRACT:

Introduction: The use of three-dimensional (3D) models of the dentition obtained from Cone Beam Computed Tomography (CBCT) is becoming increasingly more popular in dentistry. A recent trend is to replace the traditional dental casts with digital CBCT models for diagnosis, treatment planning and simulation. The accuracy of these models was previously assessed through comparing linear physical and radiographic measurements. However, this assessment technique is both observer and landmark dependent. The accuracy of 3D CBCT teeth reconstructions is yet to be reliably measured.

Objectives: To assess the accuracy of 3D CBCT reconstructions of the teeth using a semi-automated and observer-independent method and to assess the influence of Field of View (FoV) selection on reconstruction accuracy.

Methods: Fully dentate upper and lower dry human jaws, placed in a plastic box and immersed in water were scanned with CBCT with small, medium and large FoV. The teeth were then scanned separately using MicroCT. CBCT and MicroCT 3D teeth models were compared and mean surface difference was calculated per tooth for each FoV.

Results: Mean difference between MicroCT and CBCT was 120±40μm, 157±39μm and 207±80μm for the small, medium and large FoV, respectively. CBCT models were larger than MicroCT due to larger voxel size.

Conclusions: CBCT provides accurate 3D reconstructions of the teeth that can be useful for clinical applications.

Keywords: accuracy, study model, Cone Beam Computed Tomography, 3D

Introduction:

Obtaining three-dimensional (3D) models of the dental arches is becoming increasingly more important in dentistry. Employing those models to aid in diagnosis, treatment planning, simulation and outcome assessment will have a major impact on clinical practice in the near future. However, before those models can be adopted in clinical practice, their accuracy and effectiveness must be assessed. 3D surface models of the dental arches including the jawbones and teeth were previously obtained by scanning the patient with computed tomography (CT) [1,2]. However, beside the well-known limitations of medical CT of increased costs and patient dose, the technology failed to deliver accurate 3D surface reconstructions of the teeth crowns and occlusal surfaces due to limited spatial resolution [3,4]. To solve this problem, 3D models of the alveolar bone obtained from CT were combined with 3D models of teeth obtained from surface laser scanning. Those models were used for treatment of patients with severe malocclusion. However, the technique was deemed too complicated to be adopted in the clinical routine due to time and cost constraints and the extensive skills required for successful implementation [5,6].

Cone beam CT (CBCT), which is a relatively recent scanning technology in dentistry, provides images comparable to medical CT at reduced costs and radiation doses [7, 8]. More importantly, CBCT 'at present' has higher spatial resolution than MSCT with voxel sizes as small as 80 micrometers [9]. This could possibly assist in obtaining more accurate 3D reconstructions of the dentition. At the same time, several artifacts specific to CBCT technology influence the quality of 3D surface models reconstructions of the jawbones, which were found inferior to those of MSCT [10-13]. Additionally, it was recently found that scanning and reconstructions parameters including Field of View (FoV) selection and voxel size have a significant influence on the quality of 3D surface models of the dental arches from one CBCT system [14].

Previous studies assessed the accuracy of linear measurements made on 3D CBCT surface models of the maxillofacial skeleton by comparing the 3D measurements against physical measurements made on dry skulls [15-18]. Recently, the accuracy of 3D model reconstructions of the teeth from CBCT was assessed using a similar method [19]. However, the accuracy of measurements between two points using this technique is both observer and landmark dependent. Both the physical and the radiographic measurements are prone to errors due to subjective observers' judgment and landmark definition. This study aim is to assess the accuracy of CBCT 3D reconstructions of the teeth using a semi-automated and observer-independent method. The second objective is to assess the influence of FoV selection on the reconstruction accuracy.

Materials & Methods:

Sample preparation and radiographic scan:

Two fully dentate dry human jaws (maxilla and mandible) were obtained with approval from the department of functional anatomy at University of Amsterdam. The jaws were placed in a well-fitting plastic container and immersed in water to provide some level of soft tissue simulation. Then the two jaws were scanned separately with the Scanora 3D CBCT scanner (Soredex, Tuusula, Finland) with the three FOVs available in this model (small 6x6cm, medium 7.5x10cm and large 7.5x14.5cm) and exposure parameters of 85kV and 8mA. Image data were reconstructed at isotropic voxel sizes of 133μm, 200μm and 250μm for the small, medium and large FoVs, respectively. The teeth were then extracted, fixed in a Styrofoam block container and scanned with a MicroCT scanner (Skyscan1173, Skyscan, Kontich, Belgium) at the isotropic 35μm resolution and exposure settings of 130kV and 61μA.

Region of interest (ROI) selection:

The DICOM datasets from CBCT from all FoVs and MicroCT were imported into 3D analysis software (Amira® v4.2, Visage Imaging, Carlsbad, CA, USA). First step was to digitally crop the crown of each tooth in the CBCT and MicroCT data to separate it from other structures in the scan. The cropping was achieved using interactive region of interest (ROI) selection tools available in the Amira® software. A specific level was identified for cropping the crown from the rest of the tooth at the level of the cement-enamel junction (Figure1). This was done to limit the cropping as much as possible only to the tooth crown excluding the root structure. The cropped volume of each crown from both CBCT and MicroCT was then saved in a separate file for data analysis.

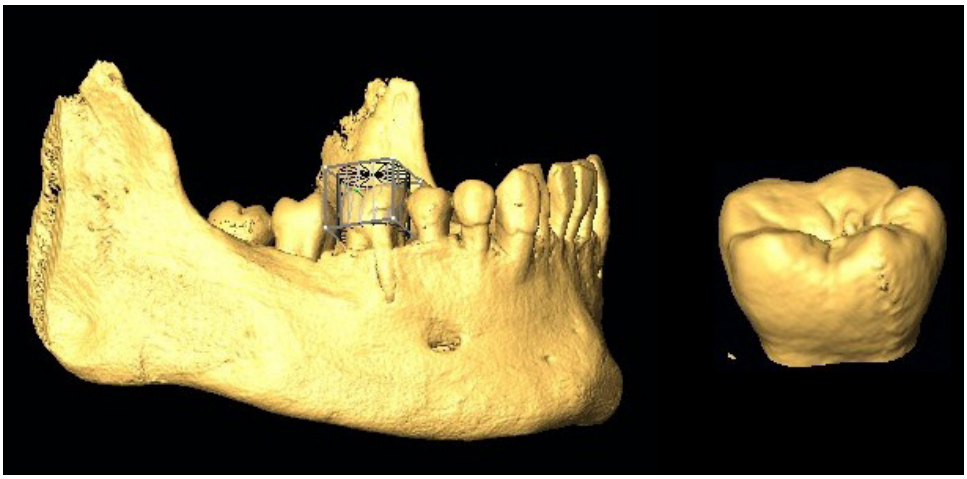

Figure1: An example of using a cubic region of interest (ROI) to extract three-dimensional crown models from the dental arch. The original dataset (left) and the cropped crown model (right).

Data segmentation and 3D surface creation:

Segmentation was performed using the segmentation tools that are available in the Amira® software. Since the crowns were cropped and other structures (e.g. bone, roots) were digitally removed from the volume, a single threshold value was selected to segment the crowns from the background for each 3D model. Based on histogram analysis of each crown, a threshold value was selected based on a local gray level value and image gradient. The selected segmentation threshold value identifies the outer border of the enamel and selects the contour of the crown to separate it from the background image. The surface models were then created using the marching cube algorithm [20].

Data registration and surface difference calibration:

The next step was superimposing the CBCT and MicroCT crowns onto one another to provide maximum alignment between the two surfaces. This was achieved using the iterative closest point (ICP) registration algorithm. This algorithm brings the two crowns into alignment by minimizing the distance between the two surfaces (CBCT and MicroCT) by calibrating six-degrees transformation parameters (three rotation and three translation) [21]. The teeth from CBCT were superimposed on the MicroCT data, which served as the reference (gold) standard. The aligned surfaces of the CBCT were compared to those of MicroCT to establish the difference between the two surfaces. The comparison metric was root mean square (RMS), which calibrates the mean distance between the two surfaces at anatomically

corresponding locations. This metric assesses the extent to which the CBCT crown surfaces differ from their MicroCT counterparts at anatomically corresponding locations.

Results:

The RMS data, which represents mean difference between CBCT and MicroCT was calibrated per tooth for the three FoV selections. The data was entered into SPSS® software (SPSS v.15, SPSS Inc., Chicago, IL, USA). One-way analysis of variance (ANOVA) was conducted to assess the difference between the three FoVs with the post-hoc Tukey HSD. Alpha level was set to 0.05. Mean differences between CBCT and MicroCT for the three FoV selections are summarized in table1. CBCT reconstructions were larger than their MicroCT counterparts in all instances. There was a statistically significant difference between the three FoVs in 3D surface accuracy in comparison with MicroCT in both jaws (p =0.0001). There was a statistically significant difference between the large and medium FoVs in both maxilla and mandible (p = 0.0001) but not between the medium and small FoVs (p = 0.16).

Tooth	Mandible (μm)			Maxilla(μm)		
	Small	**Medium**	**Large**	**Small**	**Medium**	**Large**
Central incisor	159±40	281±78	169±19	199±17	229±30	239±17
Lateral incisor	106±18	169±19	163±6	211±14	232±4	252±1
Canine	94±22	257±10	387±21	138±38	136±32	199±6
First premolar	95±11	158±7	167±13	159±8	172±37	190±26
Second premolar	85±5	149±1	161±10	180±28	194±58	199±53
First molar	126±6	164±17	179±7	132±23	179±10	178±23
Second molar	99±16	152±6	239±73	162±19	196±26	213±1

Discussion:

The study was conducted to assess the accuracy of 3D surface reconstructions of teeth crowns and occlusal surfaces from CBCT. The results show that CBCT 3D reconstructions are accurate within the limits of the spatial resolution and voxel sizes of the selected FoV available for the Scanora 3D system. The largest observed difference between CBCT and MicroCT was for the mandibular canine tooth with the large FoV (387±21μm). The accuracy found in this study is higher than what was previously reported [19]. Due to larger voxel size, CBCT 3D models were larger than their MicroCT counterparts. Specifically, the cusps and pits were larger (over-estimated) in CBCT than in MicroCT. Additionally, due to the low contrast to noise ratio in CBCT, the grooves details were less visible in comparison with MicroCT (Figure 2). In this study, the choice of large FoV reduced the visibility of the occlusal surfaces in comparison with the small or medium FoVs selections. This corroborates previous findings from Hassan et al. [14] that large FoV selection has significant influence on 3D surface model quality of the dental arches from CBCT. Also, in concordance with previous findings, there was no significant difference between the medium and the small FoVs selections [14].

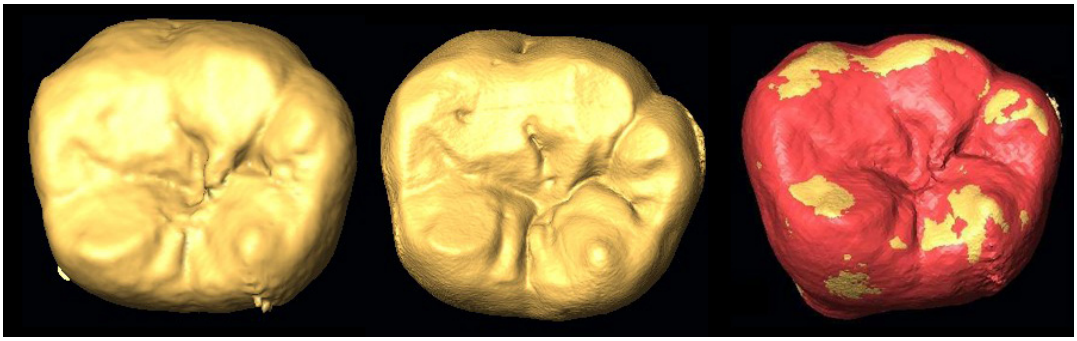

Figure2: Three-dimensional crown surface model derived from CBCT (A) and from MicroCT (B). Surface Alignment between CBCT (red) and MicroCT (yellow) in (C). Notice the over-estimation of CBCT occlusal surface reconstruction in comparison with MicroCT.

The accuracy of CBCT 3D models is mainly influenced by the segmentation approach employed. Several methods were proposed to segment 3D models of the dental arches from CBCT data. These included global and local thresholding, image gradient and active contour fitting [10-14, 22]. Recently, a multi-steps approach was proposed to *automatically* segment the teeth crowns and roots from CBCT [23, 24]. The validity and accuracy of those segmentation techniques needs to be assessed against a reliable gold standard such as MicroCT or high resolution surface laser scanning. The segmentation method used in this study is based on image threshold

and gradient. However, to segment each crown precisely, the teeth needed to be digitally cropped or 'cut-out' each one separately from the volume. This was both labor-intensive and time consuming. The objective was, however, to assess the accuracy of 3D surface teeth models so this custom segmentation approach was used to ensure the reliability of the measurements.

An important drawback of this study next to the use of dry skulls with partial soft tissue simulation is the scanning unit used and its specific settings. Only one CBCT unit has been employed with specific beam energy and FoV-voxel size settings. All these parameters influence the final image quality and the amount of artifacts in the reconstructed data. A large FoV may provide less accurate reconstructions because of the greater beam angulation in the superior and inferior volume area and reduced contrast to noise ratio. Yet, the FoVs in this study had specific voxel sizes, which were not adjustable and thus it was difficult to assess the influence of this parameter individually. Also the voxel size itself has an important influence on the noise in the orthogonal slices: the smaller the voxel size, the greater the noise, but of course the better the spatial resolution. It is therefore crucial in the future to investigate all parameters and their influence on the reconstruction accuracy.

Jacobs and van Steenberghe (1994) reported that the patient could feel small differences in his or her occlusion up to 10 micron [25]. As such, the current accuracy of CBCT 3D reconstructions is insufficient to create prosthetic appliances such as crowns with CAD/CAM systems. However, for other dental applications including orthodontics and orthognathic surgery diagnosis and treatment planning, the accuracy of the CBCT surface models currently achievable could prove sufficient for the clinical routine. And although all CBCT surfaces are larger than the 'anatomic' truth, the reliability of dental measurements between two points may not be affected depending on the type of measurement made [26].

In conclusion, CBCT provides accurate 3D reconstructions of the teeth, but more research should be conducted to adequately simulate clinical settings. The absence of metal may have influenced these promising results and teeth were also not scanned in occlusion. However, this study indicates the potential of CBCT teeth reconstructions for certain dental clinical applications

Acknowledgement:

The authors would like to thank Elke Van de Casteele and Jeroen Hostens (Skyscan) for their help with the MicroCT scanning.

References:

1. Nkenke E, Vairaktaris E, Neukam FW et al. State of the art of fusion of computed tomography data and optical 3D images. Int J Comput Dent. 2007;10:11–24.
2. Kwon T, Park H, Ryoo H, Lee S. A comparison of craniofacial morphology in patients with and without facial asymmetry--a three-dimensional analysis with computed tomography. Int J Oral Maxillofac Surg. 2006;35:43-8.
3. Macchi A, Carrafiello G, Cacciafesta V, Norcini A. Three-dimensional digital modeling and setup. Am J Orthod Dentofacial Orthop. 2006;129:605-10.
4. Nkenke E, Zachow S, Benz M et al. Fusion of computed tomography data and optical 3D images of the dentition for streak artefact correction in the simulation of orthognathic surgery. Dentomaxillofacial Radiol. 2004;33:226–32.
5. Swennen GRJ, Mommaerts MY, Abeloos J et al. The use of a wax bite wafer and a double computed tomography scan procedure to obtain a three-dimensional augmented virtual skull model. J Craniofac Surg. 2007;18:533-9.
6. Swennen GRJ, Barth E, Eulzer C, Schutyser F. The use of a new 3D splint and double CT scan procedure to obtain an accurate anatomic virtual augmented model of the skull. Int J Oral Maxillofac Surg. 2007;36:146-52.
7. Silva MAG, Wolf U, Heinicke F et al. Cone-beam computed tomography for routine orthodontic treatment planning: a radiation dose evaluation. Am J Orthod Dentofacial Orthop. 2008;133:e1–e5.
8. Loubele M, Bogaerts R, Van Dijck E, et al. Comparison between effective radiation dose of CBCT and MSCT scanners for dentomaxillofacial applications. Eur J Radiol. July 16, 2008. doi:10.1016/j.ejrad.2008.06.002
9. Bartling SH, Majdani O, Gupta R et al. Large scan field, high spatial resolution flat-panel detector based volumetric CT of the whole human skull base and for maxillofacial imaging. Dentomaxillofacial Radiol. 2007;36:317–27.
10. Loubele M, Guerrero ME, Jacobs R et al. A comparison of jaw dimensional and quality assessments of bone characteristics with cone-beam CT, spiral tomography, and multi-slice spiral CT. Int J Oral Maxillofac Implants. 2007;22:446–54.
11. Loubele M, Maes F, Schutyser F et al. Assessment of bone segmentation quality of cone-beam CT versus multislice spiral CT: a pilot study. Oral Surg Oral Med Oral Pathol Oral Radiol Endod. 2006;102:225–34.
12. Loubele M, Maes F, Jacobs R et al. Comparative study of image quality for MSCT and CBCT scanners for dentomaxillofacial radiology applications. Radiat Prot Dosimetry. 2008;129:222–6.
13. Loubele M, Jacobs R, Maes F et al. Image quality vs radiation dose of four cone beam computed tomography scanners. Dentomaxillofacial Radiol. 2008;37:309–19.
14. Hassan B, Souza PC, Jacobs R, de Azambuja Berti S, van der Stelt P. Influence of scanning and reconstruction parameters on quality of three-dimensional surface models of the dental arches from cone beam computed tomography. Clin Oral Invest. June 9, 2009 [e-pub ahead of print].
15. Stratemann SA, Huang JC, Maki K, Miller AJ, Hatcher DC. Comparison of cone beam computed tomography imaging with physical measures. Dentomaxillofac Radiol. 2008;37:80-93.
16. Hassan B, van der Stelt P, Sanderink G. Accuracy of three-dimensional measurements obtained from cone beam computed tomography surface-

rendered images for cephalometric analysis: influence of patient scanning position. Eur J Orthod. April 2009;31(2):129-134.
17. Periago DR, Scarfe WC, Moshiri M, Scheetz JP, Silveira AM, Farman AG. Linear accuracy and reliability of cone beam CT derived 3-dimensional images constructed using an orthodontic volumetric rendering program. Angle Orthod. May 2008;78(3):387-95.
18. Brown AA, Scarfe WC, Scheetz JP, Silveira AM, Farman AG. Linear accuracy of cone beam CT derived 3D images. Angle Orthod. January 2009;79(1):150-157.
19. Baumgaertel S, Palomo JM, Palomo L, Hans MG. Reliability and accuracy of cone-beam computed tomography dental measurements. American Journal of Orthodontics and Dentofacial Orthopedics. July 2009;136(1):19-25.
20. Lorensen WE, Cline HE. Marching cubes: a high resolution 3D surface construction algorithm. SIGGRAPH Comput. Graph. 1987;21:163–169.
21. Zhang Z. Iterative Point Matching for Registration of Free-form Curves and Surfaces. Int J Comput Vis. 1994; 13(2):119-1528.
22. Cevidanes LH, Bailey LJ, Tucker SF et al. Three-dimensional cone-beam computed tomography for assessment of mandibular changes after orthognathic surgery. American Journal of Orthodontics and Dentofacial Orthopedics. January 2007;131(1):44-50.
23. Hosntalab M, Zoroofi RA, Abbaspour Tehrani-Fard A, Shirani G. Segmentation of teeth in CT volumetric dataset by panoramic projection and variational level set. International Journal of Computer Assisted Radiology and Surgery. 2008;3(3):257-265.
24. Hui Gao, Oksam Chae. Touching tooth segmentation from CT image sequences using coupled level set method Int. J. electrical engineering, computer science, and electronics. 2009; 382-387
25. Jacobs R, van Steenberghe D. Role of periodontal ligament receptors in the tactile function of the teeth: a review. J Periodontal Res. 1994;29:153-67.
26. Halazonetis DJ. Commentary. Am J Orthod Dentofacial Orthop. July 2009;136(1):25-28.

Chapter III Applications of CBCT in endodontics

Part 3.1: Value of CBCT in detecting vertical root fractures in endodontically filled teeth

Hassan B, Metska ME, Ozok AR, van der Stelt P, Wesselink PR. Detection of vertical root fractures in endodontically treated teeth by a cone beam computed tomography scan. J Endod. 2009 May ;35(5):719-722.

Part 3.2: Comparison of five CBCT systems for detecting vertical root fractures in endodontically treated teeth

Hassan B, Metska ME, Ozok AR, van der Stelt P, Wesselink PR. Comparison of five Cone Beam Computed Tomography systems for detecting vertical root fractures in endodontically treated teeth. J Endod. 2009 [in press]

Part 3.3: Value of CBCT in determining the outcome of root canal treatment

Garcia de Paula-Silva FW, **Hassan B**, Bezerra da Silva LA, Leonardo MR, Wu M. Outcome of root canal treatment in dogs determined by periapical radiography and cone-beam computed tomography scans. J Endod. 2009 May ;35(5):723-726.

Part 3.1: Detection of Vertical Root Fractures in Endodontically Treated Teeth by a Cone Beam Computed Tomography Scan

Bassam Hassan, Maria Elissavet Metska, Ahmet Rifat Ozok,Paul van der and Paul Rudolf Wesselink

JOE (Journal of Endodontics) — Volume 35, Number 5, May 2009
J Endod 2009;35:719–722

Abstract

Our aim was to compare the accuracy of cone beam computed tomography (CBCT) scans and periapical radiographs (PRs) in detecting vertical root fractures (VRFs) and to assess the influence of root canal filling (RCF) on fracture visibility. Eighty teeth were endodontically prepared and divided into four groups. The teeth in groups A and B were artificially fractured, and teeth in groups C and D were not. Groups A and C were root filled. Four observers evaluated the CBCT scans and PR images. Sensitivity and specificity for VRF detection of CBCT were 79.4% and 92.5% and for PR were 37.1% and 95%, respectively. The specificity of CBCT was reduced ($p = 0.032$) by the presence of RCF, but its overall accuracy was not influenced ($p = 0.654$). Both the sensitivity ($p = 0.006$) and overall accuracy ($p = 0.008$) of PRs were reduced by the presence of RCF. The results showed an overall higher accuracy for CBCT (0.86) scans than PRs (0.66) for detecting VRF.

Key Words
Cone-beam computed tomography scan, diagnosis, periapical radiograph, root canal filling, vertical root fracture

Introduction:

A Definitive diagnosis of vertical root fractures (VRFs) in endodontically treated teeth is challenging. The clinical symptoms and radiographic signs are not completely pathognomonic (1–7), although dual sinus tracts or sinus tract–like pockets on opposite sides of a root are considered almost pathognomonic for a VRF (8). The prognosis of VRF is poor. In a 5-year follow-up study of nonsurgically endodontically treated teeth, root fracture was the untoward event in 32.1%, and the elected treatment was extraction (9).

Because periapical radiographs (PRs) are two-dimensional (2D) images of threedimensional anatomic structures, the superimposition of adjacent tissues may obscure the visibility of VRFs. Thus, direct visualization of a radiolucent fracture line on radiographs is the only explicit feature for detecting VRFs. A three-dimensional diagnostic imaging system could diagnose VRF more accurately. Conventional multidetector computed tomography (MDCT) scans were found superior to PRs in detecting VRFs (10). However, the radiation dose involved in MDCT scans, the limited availability, and the increased costs impede its use in dentistry (11, 12). Cone beam computed tomography (CBCT) scans, which provide comparable images at reduced dose and costs, are a better alternative to MDCT scans in endodontics (13, 14). CBCT scans use a cone-shaped x-ray beam to acquire a three-dimensional scan of the patient head in a single 360_ rotation (15).

Prototype local computed tomography scans and flat-panel detector CBCT systems that are used to scan ex vivo tissue samples were found useful for detecting VRFs (16, 17). The feasibility of clinical dental CBCT systems with a rotating x-ray tube and detector apparatus in detecting VRFs is thus far unknown. Also, because VRFs are most commonly associated with endodontically treated teeth, it is important to assess the possible influence of root canal filling on fracture line visibility. The first aim of this study was to evaluate the accuracy of a clinical dental CBCT system in comparison with digital PRs in detecting VRFs in root-filled and non-filled teeth. The second aim was to assess the influence of gutta-percha root canal filling on the detection of VRFs with CBCT scans or PRs.

Materials and Methods

Sample Preparation

Eighty extracted human teeth (40 premolars and 40 molars) were inspected using a stereomicroscope (Wild Photomakroscop M400, Wild, Heerbrugg, Switzerland) for the absence of VRFs. Access opening was made for each tooth, and the root canals were prepared with the ProTaper rotary system (Dentsply Maillefer, Tulsa, OK) until size F3. The teeth were divided into four groups: two experimental (A and B) and two controls (C and D). Each group consisted of 10 premolars and 10 molars (n = 20), which were decoronated to eliminate bias of enamel fractures.
In groups A and B, the teeth were stabilized in copper rings filled with light body impression material (Express 2 VPS; 3M ESPE, Zoeterwoude, The Netherlands), and a holder was used to fix the samples in place. A tapered chisel inserted in the canal space was tapped gently with a hammer to induce a VRF. The fractured teeth were inspected again under the stereomicroscope to confirm the presence of VRFs. The fracture line orientation (buccolingual or mesiodistal) was also recorded. A well-fitting gutta-percha cone was inserted in the canals of groups A and C. One investigator, who was not involved in the observation, coded the teeth and placed them in premade sockets in 10 dry human mandibles bilaterally in the posterior region. The mandibles were coated with three layers of dental wax buccally and lingually to simulate soft tissue. Agar-agar (Merck, Darmstadt, Germany) was used to fix the teeth in these holes and to fill the gaps between the root surface and the socket.

Radiographic Scan

The sample was scanned using the I-CAT CBCT (120 KvP, 5 mA; Imaging Sciences, Hatfield, PA). The scans were made according to the manufacturer's recommended protocol to scan the mandible with the 10 _ 16 cm field of View (FoV) selection. The datasets were exported in DICOM 3 file format, and the size of the isotropic voxel was 0.25 mm. The PR images were made with a fixed x-ray unit (Siemens Heliodent MD, Erlangen, Germany) and size 2 phosphor-plate films (Digora, Tuusula, Finland) following manufacturer's recommendations, two radiographs per tooth, one using parallel technique and the other with mesial angulation.

Data Analysis

The images were imported into image analysis and visualization software (Amira 4.2.0; Visage Imaging, Carlsbad, CA). Orthographic tomographic reconstructions were created in axial, sagittal, and coronal directions. Four observers (two endodontists and two fourth-year dental students) were calibrated by training them in CBCT images using dummy datasets from a pilot study. All images were displayed on a 21-inch flat-panel screen (Philips Brilliance, Amsterdam, The Netherlands). Each observer assessed the presence or absence of a VRF on a dichotomous scale (fractured/nonfractured). CBCT images were reviewed in the three reconstruction planes (axial, coronal, and sagittal), and a single score was obtained for each tooth (Fig. 1). PR images were reviewed, and a single score was also obtained per tooth.
The radiographic features for detecting a VRF on a CBCT scan were the direct visualization of a radiolucent line, which traversed the trunk of the root separating it either partially or completely into two segments that is followed on at least two consecutive slices (10). The radiographic feature for detecting VRF on PRs was also the direct visualization of a radiolucent line, which traversed the root surface on either the parallel or the mesially angulated images.

Statistical Analysis

The data were analyzed on SPSS 16.0 software (SPSS Benelux, Gorinchem, The Netherlands). A two-sided chi-square test was used to measure the sensitivity and specificity of both CBCT scans and PRs for the detection of VRF. A univariate analysis of variance was used to assess the influence of the radiographic technique (CBCT scans or PRs), filling material (filled or nonfilled), and the level of expertise (endodontists or dental students) on overall accuracy in detecting VRFs. Overall sensitivity and specificity were first calculated for all teeth and then separately for filled and nonfilled teeth. Sensitivity was also calculated per fracture orientation (buccolingual and mesiodistal). The overall agreement among the observers was measured by using Cohen’s kappa. The alpha value was set to 0.05.

Results

The sensitivity and specificity results for CBCT scans and PRs are reported in Table 1. The overall sensitivity of detecting VRFs was significantly higher for CBCT scans compared with PRs ($p = 0.0001$). The overall specificity of CBCT scans was slightly lower than PRs but not significantly different ($p = 0.489$). CBCT scans were overall significantly more accurate than PRs in detecting VRFs ($p = 0.0001$). The accuracy of CBCT scans was 0.86 and that of PRs was 0.66.

The presence of root canal filling (RCF) did not significantly influence the sensitivity of CBCT scans ($p = 0.84$), but it reduced their specificity ($p = 0.016$). For PRs, the presence of RCF reduced sensitivity ($p = 0.006$) with no significant influence on specificity ($p = 0.471$).

The presence of RCF reduced overall accuracy of PRs ($p = 0.008$) but not that of CBCT scans ($p = 0.654$). Of all fractured roots, fracture lines in 67.5% were in the buccolingual direction and 32.5% were in the mesiodistal direction (Fig. 2). The sensitivity of CBCT scans was higher than PRs for detecting both buccolingual and mesiodistal fractures (Table 1). The overall agreement among the observers was moderate ($k = 0.521$). There was no significant difference in overall accuracy between and among the observers for detecting VRFs by both CBCT scans and PRs ($p = 0.76$).

TABLE1: Overall Sensitivity and Specificity Percentages of CBCT Scans and PRs per Observer Group and Root Filling.

Scanner	Endodontists	Dental Students	Both Groups	Root-filled	Non-filled	Bucco-lingual	Mesio-distal
CBCT							
Sensitivity	77.5	81.3	79.4	78.8	80.0	87.0	63.5
Specificity	91.3	93.8	92.5	87.5	97.5	_	_
PR							
Sensitivity	37.5	36.7	37.1	26.6	47.5	51.4	7.7
Specificity	95.0	95.0	95.0	93.8	96.2	_	_

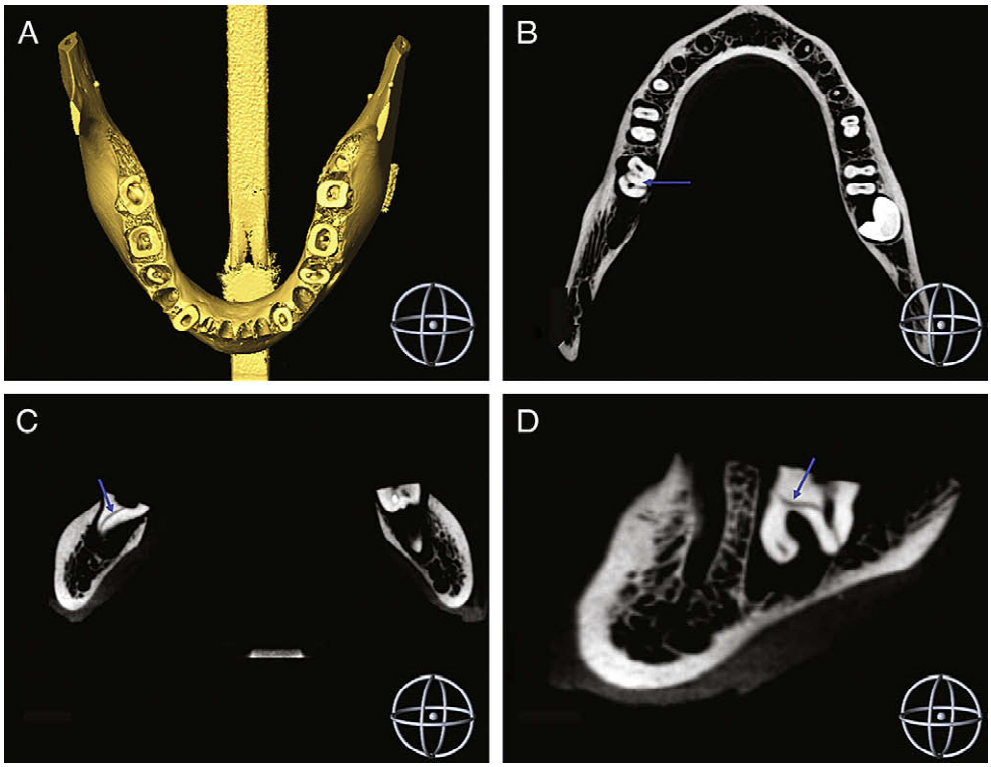

Figure 1. I-CAT CBCT reconstructions. (A) Three-dimensional surface reconstruction of the mandible. Fracture line is visible on 2D slices (arrow). (B) Axial, (C) coronal, and (D) sagittal.

Discussion

This study investigated the feasibility of CBCT scans in detecting VRFs in endodontically treated teeth. The results show an overall higher accuracy of CBCT scans in comparison with PRs. The overall sensitivity of CBCT scans was significantly higher than PRs in detecting fracture lines. The high sensitivity of CBCT scans is evidently caused by the higher inherent contrast of tomographic imaging in comparison with conventional 2D projection imaging. The three-dimensional nature of CBCT scans allows visualizing the fracture line from multiple angles and different orientations at very thin slices and at a very high contrast. Conversely, the 2D nature of PRs obscured the visibility of the fracture line because of the inherent superimposition artifact, which may explain the low sensitivity of PRs in detecting VRFs. The overall specificity was high and comparable for both CBCT scans and PRs. The high specificity for PRs could be explained by

the fact that most teeth were scored negatively for VRF because most fractures were not visible.

Although the overall accuracy of CBCT scans was not reduced by the presence of RCF, its specificity was reduced. Radiopaque substances such as gutta-percha cones create distinct star-shaped streak artifacts on tomographic slices that can mimic fracture lines on CBCT images (18), which may decrease observer confidence in diagnosing VRFs. On the other hand, RCF significantly reduced the overall accuracy of PRs and the overall sensitivity, leading to more false-negative results. In accord with previous findings, there were more buccolingual fractures (67.5%) than mesiodistal fractures (32.5%) in this study (15). Therefore, it is probable that most of the fracture lines were obscured by the filling. The sensitivity of PRs for detecting mesiodistal fractures was very low (7.7%) compared with the detection of buccolingual fractures (51.4%). The mesiodistal fractures are almost impossible to detect with 2D radiographs because the x-ray beam must be within 4_ of the fracture plane to allow detection (19). In fact, this suggests that the sensitivity of PR could have been even lower if there were more mesiodistal fractures in the sample. The sensitivity of CBCT scans was higher than PRs for both fracture types (87% and 63.5%), respectively.

Both observer groups were comparable in their ability to detect VRF on both systems with no observable predilection of the more experienced group over the less experienced group. Both groups received similar training during the calibration session and the detection criteria of a VRF on both systems were clearly defined, which can explain this lack of significant difference. The detection of VRF was limited by the voxel size (0.25 mm) and the contrast-to-noise ratio of the selected scan field. The method in which the fractures were created may not reflect the actual clinical situation. For example, the distance between the fragments may in some teeth slightly deviate from that generally seen in vivo. However, our aim was to compare the accuracy of the two radiographic techniques, and this was performed under same conditions for both techniques.

Our results corroborate previous findings that CBCT scans are superior to PRs in detecting longitudinal root fractures (16, 17). Previous studies used prototype CBCT systems, which are not clinical and cannot be used to scan patients. Also, they have different scanning and reconstruction settings from dental CBCT systems currently available. In those studies, the influence of the presence of RCF on the visibility of VRFs was not assessed either. More

research is required to determine patient scanning and data-reconstruction parameters with CBCT scans that could influence the visibility of the fracture line. In conclusion, CBCT scans are more accurate than PRs for detecting VRFs, and the presence of RCF does not reduce its accuracy.

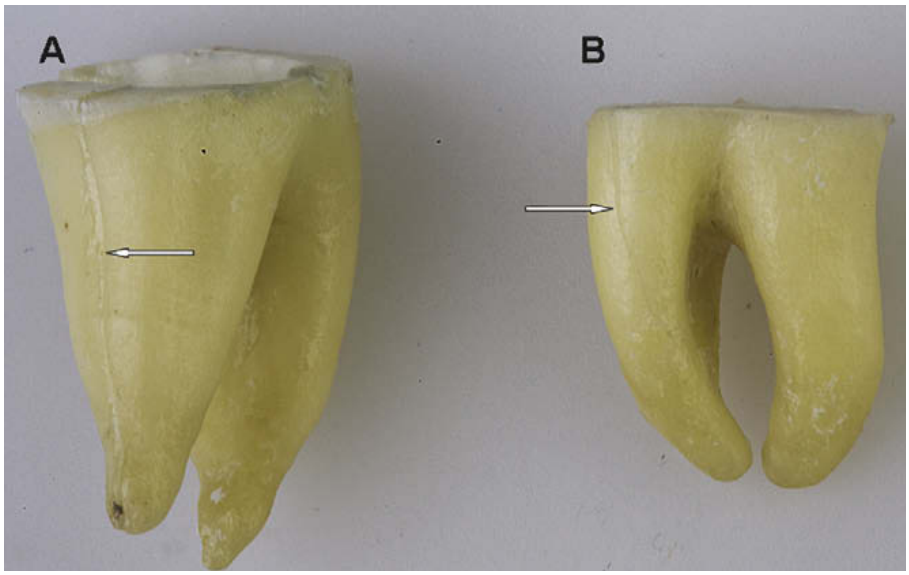

Figure 2. A light photograph showing vertical root fracture on two teeth by fracture line orientation (arrow). (A) Mesiodistal and (B) buccolingual.

Acknowledgment

We would like to thank Dr Hans Verheij for his contribution in conducting the statistical analysis and Dr H. de Jonge for his support with the I-CAT scans.

References

1. Tamse A, Fuss Z, Lustig J, Ganor Y, et al. Radiographic features of vertically fractured, endodontically treated maxillary premolars. Oral Surg Oral Med Oral Pathol Oral Radiol Endod 1999;88:348–52.
2. Tamse A, Fuss Z, Lustig J, et al. An evaluation of endodontically treated vertically fractured teeth. J Endod 1999;25:506–8.
3. Tamse A, Kaffe I, Lustig J, et al. Radiographic features of vertically fractured endodontically treated mesial roots of mandibular molars. Oral Surg Oral Med Oral Pathol Oral Radiol Endod 2006;101:797–802.
4. Tamse A. Vertical root fractures in endodontically treated teeth: diagnostic signs and clinical management. Endod Topics 2006;13:84–94.
5. Krell KV, Rivera EM. A six year evaluation of cracked teeth diagnosed with reversible pulpitis: treatment and prognosis. J Endod 2007;33:1405–7.
6. Opdam NJ, Roeters JJ, Loomans BA, et al. Seven-year clinical evaluation of painful cracked teeth restored with a direct composite restoration. J Endod 2008;34:808–11.
7. Shemesh H, van Soest G, Wu M-K, et al. Diagnosis of vertical root fractures with optical coherence tomography. J Endod 2008;34:739–42.
8. Pitts DL, Natkin E. Diagnosis and treatment of vertical root fractures. J Endod 1983; 9:338–46.
9. Chen SC, Chueh LH, Hsiao CK, et al. First untoward events and reasons for tooth extraction after nonsurgical endodontic treatment in Taiwan. J Endod 2008;34:671–4.
10. Youssefzadeh S, Gahleitner A, Dorffner R, et al. Dental vertical root fractures: value of CT in detection. Radiology 1999;210:545–9.
11. Ludlow JB, Ivanovic M. Comparative dosimetry of dental CBCT devices and 64-slice CT for oral and maxillofacial radiology. Oral Surg Oral Med Oral Pathol Oral Radiol Endod 2008;106:106–14.
12. Cotton TP, Geisler TM, Holden DT, et al. Endodontic applications of cone-beam volumetric tomography. J Endod 2007;33:1121–32.
13. Loubele M, Bogaerts R, Van Dijck E, et al. Comparison between effective radiation dose of CBCT and MSCT scanners for dentomaxillofacial applications. Eur J Radiol 2008. in press.
14. Tsiklakis K, Donta C, Gavala S, et al. Dose reduction in maxillofacial imaging using low dose cone beam CT. Eur J Radiol 2005;56:413–7.
15. Patel S, Dawood A, Ford TP, et al. The potential applications of cone beam computed tomography in the management of endodontic problems. Int Endod J 2007;40: 818–30.
16. Mora MA, Mol A, Tyndall DA, et al. In vitro assessment of local computed tomography for the detection of longitudinal tooth fractures. Oral Surg Oral Med Oral Pathol Oral Radiol Endod 2007;103:825–9.
17. Hannig C, Dullin C, Hu¨ lsmann M, et al. Three-dimensional, non-destructive visualization of vertical root fractures using flat panel volume detector computer tomography: an ex vivo in vitro case report. Int Endod J 2005;38:904–13.
18. Zhang Y, Zhang L, Zhu XR, et al. Reducing metal artifacts in cone-beam CT images by preprocessing projection data. Int J Radiat Oncol Biol Phys 2007; 67:924–32.
19. Rud J, Omnell K. Root fractures due to corrosion. Diagnostic aspects. Scand J Dent Res 1970;78:397–403.

Part 3.2: Comparison of five Cone Beam Computed Tomography systems for the detection of vertical root fractures

Bassam Hassan, Maria Elissavet Metska, Ahmet Rifat Ozok,Paul van der and Paul Rudolf Wesselink

JOE 2009 [in print]

Abstract:

Introduction: This study compared the accuracy of cone beam computed tomography (CBCT) scans made by five different systems in detecting vertical root fractures (VRFs). It also assessed the influence of the presence of root canal filling (RCF), CBCT slice orientation selection and the type of tooth (premolar/molar) on detection accuracy.
Methods: Eighty endodontically prepared teeth were divided into four groups, and placed in dry mandibles. The teeth in groups Fr-F and Fr-NF were artificially fractured; those in groups Control-F and Control-NF were not. Groups Fr-F and Control-F were root-filled. CBCT scans were made using five different commercial CBCT systems. Two observers evaluated images in axial, coronal and sagittal reconstruction planes.
Results: There was a significant difference in detection accuracy among the five systems (p=0.00001). The presence of RCF did not influence sensitivity (p= 0.16) but it reduced specificity (p= 0.003). Axial slices were significantly more accurate than sagittal and coronal slices (p=0.0001) in detecting VRF in all systems. Significantly more VRFs were detected among molars than premolars (p=0.0001).
Conclusions: RCF presence reduced specificity in all systems (p= 0.003) but did not influence accuracy (p= 0.79) except in one system (p= 0.012). Axial slices were the most accurate in detecting VRFs (p =0.0001).

Introduction:

The clinical and radiographic diagnosis of vertical root fractures (VRFs) is often complicated. A local deep pocket, dual sinus tracts and a halo type of lateral radiolucency are among the symptoms (1-8). Often these symptoms are not convincing to justify tooth extraction, which usually is the elected treatment since prognosis of VRFs is poor. Therefore, exact diagnosis of a VRF is crucial to avoid erroneous extraction. However, due to the two dimensional (2D) nature of periapical radiographs (PRs) and the inherent superimposition projection artifacts, visualizing a VRF is difficult, especially when the fracture line is mesio-distally oriented (9). The presence of a VRF is only confirmed by direct visualization (10). This may sometimes be accomplished by means of a surgical diagnostic flap, which is quite invasive.

Cone Beam Computed Tomography (CBCT) specifically designed for the maxillofacial region has become largely accessible to clinicians, and replaced conventional CT for dentomaxillofacial applications due to their reduced radiation dose, and installation and maintenance costs (11-13). Prototype flat panel CBCT systems were found useful in detecting VRFs (14, 15). Those systems, however, cannot be used to scan patients. Recently, a CBCT system was found more accurate than PR in detecting VRFs in root-filled teeth (16). The superiority of CBCT over PR is primarily due to the high contrast and three-dimensional nature of tomographic imaging, which permits direct visualization of fracture lines otherwise masked in PR.

Several dentomaxillofacial CBCT systems are currently on the market. Those systems differ from each other in detector design, patient scanning settings and data reconstruction parameters (17-21). Several scanning and reconstruction factors including scan field of view (FoV) selection and voxel size, the number of basis projections (acquisitions) used for reconstruction, and image artifacts have significant influence on image quality in CBCT. CBCT systems vary in their image quality and ability to visualize anatomical structures (22-27). This variation is most prominent with small and delicate anatomical structures such as periodontal ligament and trabecular bone (28). It is, therefore, probable that different CBCT systems vary in their ability to detect VRFs since the fractures are small. The influence of the presence of RCF on VRF visibility could also vary among the different scanners. Additionally, the selection of the reconstruction plane (axial, sagittal or coronal) used for detection or the type of tooth could have an

influence on VRF detection. This study aimed 1) to compare the accuracy of five clinical CBCT systems for detecting VRFs in endodontically-prepared teeth and 2) to assess the influence of the presence of a RCF, slice orientation selection, and the type of tooth on accuracy for detecting VRF in each system.

Material and methods:

Sample preparation:

We used the method described by Hassan *et al.* (16). Briefly, 40 extracted premolars and 40 molars were inspected on a stereomicroscope (Wild photomakroscop M400, Wild, Heerbrugg, Switzerland) for the absence of VRFs. Endodontically-prepared root canals (size F3, ProTaper, Dentsply Maillefer, Tulsa, OK) were divided into two experimental (Fr-F and Fr-NF) and two control groups (Control-F and Control-NF). Each group consisted of 10 premolars and 10 molars (n = 20). The teeth were decoronated to eliminate bias of enamel fractures.
The roots in groups Fr-F and Fr-NF were vertically fractured using the method described by Hassan *et al.* (16). The fractured teeth in these two groups were inspected again under the stereomicroscope to confirm the presence of VRFs.
Fracture line orientation (buccolingual or mesiodistal) was also recorded. A well-fitting gutta-percha cone was inserted in the canals of groups Fr-F and Control-F. One investigator, who was not involved in the observation, coded the teeth, and fixed them with agar-agar (Merck, Darmstadt, Germany) in premade sockets bilaterally in the posterior region in 10 dry human mandibles, which were coated with three layers of dental wax (Tenatex Red, Kemdent, Swindon, UK) buccally and lingually to provide some level of soft tissue simulation.

Radiographic scans:

The sample was scanned using five CBCT systems according to the protocols recommended by the manufacturer. The CBCT systems were: 1) NewTom 3G (QR SLR, Verona, Italy) 2) Next Generation I-CAT (Imaging Sciences International, Hatfield, Pennsylvania) 3) Galileos 3D (Sirona Germany, Bensheim, Germany) 4) Scanora 3D (Soredex, Tuusula, Finland) and 5) 3D AccuiTomo-xyz (J. Morita, Kyoto, Japan). Systems specifications and scan settings are shown in Table1. The scanned data were exported in DICOM 3 format.

Data analysis:

The axial, coronal and sagittal tomographic slices of the datasets were created in Amira image analysis software (V4.2.0, Visage imaging, Carlsbad, CA). Two blinded and calibrated experienced endodontists assessed the images on each slice orientation independently. The calibration included training on the radiographic features of VRF on CBCT. The visibility of a radiolucent fracture line crossing the root either completely or partially on at least two consecutive slices was the main radiographic feature for detecting a VRF (16). Images were displayed on a 21-inch flat-screen panel (Philips Brilliance, Best, Netherlands). Each observer assessed the presence of VRF on a dichotomous scale (fractured/not-fractured). A separate score for detecting VRF was obtained for each slice orientation (axial, sagittal and coronal). The root was considered fractured when a fracture line was detected on any one of the three slices.

Table1: Scan and reconstruction settings for the five CBCT systems. Sensitivity, specificity, overall accuracy for the detecting vertical root fractures and accuracy for root canal filled (RCF) teeth, for the tooth-type (premolar or molar) per CBCT system. Kappa inter-observer agreement per system.

Scanner	Manufacturer-Detector type	kVp[3]	mA[4]	Scan FoV (cm)[5]	Voxel Size (mm)	Sensitivity Overall	Specificity Overall	Accuracy Overall	Accuracy Axial	Accuracy Coronal	Accuracy Sagittal	Accuracy RCF	Accuracy Premolars	Accuracy Molars	Kappa
NewTom 3G	AFP imaging-IIT/CCD[1]	110	2,4	10 x 10	0,20	30,4	95	62,7	61,5	51,9	55,8	62,5	54,4	71,3	0.25 fair
Next Generation I-CAT	Imaging Sciences Int-FPD[2]	120	5	10 x 16	0,25	77,5	91,3	84,4	84,4	65,7	68,2	81,3	78,8	90	0.68 good
Galileos 3D	Sirona-IIT/CCD	85	7	15 x 15	0,30	18,8	85	51,9	51,9	51,3	48,8	53,8	47,5	56,3	0.03 poor
Scanora 3D	Soredex/ FPD	85	10	7.5 x 10	0,20	57,5	85	71,3	70,7	68,2	63,2	72,5	63,8	78,8	0.42 moderate
AccuiTomo-xyz	J.Morita-IIT/CCD	80	3,3	3 x 4	0,25	48,1	90,7	69,4	67,4	59,9	65,1	66,9	58,9	78,9	0.38 fair

[1] Image Intensifier Tube/Charged Coupled Device
[2] Flat Panel Detector
[3] kilo Volt Peak
[4] milli Ampere
[6] Scan Field of View selection in centimeters

Statistical analysis:

The data were analyzed on SPSS software (v16.0, SPSS Benelux, Gorinchem, Netherlands). The radiographic measurements were compared with the gold standard (physical observations) using two-sided Chi-square test to determine the sensitivity and specificity of each system in detecting VRFs. A Univariate Analysis of Variance test assessed the influence of the: 1) choice of CBCT system 2) presence of a root canal filling (RCF) 3) reconstruction slice orientation (axial, coronal or sagittal) and 4) effect of tooth type (premolar, molar) on the detection accuracy of VRF. Additionally, the influence of VRF line orientation (buccolingual or mesiodistal) was also assessed. A Cohen's Kappa measured the overall and per system agreement between the two observers. The alpha value was set to 0.05.

Results:

The Kappa agreement measure, sensitivity, specificity and accuracy results for the five CBCT systems are summarized in (Table 1). There was a statistically significant difference among the five scanners in their sensitivity for detecting VRF ($p= 0.0001$) and no statistically significant difference in their specificity ($p= 0.17$). There was a statistically significant difference in overall accuracy among the five systems ($p=0.0001$) (Table 1). The presence of RCF did not influence sensitivity ($p= 0.16$) but it reduced specificity ($p= 0.003$). RCF did not reduce overall accuracy in detecting VRF on CBCT ($p = 0.79$) except for the Galileos 3D system ($p =0.012$). Axial slices were significantly more accurate than sagittal and coronal slices ($p=0.0001$) in detecting VRF in all systems (Table 1). Significantly more VRFs were detected among molars than premolars ($p=0.0001$). There was no significant influence of VRF line orientation (buccolingual or mesiodistal) on detection accuracy ($p=0.21$). The overall agreement between the observers was fair ($\kappa = 0.385$). The agreement for i-CAT was good ($\kappa = 0.68$) and it was better compared to those for other systems (Table 1).

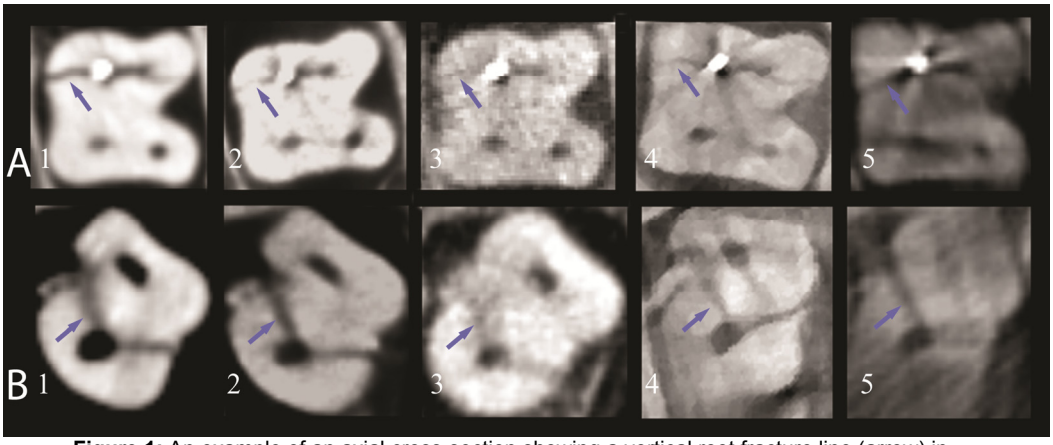

Figure 1: An example of an axial cross-section showing a vertical root fracture line (arrow) in an endodontically filled root (row A) and in a non-filled root (row B). Cone Beam Computed Tomography systems from left to right: 1) Next Generation iCAT 2) Scanora 3D 3) NewTom 3G 4) AccuiTomo MTC-1 5) Galileos 3D.

Discussion:

The Next Generation I-CAT was the most accurate system followed by the Scanora 3D. The other three systems were significantly less accurate in detecting VRF. Possible explanations for the variation include differences in detector type and characteristics, scan FoV selection and voxel size (which influence contrast and resolution) as well as system-specific image artifacts.

Based on detector design technology current CBCT systems are categorized into: 1) Image Intensifier Tube/Charged Coupled Device (IIT/CCD) combinations or 2) Flat Panel Detectors (FPD) (29). It is reported that IIT/CCD detectors are inferior to FPD in terms of reduced dynamic range, contrast and spatial resolution, increased pixel noise and image artifacts (30, 31). While ICAT and Scanora 3D are both FPD-based systems, the other three systems are IIT/CCD-based (Table1). This might explain the superiority of those two systems to the other three.

The influence of FoV selection during the scan is equally important. Broadly, based on FoV selections CBCT systems are categorized into: 1) Small (dental) volume usually used for scanning few teeth or one jaw 2) Medium (maxillofacial) volume covering both jaws, the maxillary sinus and part of the nose and c) Large (Craniofacial) volume, which covers the entire maxillofacial region extending in some systems to the cranial vertex superiorly (17-21). FoV selection is directly related to voxel size, and

influences spatial and contrast resolution. Larger FoV selection provides less resolution and contrast in comparison with small FoV and this directly influences the visibility of anatomical structures with CBCT (28-31). Some CBCT systems, such asGalileos 3D, provide a single scan FoV selection of 15x15cm, which cannot be modified. It was, therefore, impossible to standardize the FoV and voxel size selections for all of the systems included in this study. However, an attempt was made to obtain the scans with comparable scan FoVs and voxels sizes as much as possible.

The number of basis projections obtained during the scan, data reconstruction parameters (algorithms) and machine-specific image artifacts may also contribute to the variation among the systems (28-33). An image of low quality is difficult to be interpreted and a definite diagnosis cannot be done easily. More false positives and/or false negatives arise, thus reducing the systems' overall accuracy. That is a possible explanation for the fair and poor kappa scores, especially for the Galileos 3D system (Table1**)**.

The presence of RCF reduced specificity in all systems leading to more false positive results (Table1). Radio-opaque materials such as gutta-percha cones create streak artifacts that mimic fracture lines (16). However, the presence of RCF did not reduce overall detection accuracy except in the Galileos system, which was associated with many artifacts (Figure 1).

VRFs extend by definition longitudinally onto the root surface. It is therefore logical that a horizontal cross-section perpendicular to the VRF should provide best detection. Indeed, axial slices were more accurate than coronal and sagittal ones in detecting VRFs in all systems (Table 1). The fracture line orientation had no significant influence on the detection accuracy. This corroborates previous finding that CBCT is insensitive to VRF line orientation due to its three-dimensional nature (16).

The study was limited to the CBCT systems that were accessible when this study was conducted. New models with different technical specifications appear on the market each year from the same or other manufacturers. Whether those CBCT systems or models would perform differently remains to be investigated.

In conclusion, there is large variation among the different CBCT systems in their ability to detect VRFs ex-vivo possibly due to the detector characteristics of each system, FoV and voxel size selections and other

several CBCTspecific image artifacts. The presence of RCF reduced specificity in all systems but it did not influence overall accuracy except in the Galileos 3D system. Axial slices are more accurate than sagittal and coronal for detecting VRFs.

Acknowledgement:

We would like to thank Dr. Hans Verheij for his support with the statistical analysis and the following individuals and institutes for the CBCT scans: 1) Prof. Dr. R. Jacobs (Oral Imaging Centre, KULEUVEN University, Leuven, Belgium) for the Scanora 3D and the AccuiTomo-xyz scans 2) Dr. C. Politis and Sun Yi (Department of oral and maxillofacial surgery, St. John's hospital, Gent, Belgium) for the Galileos 3D scans and 3) Dr. H. De Jonge (Atrium Medical Centre, Heerlen, The Netherlands) for the I-CAT scans.

References:

1. Tamse A, Fuss Z, Lustig J, Ganor Y, Kaffe I. Radiographic features of vertically fractured, endodontically treated maxillary premolars. Oral Surg Oral Med Oral Pathol Oral Radiol Endod 1999;88:348-52.
2. Tamse A, Fuss Z, Lustig J, Kaplavi J. An evaluation of endodontically treated vertically fractured teeth. J Endod 1999;25:506-8.
3. Tamse A, Kaffe I, Lustig J, Ganor Y, Fuss Z. Radiographic features of vertically fractured endodontically treated mesial roots of mandibular molars. Oral Surg Oral Med Oral Pathol Oral Radiol Endod 2006;101:797-802.
4. Tamse A. Vertical root fractures in endodontically treated teeth: diagnostic signs and clinical management. Endod Topics 2006;13:84-94.
5. Krell KV, Rivera EM. A six year evaluation of cracked teeth diagnosed with reversible pulpitis: treatment and prognosis. J Endod 2007;33:1405-7.
6. Opdam NJ, Roeters JJ, Loomans BA, Bronkhorst EM. Seven-year clinical evaluation of painful cracked teeth restored with a direct composite restoration. J Endod 2008;34:808-11.
7. Shemesh H, van Soest G, Wu M-K, Wesselink PR. Diagnosis of vertical root fractures with optical coherence tomography. J Endod 2008;34:739-42.
8. Pitts DL, Natkin E. Diagnosis and treatment of vertical root fractures. J Endod 1983;9:338-46.
9. Rud J, Omnell K. Root fractures due to corrosion. Diagnostic aspects. Scand J Dent Res 1970;78:397-403.
10. Moule AJ, Kahler B. Diagnosis and management of teeth with vertical root fractures. Aust Dent J 1999;44:75-87.
11. Ludlow JB, Ivanovic M. Comparative dosimetry of dental CBCT devices and 64-slice CT for oral and maxillofacial radiology. Oral Surg Oral Med Oral Pathol Oral Radiol Endod 2008;106:106-14.
12. Cotton TP, Geisler TM, Holden DT, Schwartz SA, Schindler WG. Endodontic applications of cone-beam volumetric tomography. J Endod 2007;33:1121-32.

13. Loubele M, Bogaerts R, Van Dijck E, Pauwels R, Vanheusden S, Suetens P, Marchal G, Sanderink G, Jacobs R. Comparison between effective radiation dose of CBCT and MSCT scanners for dentomaxillofacial applications. Eur J Radiol 2008;16 [e-pub ahead of print].
14. Mora MA, Mol A, Tyndall DA, Rivera EM. In vitro assessment of local computed tomography for the detection of longitudinal tooth fractures. Oral Surg Oral Med Oral Pathol Oral Radiol Endod 2007;103:825-9.
15. Hannig C, Dullin C, Hulsmann M, Heidrich G. Three-dimensional, nondestructive visualization of vertical root fractures using flat panel volume detector computer tomography: an ex vivo in vitro case report. Int Endod J
2005;38:904-13.
16. Hassan B, Metska ME, Ozok AR., Van der Stelt P., Wesselink PR. Detection of vertical root fractures in endodontically treated teeth by cone beam computed tomography. J Endod 2009 (in press).
17. Mozzo P, Procacci C, Tacconi A, Martini PT, Andreis IA. A new volumetric CT machine for dental imaging based on the cone-beam technique: preliminary results. Eur Radiol 1998;8:1558-64.
18. Kobayashi K, Shimoda S, Nakagawa Y, Yamamoto A. Accuracy in measurement of distance using limited cone-beam computerized tomography. Int J Oral Maxillofac Implants 2004;19:228-31.
19. Araki K, Maki K, Seki K, Sakamaki K, Harata Y, Sakaino R, Okano T, Seo K. Characteristics of a newly developed dentomaxillofacial X-ray cone beam CT scanner (CB MercuRay): system configuration and physical properties.
Dentomaxillofac Radiol 2004;33:51-9.
20. Sukovic P. Cone beam computed tomography in craniofacial imaging. Orthod Craniofac Res 2003;6 Suppl 131-6; discussion 179-82.
21. Arai Y, Tammisalo E, Iwai K, Hashimoto K, Shinoda K. Development of a compact computed tomographic apparatus for dental use. Dentomaxillofac Radiol 1999;28:245-8.
22. Loubele M, Guerrero ME, Jacobs R, Suetens P, van Steenberghe D. A comparison of jaw dimensional and quality assessments of bone characteristics with cone-beam CT, spiral tomography, and multi-slice spiral CT. Int J Oral Maxillofac Implants 2007;22:446-54.
23. Loubele M, Maes F, Schutyser F, Marchal G, Jacobs R, Suetens P. Assessment of bone segmentation quality of cone-beam CT versus multislice spiral CT: a pilot study. Oral Surg Oral Med Oral Pathol Oral Radiol Endod 2006;102:225-34.
24. Loubele M, Maes F, Jacobs R, van Steenberghe D, White SC, Suetens P. Comparative study of image quality for MSCT and CBCT scanners for dentomaxillofacial radiology applications. Radiat Prot Dosimetry 2008;129:222-6.
25. Mischkowski RA, Scherer P, Ritter L, Neugebauer J, Keeve E, Zöller JE. Diagnostic quality of multiplanar reformations obtained with a newly developed cone beam device for maxillofacial imaging. Dentomaxillofac Radiol 2008;37:1-9.
26. Kwong JC, Palomo JM, Landers MA, Figueroa A, Hans MG. Image quality produced by different cone-beam computed tomography settings. Am J Orthod Dentofacial Orthop 2008;133:317-27.
27. Bryant JA, Drage NA, Richmond S. Study of the scan uniformity from an i-CAT cone beam computed tomography dental imaging system. Dentomaxillofac Radiol 2008;37:365-74.
28. Liang X, Jacobs R, Hassan B, Li L, Powels R, Corpas L, Couto Souza P, Marten W, Shahbazian M, Alonso A, Lambrichts I. A comparative evaluation of dentomaxillofacial CBCT and MSCT image data– Part I: on subjective image quality. Eur J Radiol 2009 (in-press).
29. Scarfe WC, Farman AG. What is cone-beam CT and how does it work? Dent Clin North Am 2008;52:707-30.

30. Katsumata A, Hirukawa A, Okumura S, Naitoh M, Fujishita M, Ariji E, Langlais RP. Effects of image artifacts on gray-value density in limited-volume cone-beam computerized tomography. Oral Surg Oral Med Oral Pathol Oral Radiol Endod 2007;104:829-36.
31. Katsumata A, Hirukawa A, Okumura S, Naitoh M, Fujishita M, Ariji E, Langlais RP. Relationship between density variability and imaging volume size in cone-beam computerized tomographic scanning of the maxillofacial region: an in vitro study. Oral Surg Oral Med Oral Pathol Oral Radiol Endod
2009;107:420-5.
32. Mora MA, Mol A, Tyndall DA, Rivera EM. Effect of the number of basis images on the detection of longitudinal tooth fractures using local computed tomography. Dentomaxillofac Radiol 2007;36:382-6.
33. van Daatselaar AN, van der Stelt PF, Weenen J. Effect of number of projections on image quality of local CT. Dentomaxillofac Radiol 2004;33:361-9.

Part 3.3: Outcome of Root Canal Treatment in Dogs Determined by Periapical Radiography and Cone-Beam Computed Tomography Scans

Francisco Wanderley Garcia de Paula-Silva, Bassam Hassan,
Le´a Assed Bezerra da Silva, Ma´rio Roberto Leonardo and Min-Kai Wu

JOE — Volume 35, Number 5, May 2009

Abstract
The purpose of this study was to compare the favorable outcome of root canal treatment determined by periapical radiographs (PRs) and cone beam computed tomography (CBCT) scans. Ninety-six roots of dogs' teeth were used to form four groups (n= 24). In group 1, root canal treatments were performed in healthy teeth. Root canals in groups 2 through 4 were infected until apical periodontitis (AP) was radiographically confirmed. Roots with AP were treated by one-visit therapy in group 2, by two-visit therapy in group 3, and left untreated in
group 4. The radiolucent area in the PRs and the volume of CBCT-scanned periapical lesions were measured before and 6 months after the treatment. In groups 1, 2, and 3, a favorable outcome (lesions absent or reduced) was shown in 57 (79%) roots using PRs but only in 25 (35%) roots using CBCT scans ($p = 0.0001$). Unfavorable outcomes occurred more frequently after one-visit therapy than two-visit therapy when determined by CBCT scans ($p = 0.023$). (J Endod 2009;
35:723–726)

Key Words
Cone-beam computed tomography (CBCT), favorable (unfavorable) outcome, periapical radiography (PR), root canal treatment

Introduction:

Both clinical and radiographic findings are used to determine treatment outcome. Because posttreatment apical periodontitis (AP) is often asymptomatic, the outcome has been determined by periapical radiographs (PRs) alone in many clinical studies (1). However, AP with bone loss may not result in an apical radiolucency on PRs, depending on the density and thickness of the overlying cortical bone and the distance between the lesion and the cortical bone (2–5). When a bone lesion is within the cancellous bone and the overlying cortical bone is substantial, the bone lesion may not be visible. Clinically, it has been reported that a large lesion of up to 8 mm in diameter can be present without radiolucency (6, 7).

The aim of root canal treatment is to reduce root infection to a minimal level and eliminate AP (8–10). In two studies in which the relationship between histologic and radiologic signs of inflammation was determined in human cadavers, the negative predictive value of radiologic inflammatory signs was 53% and 67%, respectively (11, 12). In a study on dogs, the negative predictive value of radiologic signs was 55% (13). This means that when an intact periradicular region was diagnosed radiographically, only 55% of the cases were uninflamed histologically. Because posttreatment AP could be radiographically invisible, the unfavorable treatment outcome could be underestimated in previous clinical reports (14, 15). Consequently, some risk factors determined in those reports could be false.

Computed tomography scans have been widely used in medicine since the 1970s (16) and appeared in endodontic research in 1990 (17). It has been shown that computed tomography scans can diagnose AP lesions accurately (15, 18–24). In this study, root canal treatments were performed in dogs' teeth. The purpose was to compare the treatment outcome determined by PR and cone-beam computed tomography (CBCT) scans.

Material and Methods

Sample preparation:

All animal procedures performed in this study conformed to protocols reviewed and approved by the Animal Care Committee of the University of Sa˜o Paulo (Protocol #2007.1.192.53.6).
The third and fourth mandibular premolars of 12 dogs (12 months of age, body weight from 10 to 15 kg) were selected for treatment with a total of 96 root canals. The animals were anesthetized intravenously with sodium thiopental (30 mg/kg body weight; Thionembutal; Abbott Laboratories, Sa˜o Paulo, Brazil). All endodontic procedures were performed aseptically with sterile instruments under a rubber dam, which was surface disinfected with 2% chlorhexidine. Different treatments were performed in four groups, each group consisting of three dogs, for a total of 24 roots per group.
In group 1, root canal treatment was performed in healthy teeth. After coronal pulp exposure, the pulp tissue was extirpated, and the apical cementum layer was perforated with the sequential use of size #15 to #30 K-files, thus creating standardized apical openings. All roots were instrumented to ISO K-file size 60. Root canal filling was performed with gutta-percha cones and AH Plus Jet Mix (Dentsply De Trey, Konstanz, Germany) using a lateral condensation technique.

In groups 2, 3, and 4, crown access was created on the occlusal surface with spherical carbide burs. After pulp removal, the root canals were left exposed to the oral cavity for 7 days to allow microbial contamination. Access openings were then sealed with a quick-setting zinc oxide-eugenol cement (IRM; Dentsply Indu´ stria e Come´rcio Ltda, Petro ´ polis, Rio de Janeiro, Brazil). After 45 days, the development of AP was radiographically confirmed.

Group 2 roots with AP were treated as in group 1. In group 3, root canal instrumentation was performed as in groups 1 and 2. The root canal dressing with a calcium hydroxide paste (Calen; SS White Artigos Denta´ rios Ltda, Rio de Janeiro, Brazil) was applied by using an ML syringe (SS White Artigos Denta´ rios Ltda). A sterile cotton pledget was placed in the pulp chamber, and the access cavity was filled with IRM. Fifteen days later, intracanal dressing was removed, and root canal filling was performed as in groups 1 and 2. Group 4 roots with AP were left untreated.

In groups 1, 2, and 3, each canal was irrigated with a 1% solution of sodium hypochlorite between each instrument during the preparation procedure. After the completion of instrumentation, the root canals were dried with sterile paper points, filled with EDTA solution pH 7.4 (Odahcan-Herpo Produtos Denta´rios Ltda, Rio de Janeiro, Brazil) for 3 minutes, and then irrigated with saline and dried. After the completion of root canal obturation, the crown openings of the three groups were permanently restored with silver amalgam (Velvalloy; SS White Artigos Denta´ rios Ltda), which was condensed on a glass ionomer cement base (Vitremer; 3M/ESPE, Saint Paul, MN). Both PRs and CBCT scans were obtained at three time points: (1) before any intervention (all groups), (2) confirmation of AP (45 days after root canal infection), and (3) 6 months after filling (groups 1, 2, 3, and 4).

PR Scans and Analysis

Radiographs were taken according to the parallel technique using a Heliodent dental X-ray machine (Siemens, Erlanger, Germany) with exposure factors set at 60 kV, 10 mA, and 0.4 seconds. Ultraspeed periapical films (Eastman Kodak, Rochester, NY) were used. The images were digitized through an optical scanning process (Scanjet 7450C; Hewlett-Packard, Palo Alto, CA) with a resolution of 1,200 dpi. The radiolucent areas of the periapical lesion were delineated on the radiographic image excluding tooth structure (root apex) and including only the area of rarefaction. The lesion size was measured in square millimeters using Image J 1.28 u software (National Institutes of Health, Bethesda, MD) as previously described (25, 26). Three calibrated examiners evaluated the PR images independently (k = 0.9636).

CBCT Scans and Analysis

The NewTom 3G (QR Srl, Verona, Italy) apparatus operating at 120 kVp, 3.6 mA, 9 inches field-of-view, matrix size 512 _ 512, bit depth of12 bits, and exposure time of 36 seconds was used. Scans were made according to the manufacturer's recommended protocol. The same scan and reconstruction protocol was used at the three time points in the study. Volumetric studies were exported in DICOM3 format, and the isotropic voxel size was 0.3 mm. The data were imported into Amira software (v.4.2; Visage Imaging Inc, Carlsbad, CA), and the scan position was corrected using realignment tools. Tomographic sections of 0.3 mm in three planes (axial, coronal, and sagittal) were created.

A single observer who was blind to the groups' order measured the size of each lesion twice with 2 weeks separation between the first and the second measurements, and the mean values were used. Details of the segmentation technique are as follows: a region of interest limited only to the apical third of each root and 5mm below the apex was selected to ensure standardized measurements of the lesion size. The lesion was then followed on the axial, coronal, and sagittal slices, and the area of the lesion was segmented on each slice using interactive brush segmentation tools. On each slice, the AP lesion border was delineated to include the lesion radiolucency while excluding the root apex. The segmentation criterion for lesion inclusion is that the gray level value of the lesion lies between +380 and _100 (27). This value is valid only for the NewTom3G scanner and only for the 9-inch field because the histogram scales differ among the different CBCT scanners and scan-field selections (28). The lesion size was calculated as the volume summation of the lesion surface areas across all the segmented slices (29). The software automatically calculates the lesion volume for each root in cubic millimeters.

Evaluation of Treatment Outcome

The treatment outcome for each root was presented in one of the following four categories based on the change of lesions during the 6 months after the treatment: (1) emerged or enlarged, (2) unchanged, (3) reduced, and (4) absent. When a lesion grew or shrank at least 1 mm2 (PRs) or 1 mm3 (CBCT scans), enlargement or reduction of the lesion was determined. The outcome of categories 3 and 4 were considered favorable.

Statistical Analysis

Data were analyzed statistically by the chi-square test and the Kruskal-Wallis Test. The level of significance was set at a = 0.05.

Results

All 96 roots showed healthy periapex preoperatively determined by PRs and CBCT scans. A periapical lesion was diagnosed in all roots in groups 2, 3,

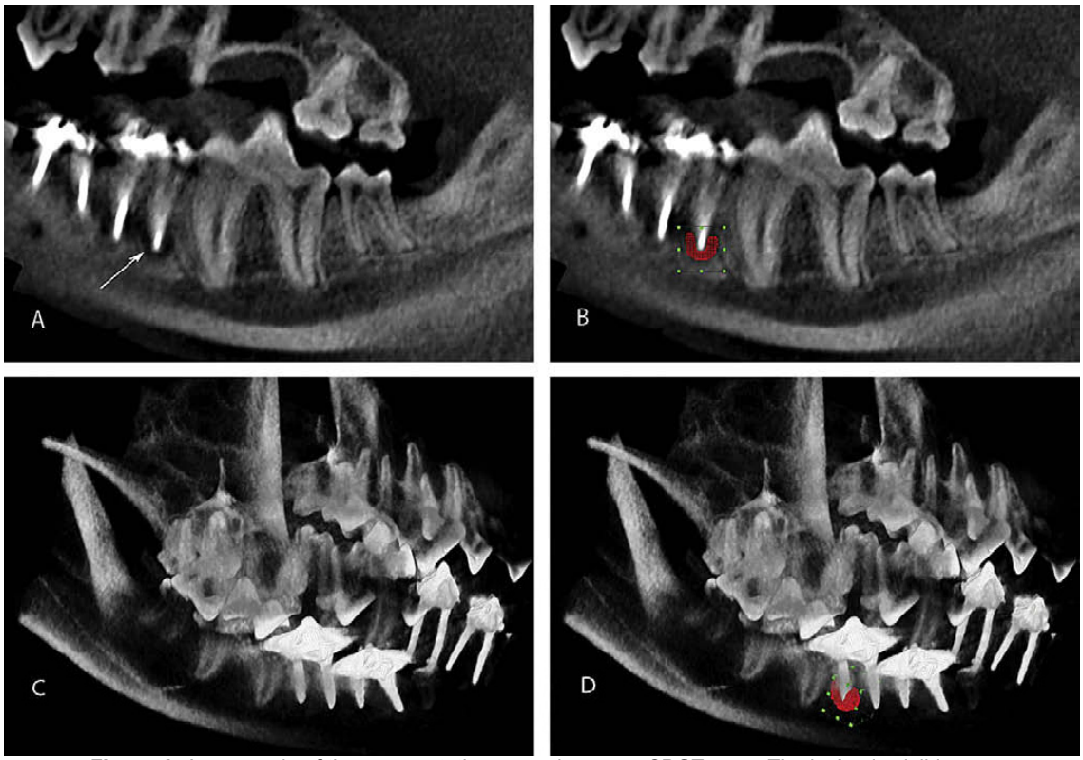

Figure 1. An example of the segmentation procedure on a CBCT scan. The lesion is visible (arrow) on (A) a two-dimensional sagittal slice and is highlighted in red (B). A three-dimensional volume-rendered image of the jaw is shown in C, and the lesion is highlighted in a three-dimensional view in D. The green box shows the region of interest selection.

and 4 after root canal infection. All groups had pretreatment lesions of similar sizes ($p > 0.05$). Favorable outcomes (lesion reduced or absent) was shown in 57 (79%) roots in groups 1, 2, and 3 when determined by a PR but in merely 25 (35%) roots when determined by a CBCT scan (Table 1) ($p = 0.0001$). Unfavorable outcomes occurred more frequently after one-visit therapy than two-visit therapy when determined by a CBCT scan ($p = 0.023$). However, the difference was not significant when determined by PR ($p = 0.093$). In group 4, when determined by a PR, all lesions were enlarged; when determined by a CBCT scan, 22 lesions were enlarged, whereas 2 lesions were slightly reduced.

TABLE 1. Outcome of Root Canal Treatment in Three groups (G1, G2, and G3)* Determined by CBCT Scans and (PRs)

Treatment outcome	Periapical lesion	CBCT			PR		
		G1 (n = 24)	G2 (n = 24)	G3 (n = 24)	G1 (n = 24)	G2 (n = 24)	G3 (n = 24)
Favorable	Reduced	—	1	5	—	15	15
	Absent	16	0	3	21	0	6
	Total (%)		25 (35)			57 (79)	
Unfavorable	Emerged/enlarged	8	23	16	3	5	2
	Unchanged	—	0	0	—	4	1
	Total (%)		47 (65)			15 (21)	

*CBCT, cone beam computed tomography; PR, periapical radiography. In G1, root canal treatments were performed in healthy teeth; in G2, roots with AP were treated by one-visit therapy; and in G3, roots with AP were treated by two-visit therapy.

Discussion

The volume of extraction sockets has been previously measured using CBCT scans (29), and, to our knowledge, this is the first time that the volume of AP lesions has been measured. Using Amira software, the lesion size was calculated as the volume summation of the lesion surface areas across all the segmented slices (Fig. 1). Lesion visibility on each slice is dependent on the slice orientation relative to the lesion (ie, different cuts in different orientation will show different views of the same lesion). The effect of this dependency was minimized by correcting the scan position and by segmenting the slices in three orthographic directions (axial, coronal, and sagittal) in order to reduce bias from single-slice orientation.

In groups 1 through 3, a total of 72 roots was treated. Forty-seven roots presenting unfavorable outcomes were detected by CBCT scans, three times more than those detected by PR (Table 1). PR was unreliable not only in diagnosing the absence of a lesion but also in diagnosing a reduction in lesion size in 24 roots (Table 1). It could be that when lesions expanded in the cancellous bone and in the buccolingual direction, the lesion's enlargement was only revealed by volumetric measurements using CBCT (2–5). One possible reason for the poor outcome in this study would be the short timeframe in animal experiments (30, 31).

The superiority of CBCT scans over PRs in detecting bone lesions has been reported in several articles (15, 19, 21). No AP lesions were detected with PRs at day 14 after root canal infection and 47% could be detected at day 21, whereas CBCT evaluation detected AP in 33% at day 14 and 83% at day 21 (21). Estrela et al (15) showed the absence of posttreatment AP in 65% of teeth using PRs but only in 37% using CBCT scans. Obviously, the prevalence of posttreatment AP was underestimated by PRs, whereas additional relevant information was obtained through CBCT images.

One controversy in endodontics is whether two-visit therapy is superior to one-visit therapy (32–36). In several studies, no significant difference in periapical healing was found between them (32–34). The outcome was evaluated by PRs, which was not sensitive in diagnosing AP lesions (15). In the current study, the unfavorable outcomes occurred more frequently after one visit than two visits when inspected by CBCT scans ($p < 0.05$). Poor periapical healing after one-visit therapy has been reported in other dog experiments (30, 31), and it could be attributed to the presence of

microorganisms that were not properly removed during the cleaning and shaping step of the root canal procedure. Even though it has been reported that the anatomy of the apical portion of the dog root canal differs from that in humans because it consists of a delta of many small canals that cannot be cleaned or filled (37, 38), we attempted to eliminate these small canals by creating a single standardized apical opening. It could be that infection remaining in the apical root canal caused posttreatment AP and the use of Ca(OH)2 as a antimicrobial root canal dressing did, to a certain degree, lead to a more favorable outcome for the two-visit therapy group.

In conclusion, our findings provide evidences of the superiority of CBCT scans for the detection of periapical disease compared with PR. Furthermore, unfavorable outcomes determined by CBCT occurred more frequently after one-visit therapy compared with two-visit therapy.

References

1. Ng Y-L, Mann V, Rahbaran S, Lewsey J, Gulabivala K. Outcome of primary root canal treatment: systematic review of the literature – Part 1. Effects of study characteristics on probability of success. Int Endod J 2007;40:921–39.
2. Bender IB, Seltzer S. Roentgenographic and direct observation of experimental lesions in bone: I. JADA 1961;62:152–60.
3. Bender IB. Factors influencing the radiographic appearance of bone lesions. J Endod 1982;8:161–70.
4. van der Stelt PF. Experimentally produced bone lesions. Oral Surg Oral Med Oral Pathol 1985;59:306–12.
5. Huumonen S, Ørstavik D. Radioological aspects of apical periodontitis. Endod Topic 2002;1:3–25.
6. Stabholz A, Friedman S, Tamse A. Endodontic failures and re-treatment. In: Cohen S, Burns RC, eds. Pathways of the pulp. 6th ed. St Louis, MO: Mosby; 1994:692–3.
7. Ricucci D, Bergenholtz G. Bacterial status in root-filled teeth exposed to the oral environment by loss of restoration and fracture or caries—a histobacteriological study of treated cases. Int Endod J 2003;36:787–802.
8. Ørstavik D, Pitt Ford TR. Apical periodontitis: microbial infection and host responses. In: Ørstavik D, Pitt Ford TR, eds. Essential endodontology. Oxford: Blackwell Science; 1998:1–8.
9. Friedman S, Abitbol S, Lawrence HP. Treatment outcome in endodontics: the Toronto Study. Phase 1: initial treatment. J Endod 2003;29:787–93.
10. Trope M. The vital tooth-its importance in the study and practice of endodontics. Endod Topic 2003;5:1–11.
11. Brynolf I. A histological and roentgenological study of periapical region of human upper incisors. Odontol Revy 1967;18:1–97.
12. Barthel CR, Zimmer S, Trope M. Relationship of radiologic and histologic signs of inflammation in human root-filled teeth. J Endod 2004;30:75–9.
13. Rowe AHR, Binnie WH. Correlation between radiological and histological changes following root canal treatment. J Br Endod Soc 1974;7:57–63.

14. Wu M-K, Dummer PMH, Wesselink PR. Consequences of and strategies to deal with residual post-treatment root canal infection. Int Endod J 2006;39:343–56.
15. Estrela C, Bueno MR, Leles CR, et al. Accuracy of cone beam computed tomography and panoramic and periapical radiography for detection of apical periodontitis. J Endod 008;34:273–9.
16. Brenner DJ, Hall EJ. Computed tomography—An increasing source of radiation exposure. N Eng J Med 2007;357:2277–84.
17. Tachibana H, Matsumoto K. Applicability of X-ray computerized tomography in endodontics. Endod Dent Traumatol 1990;6:16–20.
18. Huumonen S, Kvist T, Gro¨ ndahl K, et al. Diagnostic value of computed tomography in re-treatment of root fillings in maxillary molars. Int Endod J 2006;39:827–33.
19. Lofthag-Hansen S, Huumonen S, Gro¨ ndahl K, et al. Limited cone beam CT and intraoral radiography for the diagnosis of periapical pathology. Oral Surg Oral Med Oral Pathol Oral Radiol Endod 2007;103:114–9.
20. Stavropoulos A, Wenzel A. Accuracy of cone beam dental CT, intraoral digital and conventional film radiography for the detection of periapical lesion. An ex vivo study in pig jaws. Clin Oral Invest 2007;11:101–6.
21. Jorge EG, Tanomaru-Filho M, Gonc¸alves M, et al. Detection of periapical lesion development by conventional radiography or computed tomography. Oral Surg Oral Med Oral Pathol Oral Radiol Endod 2008;106:e56–61.
22. Aggarwal V, Logani A, Shab N. The evaluation of computed tomography scans and ultrasounds in the differential diagnosis of periapical lesions. J Endod 2008;34: 1312–5.
23. Estrela C, Bueno MR, Azevedo BC, et al. A new periapical index based on cone beam computed tomography. J Endod 2008;34:1325–31. 24. Nair MK, Nair UP. Digital and advanced imaging in endodontics: a review. J Endod 2007;33:1–6.
25. De Rossi A, Silva LAB, Leonardo MR, et al. Effect of rotary or manual instrumentation, with or without a calcium hydroxide/1% chlorhexidine intracanal dressing, on the healing of experimentally induced chronic periapical lesions. Oral Surg Oral Med Oral Pathol Oral Radiol Endod 2005;99:628–36.
26. Silva LA, Paula-Silva FWG, Leonardo MR, et al. Radiographic evaluation of pulpal and periapical response of dogs' teeth after pulpotomy and use of recombinant human bone morphogenetic protein-7 as a capping agent. J Dent Child 2008;75:14–9.
27. Simon JHS, Enciso R, Malfaz J, et al. Differential diagnosis of large periapical lesions using cone-beam computed tomography measurements and biopsy. J Endod 2006; 32:833–7.
28. Loubele M, Jacobs R, Maes F, et al. Image quality vs radiation dose of four cone beam computed tomography scanners. Dentomaxillofac Radiol 2008;37:309–19.
29. Agbaje JO, Jacobs R, Maes F, et al. Volumetric analysis of extraction sockets using cone beam computed tomography: a pilot study on ex vivo jaw bone. J Clin Periodontol 2007;34:985–90.
30. Leonardo MR, Almeida WA, Ito IY, et al. Radiographic and microbiologic evaluation of posttreatment apical and periapical repair of root canals of dogs' teeth with experimentally induced chronic lesion. Oral Surg Oral Med Oral Pathol 1994;78:232–8.
31. Katebzadeh N, Hupp J, Trope M. Histological periapical repair after obturation of infected root canals in dogs. J Endod 1999;25:364–8.
32. Trope M, Delano EO, Ørstavik D. Endodontic treatment of teeth with apical periodontitis: single vs. multivisit treatment. J Endod 1999;25:345–50.
33. Weiger R, Rosendahl R, Lo¨ st C. Influence of calcium hydroxide intracanal dressing on the prognosis of teeth with endodontically induced periapical lesions. Int Endod J 2000;33:219–26.

34. Peters LB, Wesselink PR. Periapical healing of endodontically treated teeth in one and two visits obturated in the presence or absence of detectable microorganisms. Int Endod J 2002;35:660–7.
35. Bergenholtz G, Spangberg L. Controversies in endodontics. Crit Rev Oral Biol Med 2004;15:99–114.
36. Gesi A, Hakeberg M, Warfvinge J, et al. Incidence of periapical lesions and clinical symptoms after pulpectomy—A clinical and radiographic evaluation of 1- versus 2-session treatment. Oral Surg Oral Med Oral Pathol Oral Radiol Endod 2006; 101:379–88.
37. Holland GR. Periapical innervation of the ferret canine one year after pulpectomy. J Dent Res1992;71:70–74.
38. Nair PNR, Henry S, Cano V, et al. Microbial status of apical root canal system of human mandibular first molars with primary apical periodontitis after ‘‘one-visit’’endodontic treatment. Oral Surg Oral Med Oral Pathol Oral Radiol Endod 2005;
99:231–52.

Chapter IV Discussion

The specific aim of this dissertation was to explore some of the potential applications of CBCT in the clinical fields of orthodontics and endodontics. On a larger scale this work is part of an ongoing international effort to assess the efficacy of CBCT for various dental applications. CBCT was first introduced in clinical dentistry back in 1997 and was quickly dubbed a 'revolutionary technique' in maxillofacial imaging since it brought CT imaging technology to the dental clinic, which was largely inaccessible to most dentists due to radiation dose, cost and labor constraints. However, as more research evidence became available, some concerns were raised about the accuracy and applicability of this imaging modality for the many 'proclaimed' applications. The concerns stemmed from the observation that there were many different CBCT systems on the market with very different technical designs. Currently, there are more than 20 different commercial clinical CBCT available from different manufacturers. The characteristics of those scanners in terms of specifications of technical design, image quality, radiation dose and scan protocols are so distinct from each other that the efficacy results from one scanner cannot be automatically extrapolated to another system. The research results published in literature and the conclusions about the value of CBCT for a certain clinical application are largely confined to the system used and the specific model from that particular manufacturer.

Different CBCT systems operate at different kVp values ranging from the low (40 kV for Picasso) to high (120 kV for iCAT). Additionally, those systems provide different field of views (FoV) selections to choose from, different radiation exposure levels, different scan positions including sitting, standing or lying flat on a table bed plus several other relevant scanning and reconstruction factors including scan time, number of basis acquisitions (projections), data reconstruction kernels and nominal voxel sizes. It was recently reported in a systematic review of the literature regarding CBCT applications and technical factors that there is still a lack of uniformity in the design of the models produced from different manufacturers [1]. This lack of uniformity in technical specifications of different systems and different models resulted in a wide disparity in the resulting image quality and radiation dose delivered to the patient [2,3]. And due to differences in image quality among the different systems there was a large variability in the visibility of anatomical structures in the dental arches [4,5]. Consequently, repeated experiments and radiographic measurements with several CBCT

scanners are necessary to assess whether the results and findings are valid across the different systems or not. Our results in chapter 3.2 indicate that there are large differences in the accuracy of the different systems for a particular diagnostic task (detection of vertical root fractures). This situation persists to date with the systems currently available.

Additionally, image quality within any one CBCT system is itself inconsistent. Scanning and reconstruction parameters play major role in determining image contrast and spatial resolution. Image quality is not only variable among the different systems but is also dependant on the scan protocol used and the chosen FoV for each system. The results in chapter 2.2 demonstrate that optimizing scan protocol for each particular application is required to improve image quality. However, this makes it almost impossible to objectively compare image quality and accuracy of the different CBCT systems for a particular task with a single standardized protocol. A concentrated research effort is most certainly needed to resolve this issue in the future. A standardized anthropometric phantom specific for CBCT must be developed to allow comparison among different scanners. Future CBCT systems should provide more flexibility and user interactivity to permit FoV selection of various sizes with varying kVp, mA and exposure time settings. This will facilitate standardized comparison of different CBCT systems for a specific diagnostic task and will allow optimizing the patient scan protocol.

Cone Beam CT in Orthodontics: future developments trends

The literature over the role of CBCT in clinical orthodontics is inconsistent. Several review articles and short communications in orthodontic journals describe the potential applications of 3D CBCT imaging in orthodontics [6,7] while currently scarce research evidence actually exists on the accuracy and efficacy of CBCT for those cited applications. Localization of tooth in impacted canines has been regarded as an important clinical application. The added value of CBCT 3D information on the decision making of management of orthodontic patients with tooth impaction was demonstrated [8]. Assessment of the amount of bone available in the pre-maxilla and hard palate regions for the placement of mini-screws has also been marked as a potential application [9]. Nevertheless, the current debate in orthodontics is on the use of CBCT scans as replacements for the conventional orthodontic records. Specifically, the proposal is to replace the traditional dental

impression and cast system with digital 3D surface models of the dental arches from CBCT and to substitute the conventional 2D lateral cephalogram with 3D surface models reconstructions of the maxillofacial region [10]. Those models can potentially be used to aid in diagnosis and treatment planning, simulation and outcome assessment. Three-dimensional surface models are superior to conventional records because they depict the actual patient in full 3D revealing the state of dentition including teeth crowns and roots structures, impactions and stage of development. With digital study models, inter-arch linear measurements can be made, teeth can be digitally relocated to their desired location using special software tools and treatment outcomes can be assessed by superimposing pre and post operative models on each other [11,12]. The cephalometric planes can be defined in 3D based on three or four bilateral points instead of the traditional two points approach adhered to with conventional cephalometry [13,14]. This allows distinguishing the right and left sides and virtually eliminates any superimposition artifacts.

Nonetheless, those proposed applications can only be realized and tested in the clinic if accurate 3D models are made available first. The accuracy of 3D surface reconstructions of the maxillofacial skeleton for cephalometric applications was assessed in part 2.1 and high correlation between the physical and radiographic measurements was found suggesting high accuracy. However, our sample model was based on sectioned maxillas and mandibles immersed in water. The cranium was not covered in the scan and the visibility of important cephalometric landmarks such as the sella turcica was not assessed. The visibility of cephalometric landmarks on 3D models from CBCT is to date not accurately established. In-vitro studies that utilize dry skull over-estimate the quality of the 3D models since no realistic soft-tissue equivalent material is provided. In an in-vivo situation, the visibility of cephalometric landmarks in the maxilla, mandible and the cranial base is largely affected by bone border definition (i.e. the ability to separate bone from surrounding soft-tissue and background). Image segmentation becomes more complicated when bone border definition is unclear due to thin bone plate, soft-tissue presence and patient movement during the scan in addition to CBCT image artifacts. As described in chapters 2.2 and 2.3, beside the limitation of any in-vitro model that no realistic soft tissue simulation material is present, the quality of the 3D model is also influenced by the scanner type and FoV selection.

It is still difficult to ‘automatically’ obtain good quality and highly accurate 3D surface reconstructions of the dental arches from CBCT scans. Artifacts

inherent to CBCT plus limitations in the segmentation approach make it difficult to segment the tooth root and to separate teeth from each other in the upper and lower jaws to visualize the occlusal surfaces of teeth. And as before, scan protocols still need to be optimized before good quality models can be obtained. In this thesis we have suggested a scan protocol to optimize quality of 3D model reconstructions of the dental arches from CBCT. Recent developments in CBCT technology hardware and software algorithm will probably provide means for more accurate 3D reconstructions of both the dental arches and the maxillofacial skeleton. New generation systems using flat panel detector technology have less image noise, higher spatial resolution, less artifacts and larger matrix sizes than what was achievable with previous systems. Also, recent advances in CBCT reconstruction algorithms led to sharper images and better visibility of the border of the alveolar bone, periodontal ligament space and occlusal surface of teeth. Rapid developments in image processing and segmentation algorithms facilitated both bone and tooth segmentation. Future research should concentrate on optimizing the segmentation algorithms to automatically create 3D models of the dental arches, on assessing the accuracy of the selected segmentation approach and on developing user-friendly software for orthodontic practice.

Whether the usefulness of those 3D models outweighs the risk of increased radiation to the patient and the relatively high cost of the scan remains to be investigated. However, the added value of those models should not be under or over estimated until more evidence from both research and clinical experience becomes available advocating or contra-indicating their use.

Cone Beam CT in Endodontics: Future developments trends

In many reviews of the literature there is a large consensus regarding the role of CBCT in clinical endodontics [15-18]. The diagnostic value of CBCT in detecting periapical lesions was previously demonstrated [19,20]. CBCT proved to be superior to both periapical and panoramic radiographs in detection of apical periodontitis [21]. However, a major drawback of many clinical studies is the absence of a true gold standard such as histology sectioning to confirm the presence or absence of the disease to verify the accuracy of the radiographic measurements. Only in one study, the radiographic measurements were compared to histological findings [22]. In part 3.3, CBCT was used to follow-up patients to assess treatment outcomes after

endodontic therapy. In our model, CBCT was found more accurate than conventional 2D periapical radiographs in detecting post-treatment lesions. CBCT also permitted exact measurements of the size of the lesion prior to and after endodontic therapy. The CBCT measurements were then compared with histological analysis and high correlation between the two modalities was found [23]. Periapical lesions cannot be detected on 2D periapical radiographs if the cortical bone is intact [24,25]. That means lesions confined only to the inner trabecular bone cannot be seen on conventional radiographs due to superimposition of the thick cortical bone on the image. CBCT thin slices can reveal lesion in the trabecular bone. However, it was recently found that the visibility of the trabecular bone itself in CBCT is variable among the different scanner systems and across the different scanning and reconstruction settings [4]. Optimizing scan protocol to improve image quality and visibility of the trabecular bone is therefore also necessary here for this application.

For detection of vertical root fractures in endodontically treated teeth, the results shown in parts 3.1 and 3.2 demonstrate that detection of the hair-thin fractures is possible with CBCT yet the variability in image quality among the different CBCT systems has a large influence on detection accuracy. As expected, more fractures were detected on axial slices than on sagittal or coronal reconstructions and also not too surprising was the result that endodontic filling material create streak artifacts that mimic facture lines and mask the actual fracture leading to reduced specificity. The limitations of our ex-vivo model still apply that the soft-tissue simulation was not sufficiently realistic and that the fracture sizes may differ from that seen in the clinic. In a subsequent study, the size of the fractures was found in the range between 60-550µm (unpublished results). There was also a strong correlation between fracture size and its visibility on CBCT images.

Several important developments in CBCT hardware and software will have major impact on the future role of this imaging modality in clinical endodontics. First, the introduction of ‘high-resolution’ collimated scan mode in recent scanners permits the selection of a limited region of interest confined only to the tooth under investigation thus reducing radiation dose delivered to the patient whilst providing maximum resolution and sharp visibility of the canal space. Additionally, many of the so-called metal artifact reduction algorithms are being introduced in new CBCT systems in order to minimize the effect of streak-artifacts caused by root canal filling material and metallic posts. This will certainly lead to improvement in the visibility of fracture lines, internal calcifications and resorptions. Some new systems can

also scan both the maxilla and the mandible while maintaining high spatial resolution. This coupled with high performance computing and recent improvements in reconstruction algorithms will allow for very high-resolution imaging of the dentition. Studies regarding the prevalence of periapical lesions will become possible in the near future. New image processing algorithms would permit automatic segmentation of the root canal and could possibly allow for studying and comparing the morphology of the root canal across populations. Registration algorithm will be used to automatically assess changes in the size of periapical lesions to determine treatment outcome. Automatic tooth segmentation is becoming more feasible that in the future 3D CBCT images can be combined with the imagery from the endodontic microscope in order to provide a complete and exact clinical and radiographic view of the root canal space intra-operatively.

In conclusion, it is clearly demonstrated that CBCT has a lot of potential for many important clinical applications in dentistry. CBCT technology provides a novel insight in the intricate anatomy of the maxillofacial region and clinical diagnosis. And the volumetric nature of the scan allows creation of 3D models of the jaws and dentition opening the door for new applications never deemed possible before. However, as with any new imaging modality, there are several issues related to image quality that need to be resolved first before the full potential of this technology is realized.

References:

1. De Vos W, Casselman J, Swennen GRJ. Cone-beam computerized tomography (CBCT) imaging of the oral and maxillofacial region: a systematic review of the literature. Int J Oral Maxillofac Surg. 2009 Jun ;38(6):609-625.
2. Loubele M, Maes F, Jacobs R, van Steenberghe D, White SC, Suetens P. Comparative study of image quality for MSCT and CBCT scanners for dentomaxillofacial radiology applications. Radiat Prot Dosimetry. 2008 ;129(1-3):222-226.
3. Loubele M, Jacobs R, Maes F, Denis K, White S, Coudyzer W, Lambrichts I, van Steenberghe D, Suetens P. Image quality vs radiation dose of four cone beam computed tomography scanners. Dentomaxillofac Radiol. 2008 Sep ;37(6):309-318.
4. Liang X, Jacobs R, Hassan B, Li L, Pauwels R, Corpas L, Souza PC, Martens W, Shahbazian M, Alonso A, Lambrichts I. A comparative evaluation of Cone Beam Computed Tomography (CBCT) and Multi-Slice CT (MSCT) Part I. On subjective image quality [Internet]. Eur J Radiol. 2009 Apr 30;[cited 2009 Oct 6]
5. Liang X, Lambrichts I, Sun Y, Denis K, Hassan B, Li L, Pauwels R, Jacobs R. A comparative evaluation of Cone Beam Computed Tomography (CBCT) and Multi-Slice CT (MSCT). Part II: On 3D model accuracy [Internet]. Eur J Radiol. 2009 May 5;[cited 2009 Oct 6]
6. Holberg C, Steinhäuser S, Geis P, Rudzki-Janson I. Cone-beam computed tomography in orthodontics: benefits and limitations. J Orofac Orthop. 2005 Nov ;66(6):434-444.
7. Müssig E, Wörtche R, Lux CJ. Indications for digital volume tomography in orthodontics. J Orofac Orthop. 2005 May ;66(3):241-249.
8. Walker L, Enciso R, Mah J. Three-dimensional localization of maxillary canines with cone-beam computed tomography. Am J Orthod Dentofacial Orthop. 2005 Oct ;128(4):418-423.
9. Korbmacher H, Kahl-Nieke B, Schöllchen M, Heiland M. Value of two cone-beam computed tomography systems from an orthodontic point of view. J Orofac Orthop. 2007 Jul ;68(4):278-289.
10. Chenin D., Chenin D., Chenin S., Choi J.THE CUTTING EDGE Dynamic Cone-Beam Computed Tomography in Orthodontic Treatment J Clinical Ortho 2009 Aug;43(8) [e-pub ahead of print]
11. Cevidanes LHC, Heymann G, Cornelis MA, DeClerck HJ, Tulloch JFC. Superimposition of 3-dimensional cone-beam computed tomography models of growing patients. Am J Orthod Dentofacial Orthop. 2009 Jul ;136(1):94-99.
12. Cevidanes LHS, Bailey LJ, Tucker SF, Styner MA, Mol A, Phillips CL, Proffit WR, Turvey T. Three-dimensional cone-beam computed tomography for assessment of mandibular changes after orthognathic surgery. Am J Orthod Dentofacial Orthop. 2007 Jan ;131(1):44-50.
13. Olszewski R, Cosnard G, Macq B, Mahy P, Reychler H. 3D CT-based cephalometric analysis: 3D cephalometric theoretical concept and software. Neuroradiology. 2006 Nov ;48(11):853-62.
14. Swennen GRJ, Schutyser F, Barth E, De Groeve P, De Mey A. A new method of 3-D cephalometry Part I: the anatomic Cartesian 3-D reference system. J Craniofac Surg. 2006 Mar ;17(2):314-25.

15. Tyndall DA, Rathore S. Cone-beam CT diagnostic applications: caries, periodontal bone assessment, and endodontic applications. Dent. Clin. North Am. 2008 Oct ;52(4):825-841, vii.
16. Cotton TP, Geisler TM, Holden DT, Schwartz SA, Schindler WG. Endodontic applications of cone-beam volumetric tomography. J Endod. 2007 Sep ;33(9):1121-1132.
17. Patel S, Dawood A, Ford TP, Whaites E. The potential applications of cone beam computed tomography in the management of endodontic problems. Int Endod J. 2007 Oct ;40(10):818-830.
18. Patel S. New dimensions in endodontic imaging: Part 2. Cone beam computed tomography. Int Endod J. 2009 Jun ;42(6):463-475.
19. Stavropoulos A, Wenzel A. Accuracy of cone beam dental CT, intraoral digital and conventional film radiography for the detection of periapical lesions. An ex vivo study in pig jaws. Clin Oral Investig. 2007 Mar ;11(1):101-106.
20. Lofthag-Hansen S, Huumonen S, Gröndahl K, Gröndahl H. Limited cone-beam CT and intraoral radiography for the diagnosis of periapical pathology. Oral Surg Oral Med Oral Pathol Oral Radiol Endod. 2007 Jan ;103(1):114-119.
21. Estrela C, Bueno MR, Leles CR, Azevedo B, Azevedo JR. Accuracy of cone beam computed tomography and panoramic and periapical radiography for detection of apical periodontitis. J Endod. 2008 Mar ;34(3):273-9.
22. Simon JHS, Enciso R, Malfaz J, Roges R, Bailey-Perry M, Patel A. Differential diagnosis of large periapical lesions using cone-beam computed tomography measurements and biopsy. J Endod. 2006 Sep ;32(9):833-7.
23. Garcia de Paula-Silva FW, Júnior MS, Leonardo MR, Consolaro A, da Silva LAB. Cone-beam computerized tomographic, radiographic, and histologic evaluation of periapical repair in dogs' post-endodontic treatment. Oral Surg Oral Med Oral Pathol Oral Radiol Endod. 2009 Sep [e-pub ahead of print]
24. Bender I.B, Factors influencing the radiographic appearance of bone lesions, *J Endod* **8** (1982), pp. 161–170.
25. Van der Stelt P.F., Experimentally produced bone lesions, *Oral Surg Oral Med Oral Pathol* **59** (1985), pp. 306–312.

Chapter V Summary and conclusions

The aim of this work was to explore some of the potential clinical applications of CBCT in dentistry. The emphasis was to assess the efficacy of CBCT for selected clinical applications in the fields of orthodontics and endodontics.

Chapter I starts with an introduction to three-dimensional imaging in medicine and dentistry followed by a technical description of the principles of CBCT imaging. The clinical applications of CBCT in dentistry are then discussed as evidenced in the literature. Several important applications in different dental specialities are detailed including tooth impaction, TMJ imaging, maxillofacial surgery, jaw defects, dental implant rehabilitation, endodontics and orthodontics.

In **Chapter II** in orthodontics, the aims were to assess the accuracy of 3D CBCT models of the dental arches and the maxillofacial skeleton for orthodontic diagnosis and treatment planning. *In part 2.1* the accuracy of CBCT 3D models reconstructions was assessed by comparing linear measurements made on 3D models against physical measurements made on dry skulls. The results showed high correlation between the radiographic and physical measurements suggesting high accuracy of CBCT 3D reconstructions. However, on further analysis *in part 2.2*, several scanning and reconstruction parameters including scan FoV and voxel size selections had significant influence on the quality of 3D reconstructions of the alveolar bone and the visibility of the occlusal surfaces of teeth. This was further confirmed *in part 2.3* when the CBCT 3D teeth and occlusal surfaces reconstructions were quantitatively compared against microCT as a reliable gold standard. Again, it was found that scan FoV and voxel size selections have significant influence on 3D models quality and accuracy and this has corroborated our subjective findings in part 2.2. Most CBCT systems currently available provide many scanning and reconstruction parameters to choose from. Scan FoV, which determines the volume coverage of the anatomical region of interest, has significant influence on image quality in CBCT. Smaller FoV selections are recommended to improve spatial resolution and to improve the visibility of anatomical structures.

In **Chapter III** in endodontics, the aims were to assess the feasibility of CBCT in detection of vertical root fractures (VRFs) and in assessment of endodontic treatment outcomes. *In part 3.1*, the accuracy of CBCT in detecting VRFs was compared to that of conventional 2D periapical radiographs (PR) against a reliable gold standard (microscopy). CBCT was found significantly more accurate than PR in detecting VRFs. *In part 3.2*, however, the accuracy of five clinical CBCT systems for detecting VRFs was compared and large differences in detection accuracy among the different systems were found. Significant differences exist in the visibility of small structures among the different CBCT systems and across the different scanning and reconstruction settings. *In part 3.3* CBCT was used to follow-up a sample of dogs with periapical lesions to assess the changes in the size of the lesions after endodontic treatment. Interestingly, the study found that in several cases, endodontic treatment did not reduce the size of the lesion leading to unfavourable outcome. CBCT was more accurate than conventional 2D PR images in detecting post-treatment lesions and it also permitted accurate assessment of the volume of the lesion pre and post operatively.

Chapter IV discusses the results of the published studies and comments on the limitations of the methodologies employed in this work. Also proposals for future research directions are made. The underlying conclusion is that CBCT is a promising technology that can provide new insights in diagnosis and treatment planning for many dental applications. Future CBCT fundamental and clinical research coupled with rapid advances in image processing and high performance computing will most certainly revolutionize modern dental practice. However, several issues with respect to image quality, scanning and reconstruction protocols need to be addressed first before the full-potential of this modality can be realized.

Samenvatting en conclusies

Het doel van dit werk was enkele potentiële klinische toepassingen van CBCT in tandheelkunde te gaan onderzoeken. De nadruk was om de nauwkeurigheid en haalbaarheid van CBCT voor geselecteerde toepassingen binnen orthodontie en endodontologie gebieden te gaan beoordelen.

Hoofdstuk I begint met een inleiding aan driedimensionele beeldvorming in geneeskunde en tandheelkunde en het is wordt gevolgd met een technische beschrijving van de principes van CBCT. De klinische toepassingen van CBCT in tandheelkunde worden vervolgens besproken zoals in de literatuur staan. Verscheidene belangrijke toepassingen in verschillende tandspecialiteiten zijn gedetailleerd (tandimpaction, CMD, maxillofacial chirurgie, kaak defecten, tand implant rehabilitatie, endodontics en orthodontie.

In Hoofdstuk II in orthodontie, de doelstelling was de nauwkeurigheid van CBCT 3D modellen van de tandbogen en het maxillofacial skelet voor orthodontische diagnose en behandeling planning te gaan beoordelen. *In deel 2.1* de nauwkeurigheid van CBCT 3D reconstructies werd beoordeeld door vergelijken tussen de lineaire radiografische en fysieke metingen op droge schedels. De resultaten toonden hoge correlatie tussen de radiografische en fysieke metingen en die toonde hoge nauwkeurigheid van 3D reconstructies CBCT. Nochtans, bij verdere analyse *in deel 2.2*, hadden verscheidene scanning en reconstructie parameters met inbegrip van field of view (FoV) en voxel grotte selecties significante invloed op de kwaliteit van de 3D reconstructies van het alveolare bot en het zichtbaarheid van de occlusal oppervlakten van tande. Dit werd verder bevestigd *in deel 2.3* toen de 3D tanden CBCT en de occlusal oppervlakten reconstructies kwantitatief tegen microCT als betrouwbare goudstandaard werden vergeleken. Weer eens, het was gevonden dat de selecties van de FoV en voxel grootte significante invloed op 3D modellenkwaliteit en nauwkeurigheid hebben en dit heeft onze subjectieve bevindingen *in deel 2.2* bevestigd. Tegenwoordig, meeste verkrijgbare CBCT systemen leveren velen scanning en reconstructie parameters om tussen te kiezen. FoV selectie bepaalt het volume van het anatomische gebied die in de scan binnengaat en die heeft een significante invloed op beeldkwaliteit in CBCT. De kleinere selecties van FoVs worden geadviseerd om resolutie en het zichtbaarheid van anatomische structuren te verbeteren.

In Hoofdstuk III in endodontie, de doelstellingen waren om de haalbaarheid van CBCT in detectie van verticale wortel fracturen (VRFs) en endodontic behandelingsresultaten te gaan onderzoeken. *In deel 3.1*, werd de nauwkeurigheid van CBCT in de detectie van VRFs vergeleken bij dat van conventionele 2D periapical röntgenfoto's (PR) tegen een betrouwbare goudstandaard (de microscopie). CBCT werd gevonden beduidend nauwkeuriger dan PR in het ontdekken van VRFs. In deel 3.2, echter, werd de nauwkeurigheid van vijf klinische CBCT systemen vergeleken en grote verschillen tussen de systemen in detectienauwkeurigheid werden gevonden. Er bestaan significante verschillen in de zichtbaarheid van kleine structuren tussen de verschillende CBCT systemen en over de verschillende scanning en reconstructie parameters. *In deel 3.3* werd CBCT gebruikt om een steekproef van honden met periapical laesies op te volgen om de veranderingen in de grootte van de laesies na endodontisch behandeling te gaan beoordelen. De studie vond dat in verscheidene gevallen, de endodontic behandeling heeft de grootte van de laesies niet verminderd dat de behandelingsresultaten waren ongunstig. CBCT was nauwkeuriger dan de conventionele 2D beelden van PR in het ontdekken van periapicale laesies na de behandeling.

Hoofdstuk IV discussieert de resultaten van de gepubliceerde studies en geeft een commentaar op de beperkingen van de methodologieën die in dit werk worden gebruikt. Ook er zijn voorstellen voor toekomstige onderzoekrichtingen. In conclusie CBCT is een veelbelovende technologie die nieuw inzicht in diagnose en behandeling planning voor vele tandheelkunde toepassingen kan verstrekken. Het toekomstige fundamentele en klinische CBCT onderzoek samen met snelle ontwikkelingen in beeldvorming en verwerking en high performance computing wordt gekoppeld zal het zekerst moderne tandpraktijk hervormen. Nochtans, moeten verscheidene kwesties met betrekking tot beeldkwaliteit eerst worden opgelost alvorens de volledig potentieel van deze modaliteit kan worden gerealiseerd.

International publications:

1) **Hassan B**, Metska ME, Ozok AR, van der Stelt P, Wesselink PR. Detection of vertical root fractures in endodontically treated teeth by a cone beam computed tomography scan. J Endod. 2009 May ;35(5):719-722.
2) **Hassan B**, Metska ME, Ozok AR, van der Stelt P, Wesselink PR. Comparison of five Cone Beam Computed Tomography systems for detecting vertical root fractures in endodontically treated teeth. (J Endod 2010;36:126–129)
3) Garcia de Paula-Silva FW, **Hassan B**, Bezerra da Silva LA, Leonardo MR, Wu M. Outcome of root canal treatment in dogs determined by periapical radiography and cone-beam computed tomography scans. J Endod. 2009 May ;35(5):723-726.
4) **Hassan B**, van der Stelt P, Sanderink G. Accuracy of three-dimensional measurements obtained from cone beam computed tomography surface-rendered images for cephalometric analysis: influence of patient scanning position. Eur J Orthod. 2009 Apr ;31(2):129-134.
5) **Hassan B**, Couto Souza P, Jacobs R, de Azambuja Berti S, van der Stelt P. Influence of scanning and reconstruction parameters on quality of three-dimensional surface models of the dental arches from cone beam computed tomography [Internet]. Clinical Oral Investigations 2009 DOI 10.1007/s00784-009-0291-3
6) Bassam Al-Rawi, **Bassam Hassan**, Bart Vandenberge, Reinhilde Jacobs. Accuracy assessment of three-dimensional surface reconstructions of teeth from Cone Beam Computed Tomography scans. JOOR Feb 2010 [Epub ahead of print]
7) **Bassam Hassan**. Reliability of Periapical Radiographs and Orthopantomograms in Detection of Tooth Root Protrusion in the Maxillary Sinus: Correlation Results with Cone Beam Computed Tomography. J Oral Maxillofac Res 2010 (Jan-Mar);1(1):e6
8) **Bassam Hassan** and Reinhilde Jacobs. Cone Beam Computed Tomography 3D imaging in Oral and Maxillofacial Surgery. Euro Medical Imaging Review 2008 1(1): 38-40.
9) Liang X, Jacobs R, **Hassan B**, Li L, Pauwels R, Corpas L, Souza PC, Martens W, Shahbazian M, Alonso A, Lambrichts I. A comparative evaluation of Cone Beam Computed Tomography (CBCT) and Multi-Slice CT (MSCT) Part I. On subjective image

quality [Internet]. Eur J Radiol. 2009 April [in-press, available online].
10) Liang X, Lambrichts I, Sun Y, Denis K, **Hassan B**, Li L, Pauwels R, Jacobs R. A comparative evaluation of Cone Beam Computed Tomography (CBCT) and Multi-Slice CT (MSCT). Part II: On 3D model accuracy. European Journal of Radiology May 2009 [in-press, available online]
11) E. Gorisse, A. de Jongh, **B. Hassan**. Behandeling idiopathische aangezichtspijn na plaatsing implantaat. Nederlands Tijdschrift voor Tandheelkunde (Dutch Journal of Dentistry). Feb 2010 [e-pub ahead of print].
12) **Hassan BA**, R Jacobs, WC Scarfe, WT Al-Rawi. A web-based instruction module for interpretation of craniofacial cone beam CT anatomy. Dentomaxillofac Radiol 2007 36: 348-355.
13) Al-Rawi WT, Jacobs R, **Hassan BA**, Sanderink G, Scarfe WC. Evaluation of web-based instruction for anatomical interpretation in maxillofacial cone beam computed tomography. Dentomaxillofac Radiol. 2007 36(8):459-64.
14) Bert Van Thielen, Francis Siguenza, **Bassam Hassan**. Experimental Results of Cone Beam Computed Tomography in Dental Veterinary Medicine. Journal of Veterinary Dentistry 2010 [in-press].
15) **Bassam Hassan**, Peter Nijkamp, Christian Vink, Jamshed Tairie, Hans Verheij, Paul van der Stelt, Herman van Beek. Identifying cephalometric landmarks in-vivo on 3D surface rendered Cone beam Computed Tomography Models. American Journal or Orthodontics Orofacial Orthopaedics 2010 [In submission to AJODO].

Acknowledgement:

After spending the best part of the last four years sitting in a tiny windowless room at the oral and maxillofacial radiology department at ACTA pondering over the perplexes of Cone Beam CT, it is tempting for me to claim the sole credit for this work. However, as much as I am inclined to do so, I cannot ignore that in the past four years lots of people were gracefully knocking on my door, disturbing my solitary confinement, exchanging ideas and offering advice. Without them, this work would have never seen the daylight. Orderly, I would like first to thank my promoter Prof. Paul van der Stelt for granting me the opportunity to work on this project and for teaching me how to stay organized and focused and how to take on one thing at a time. Thank you, professor for steering me in the right direction. Second, many thanks go to my co-promoter Dr. Gerard Sanderink for supporting me all those years and for teaching me how to remain critical to my results. I have surely developed lots of enthusiasm for criticising my own work because of him!

From the department of endodontics, great thanks go to my co-promoter Dr. Rifat Ozok for his enormous effort and contribution to the endodontic part of my thesis and for his insight and advice. I learned from him how to write thoroughly yet succinctly and how to remain 'diplomatic' to the reviewers' rather aggressive comments. Those two skills are essential for anyone who is taking on an academic career. Thanks go also to Dr. Min-Kai Wu for the unique opportunity he granted me to collaborate with the research group in Brazil on one of the most interesting and exciting projects in this thesis. His enthusiasm pushed me forward to analyze and actually produce results! I'm greatly thankful also to my dear friend and colleague Dr. Marelli Metska who co-authored the endodontic part of the thesis. The constant bickering, the heated discussions, the arguments, the coffee breaks, the frustrations, the failed experiments, the drilling and hammering of teeth… I will miss all that. THANK YOU Marelli in capital letters and I wish you all the happiness and fortune in this world. And finally I want to thank the head of the endodontics department Prof. Paul Wesselink for the opportunity for this constructive collaboration between the endodontics and radiology departments.

In the orthodontics department I'm indebted to Prof. Herman van Beek and Dr. Luc Habets for their continuous support for my work at their department. I'm also duly obliged to Prof. Prahl Anderson for her heart-full, warm and continuous support and compassion. And also my colleague Dr. Peter van Nijkamp for his constructive insights and comments. In the radiology department I would like to thank Dr. Hans Verheij for teaching me statistics and research design and for constructively influencing this thesis in numerous ways that I cannot count. I would also like to thank my dearest friend Dr. Kostas Syriopoulos who had been like a big brother to me all those years. For helping me out with almost everything from housing to times when I was ill or in need and for always standing beside me and for your persistent support and friendship, I'm ever thankful. I would also like to thank Dr. Wil Geraets for all the thoughtful discussions about life, science, the cosmos, religions and other cultures and for expanding my horizons about the Dutch customs and habits. Lastly, I'm utterly thankful to Dr. Erwin Berkhout and the lovely ladies 'Ignes', 'Mika', 'Yvonne', 'Yvonna' and 'Vida' for *forcing me* to speak Dutch, for their help and for their friendship. Without them, I would still be muttering, mumbling and stuttering in this language (not that I don't do that now!). For that 'Dank u wel'.

I would like to thank Prof. Reinhilde Jacobs head of the Oral Imaging Centre at KUL in Leuven, Belgium. I would not have been able to get into dental radiology in Europe without her support. I'm forever grateful to Reinhilde for helping and supporting me so much for so long! I would also want to thank Prof. Xin Liang for her support, smiles and friendship. From Brazil I would like to thank Prof. Paulo Couto Souza and his lovely wife Dr. Soraya Berti. I'm sure that there are lots of other people I forgot to mention but don't blame me because the thing they say about PhD students having short memories is in fact true! Triple cheers to ACTA, research and Cone Beam CT; PROST!